NUREG/CR-6917
PNNL-16313

Experimental Measurements of Pressure Drop Across Sump Screen Debris Beds in Support of Generic Safety Issue 191

Pacific Northwest National Laboratory

U.S. Nuclear Regulatory Commission
Office of Nuclear Regulatory Research
Washington, DC 20555-0001

AVAILABILITY OF REFERENCE MATERIALS IN NRC PUBLICATIONS

NRC Reference Material

As of November 1999, you may electronically access NUREG-series publications and other NRC records at NRC's Public Electronic Reading Room at http://www.nrc.gov/reading-rm.html. Publicly released records include, to name a few, NUREG-series publications; *Federal Register* notices; applicant, licensee, and vendor documents and correspondence; NRC correspondence and internal memoranda; bulletins and information notices; inspection and investigative reports; licensee event reports; and Commission papers and their attachments.

NRC publications in the NUREG series, NRC regulations, and *Title 10, Energy*, in the Code of *Federal Regulations* may also be purchased from one of these two sources.

1. The Superintendent of Documents
   U.S. Government Printing Office
   Mail Stop SSOP
   Washington, DC 20402–0001
   Internet: bookstore.gpo.gov
   Telephone: 202-512-1800
   Fax: 202-512-2250
2. The National Technical Information Service
   Springfield, VA 22161–0002
   www.ntis.gov
   1–800–553–6847 or, locally, 703–605–6000

A single copy of each NRC draft report for comment is available free, to the extent of supply, upon written request as follows:

Address: U.S. Nuclear Regulatory Commission
Office of Administration
Mail, Distribution and Messenger Team
Washington, DC 20555-0001
E-mail: DISTRIBUTION@nrc.gov
Facsimile: 301–415–2289

Some publications in the NUREG series that are posted at NRC's Web site address http://www.nrc.gov/reading-rm/doc-collections/nuregs are updated periodically and may differ from the last printed version. Although references to material found on a Web site bear the date the material was accessed, the material available on the date cited may subsequently be removed from the site.

Non-NRC Reference Material

Documents available from public and special technical libraries include all open literature items, such as books, journal articles, and transactions, *Federal Register* notices, Federal and State legislation, and congressional reports. Such documents as theses, dissertations, foreign reports and translations, and non-NRC conference proceedings may be purchased from their sponsoring organization.

Copies of industry codes and standards used in a substantive manner in the NRC regulatory process are maintained at—

The NRC Technical Library
Two White Flint North
11545 Rockville Pike
Rockville, MD 20852–2738

These standards are available in the library for reference use by the public. Codes and standards are usually copyrighted and may be purchased from the originating organization or, if they are American National Standards, from—

American National Standards Institute
11 West 42nd Street
New York, NY 10036–8002
www.ansi.org
212–642–4900

Legally binding regulatory requirements are stated only in laws; NRC regulations; licenses, including technical specifications; or orders, not in NUREG-series publications. The views expressed in contractor-prepared publications in this series are not necessarily those of the NRC.

The NUREG series comprises (1) technical and administrative reports and books prepared by the staff (NUREG–XXXX) or agency contractors (NUREG/CR–XXXX), (2) proceedings of conferences (NUREG/CP–XXXX), (3) reports resulting from international agreements (NUREG/IA–XXXX), (4) brochures (NUREG/BR–XXXX), and (5) compilations of legal decisions and orders of the Commission and Atomic and Safety Licensing Boards and of Directors' decisions under Section 2.206 of NRC's regulations (NUREG–0750).

NUREG/CR-6917
PNNL-16313

Experimental Measurements of Pressure Drop Across Sump Screen Debris Beds in Support of Generic Safety Issue 191

Manuscript Completed: December 2006
Date Published: February 2007

Prepared by
C.W. Enderlin, B.E. Wells, M. White, F. Nigl,
D.R. Rector, T.J. Peters, A.D. Guzman

Pacific Northwest National Laboratory
Richland, WA 99352

W.J. Krotiuk, NRC Project Manager

Prepared for
Division of Risk Assessment and Special Projects
Office of Nuclear Regulatory Research
U.S. Nuclear Regulatory Commission
Washington, DC 20555-0001
NRC Job Code N6106

Abstract

The U.S. Nuclear Regulatory Commission (NRC) Generic Safety Issue-191 deals with the possibility that, during a loss of coolant accident in a pressurized water reactor, thermal insulation and other materials may be damaged and the debris transported to accumulate on the sump screens of the emergency core cooling system and containment sump. Over time, a debris bed could form, blocking the sump screen, increasing the pressure drop across the sump screen, and reducing the available suction head for the recirculation pumps resulting in the safety margins for pump operations being exceeded.

Pacific Northwest National Laboratory (PNNL) conducted experiments to help the NRC predict the flow through debris beds consisting of fiberglass and calcium silicate particulate. The effects of debris preparation on debris bed formation and pressure drop were evaluated and a metric developed for characterizing the preparation. Testing consisted of forming the debris bed within the test loop and obtaining a steady-state pressure drop at the bed formation velocity. The velocity was then changed incrementally through several cycles—increasing and decreasing—with a steady pressure measurement obtained at each flow set point. The loop temperature was then changed and the velocity variation sequence repeated.

The test setup, data acquisition system, procedures, experimental results, and observations are presented. In situ measurements and photographs show the debris beds contracting and relaxing with the cycling of flow velocity.

Foreword

During a loss-of-coolant accident (LOCA) at a nuclear power plant, the impingement of a high-energy steam-water jet or exposure to the high containment temperature, pressure, and humidity environment may dislodge thermal insulation, coatings, and other material. Some dislodged debris may fall near the containment sump or be transported in the containment water pool to the vicinity of the sump. After recirculation starts, the debris may accumulate on the sump screen surface and increase the pressure drop (i.e., head loss) across the sump screens. The increased head loss could challenge the ability of the recirculation pumps to provide adequate long-term cooling water to the emergency core cooling system (ECCS) and the containment spray system pumps.

The nuclear industry has recognized this phenomenon. The United States and other countries have performed tests to characterize the pressure drop across a debris clogged sump screen. An October 1995, U.S. Nuclear Regulatory Commission (NRC) study documented in NUREG/CR-6224, *Parametric Study of the Potential for BWR ECCS Strainer Blockage Due to LOCA-Generated Debris*, used test data to develop a head loss correlation to evaluate suppression pool strainer performance in boiling-water reactors but did not address the range of potential debris characteristics postulated for accidents in pressurized-water reactors (PWRs). A significant number of PWR plants use calcium silicate (CalSil) thermal insulation, often in combination with other materials such as fiberglass (i.e., NUKON^{TM}) or reflective metal insulation.

Consequently, NRC sponsored another study to provide test data for head losses resulting from the accumulation of CalSil-laden insulation debris on a PWR sump screen and to evaluate the suitability of the NUREG/CR-6224 correlation for application to PWR plants that can accumulate CalSil insulation in combination with other debris on a sump screen. This study was documented in NUREG/CR-6874, *GSI-191 Experimental Studies of Loss-of-Coolant-Accident-Generated Debris Accumulation and Head Loss with Emphasis on the Effects of Calcium Silicate Insulation*, dated May 2005.

NRC's Advisory Committee on Reactor Safeguards (ACRS), Thermal-Hydraulic Subcommittee, raised concerns regarding the application of the NUREG/CR-6224 methodology for calculating head loss through debris-clogged PWR sump screens in letter ACRSR-2096, "Safety Evaluation of the Industry Guidelines Related to Pressurized Water Sump Performance," dated October 18, 2004. As a result of these technical comments, the staff of NRC's Office of Nuclear Regulatory Research concluded that the head loss methodology should be redeveloped and correlated against test data. NRC recognized that the available head loss test data did not include the effects of water temperature on a debris laden sump screen, did not provide data for a broad enough range of CalSil and NUKON concentrations on a sump screen to address a large portion of expected PWR sump screen conditions, and did not address head loss resulting from accumulation of coating debris on a sump screen. In addition, previous testing was performed using a woven metal screen to represent the sump screen, while many of the proposed PWR sump designs use perforated metal plates instead and are designed for lower water approach velocities.

NRC sponsored additional testing to address these concerns and to support development of an improved head loss correlation, as described in this document. The data provided can be used to develop a conservative bounding methodology for calculating pressure drop across a porous medium that might be present on a debris laden sump screen.

Brian Sheron, Director
Office of Nuclear Regulatory Research
U.S. Nuclear Regulatory Commission

Contents

Figures

Tables

Abbreviations and Acronyms

A/D	analog to digital
ACRS	Advisory Committee on Reactor Safeguards
ALK	Ameron's Amercoat 5450 alkyd topcoat
ANL	Argonne National Laboratory
BAP	boiled after preparation
BPP	boiled prior to preparation
BT	benchtop
BWR	boiling water reactor
CalSil	calcium silicate
CO	CalSil only
CSS	containment spray system
DAS	data acquisition system
DP	differential pressure
ECCS	emergency core cooling system
ENS	European Nuclear Society
ft	feet
ft/sec	feet per second
g/m^2	grams per square meter
gpm	gallons per minute
GSI	Generic Safety Issue
Hp	horsepower
Hz	Hertz
ID	inner diameter
in.	inches
Inc.	incorporated
ISA	ionic strength adjuster
ISE	ion selective electrode
L	liter
L/D	length/diameter; nondimensionalized distance expressed in terms of number of diameters
LANL	Los Alamos National Laboratory
LOCA	loss-of-coolant accident
m	meters
M&TE	measurement and testing equipment
m/s	meters/second
mA	milliamperes
mL	milliliters
mm	millimeters
mV	millivolts

NA	not applicable
N/A	not applicable
NC	NUKON and CalSil combined
NO	NUKON only
NPSH	net positive suction head
NPT	National Pipe Thread
NRC	U.S. Nuclear Regulatory Commission
NRR	NRC Office of Nuclear Reactor Regulation
PC	personal computer
PNNL	Pacific Northwest National Laboratory
PNPP	Perry Nuclear Power Plant
PO	perforated plate only
PSD	particle size distribution
psi	pounds per square inch
PVC	polyvinyl chloride
PWR	pressurized water-reactor
Re	Reynolds Number
RES	NRC Office of Nuclear Regulatory Research
RHR	residual heat removal
RTD	resistive temperature device
RWST	refueling water storage tank
SEM	scanning electron microscopy
SO	screen only
TC	thermocouple
TTS	transparent test section
V	volts
VFD	variable frequency drive
ZE	Ameron's Dimetcote 6 inorganic zinc primer with Amercoat 90 epoxy topcoat

Executive Summary

In 1996, the U.S. Nuclear Regulatory Commission (NRC) established Generic Safety Issue (GSI) 191, "Assessment of Debris Accumulation on PWR Sump Performance," to identify, prioritize, and resolve concerns regarding the blockage of sump screens following a loss-of-coolant accident (LOCA). The primary concern associated with GSI-191 is the possibility that, during a LOCA within the containment of a pressurized water reactor (PWR), thermal insulation and other materials (e.g., coatings and concrete) may be damaged and dislodged. Dislodged material (i.e., debris) may subsequently be transported and accumulate on the sump screens of the emergency core cooling system and containment spray system sump. Over time, a debris bed could form on the sump screen that progressively restricts flow, inducing a head loss that could reduce the available net positive suction head below that required for these pumps.

Pacific Northwest National Laboratory (PNNL) was tasked with conducting experiments to obtain data for the pressure drop across debris beds as a function of the approach velocity. The data will assist the NRC in developing correlations for predicting the pressure drop for flow through a compressible porous-medium debris bed composed of NUKON ™ (a fiberglass insulation) low-density fiberglass and calcium silicate (CalSil) particulate.

Two test loops with test sections 4 and 6 inches in diameter were constructed for generating debris beds and measuring the associated pressure drop. Debris beds were generated and pressure drop measurements made for beds consisting of NUKON fiberglass, CalSil particulate, and combinations of fiberglass and particulate.

During the test program, the effects of debris preparation on debris bed formation and pressure drop were evaluated and a metric developed for characterizing the disassociation of the debris after preparation. Testing consisted of forming the debris bed within the test loop and obtaining a steady-state pressure drop at the bed formation velocity. The approach velocity was then changed incrementally through several cycles of increasing and decreasing velocity with a steady pressure measurement obtained at each flow set point. The loop temperature was then changed and the velocity variation sequence repeated.

During testing, in situ measurements of the debris bed height were taken using an optical triangulation system developed for the test program. Selected retrieved debris beds were impregnated with epoxy and sectioned, and subsequently imaged using scanning electron microscopy to evaluate the debris bed structure. A process for assessing the CalSil mass in a NUKON/CalSil debris bed was employed using chemical dissolution and a calcium ion selective electrode. The test program also evaluated the effects of the debris loading sequence and flow history through the debris bed on the resulting pressure drop.

The initial set of tests conducted by PNNL was performed at test conditions similar to those of tests performed at the University of New Mexico under the direction of Los Alamos National Laboratory in 2004. Limited testing was also conducted using coating materials (Ameron's Amercoat 5450 alkyd topcoat and Ameron's Dimetcote 6 inorganic zinc primer with Amercoat 90 epoxy topcoat) as debris. The test setup, data acquisition system, procedures, experimental results, and observations are described in this report.

The preparation of the debris material and the constituent loading sequence during debris bed formation were shown to strongly influence the resulting pressure drop and physical integrity of a debris bed. NUKON/CalSil debris beds were formed by:

- CalSil being deposited on an existing NUKON debris bed (referred to as NUKON bed first)
- NUKON being introduced into a flow stream with CalSil already well dispersed in the flow (referred to as NUKON time lag)
- Premixing the NUKON and CalSil material before introducing it into the flow stream (referred to as premixed).

The debris loading sequences of NUKON bed first and NUKON time lag yielded pressure drops approximately 3 orders of magnitude higher than those achieved from the premixed condition, with the NUKON time lag yielding the larger pressure drop.

PNNL-generated debris beds consisting only of fiber material yielded relatively repeatable results. Complete debris beds were generated at debris loadings ≥171 g/m^2 in the 6-in.-diameter test loop and ≥56 g/m^2 in the 4-in.-diameter loop. Complete debris beds consisting of only calcium silicate particulate material were not formed at loadings up to 4350 g/m^2.

In situ measurements of debris bed height and accompanying photographs show the debris beds contracted and relaxed with continued cycling of the approach velocity. For most cases, the pressure drop decreased with increased temperature; however, the flow history to which the debris bed had been subjected affected the measured pressure drop. Negligible differences in the measured pressure drop were obtained for similar debris loadings between debris beds generated on 5-mesh woven wire and 1/8-in. perforated plate.

A relative bulk density was calculated for the debris beds based on the in situ bed height measurements obtained with the optical triangulation system. For both the NUKON-only and the NUKON/CalSil debris beds, the pressure drop across the debris bed increased with an increase in the relative bulk density of the debris bed. For each elevated temperature case in which the head loss increased with temperature, the relative bulk density of the debris was observed to be significantly higher.

1.0 Introduction

This report details experimental work conducted by Pacific Northwest National Laboratory (PNNL) for the U.S. Nuclear Regulatory Commission (NRC) Office of Nuclear Regulatory Research (RES). The experiments focused on measuring the pressure drop as a function of approach velocity across debris beds formed on a section of 5-mesh screen or 1/8-inch perforated plate. The test conditions were intended to be representative of a section of pressurized water reactor (PWR) sump strainer debris beds following a loss-of-coolant accident (LOCA). The work was performed as part of the NRC's effort to resolve Generic Safety Issue 191 (NRC 1996).

Two test loops with test sections 4 and 6 inches in diameter were constructed for generating debris beds and measuring the associated pressure drop as a function of the upstream approach velocity. Debris beds consisting of NUKON^{TM} low-density fiberglass, calcium silicate particulate, and combinations of fiberglass and particulate were generated. A limited number of tests were also conducted using coatings (e.g., epoxy paint) as the debris.

During the test program, the effects of debris preparation on debris bed formation and pressure drop were evaluated and a metric developed for characterizing the disassociation (preparation) of the prepared debris. This effort also investigated the impact of the debris loading sequence (i.e., the order in which debris components arrive at the screen) on the measured pressure drop. The work was initiated in May 2005, and large-scale tests were conducted between November 2005 and August 2006.

A brief background of the circumstances that have led to this test effort is given in Section 1.1. The objectives for this body of work are presented in Section 1.2, and an outline of the rest of this report is provided in Section 1.3.

1.1 Background

During a design basis LOCA, the emergency core cooling system (ECCS) provides water to the reactor core, and the containment spray system (CSS) sprays water into (to avoid excluding scrubbing radionuclide function) the containment atmosphere. To provide sufficient cooling to the reactor core, the ECCS is required to operate for the extended period required by the long-lived radioactivity in the core (often assumed to be 30 days for analytical purposes). The cooling water is initially obtained from the refueling water storage tank (RWST). When the RWST liquid is depleted, water from the sump pool that accumulates at the bottom of the reactor containment is circulated through the core. In the event of a LOCA within the containment, the potential exists for insulation, coatings, and other materials to be dislodged and introduced into the sump water. The accumulation of such debris after a LOCA may adversely affect the flow paths necessary for proper operation of the ECCS and CSS. In particular, the accumulation of debris on the sump screens upstream of the pump inlets could result in a head loss that reduces the available net positive suction head required for operation of the ECCS and/or CSS pumps.

In 1979, the NRC established USI A-43, "Containment Emergency Sump Performance," to study safety issues related to the ability of PWRs and boiling water reactors (BWRs) to circulate water to the reactor core following a LOCA.

In July of 1992, Barsebäck-2, a Swedish BWR, experienced the clogging of two ECCS pump suction strainers from the accumulation of fibrous insulation. The clogging occurred following the release of steam from a safety valve that inadvertently opened at low power (ENS 1992). In 1993, the Perry Nuclear Power Plant, with a BWR/6 reactor, experienced two instances of ECCS strainer plugging (PNPP 1993). One of the events resulted in deformation of the pump suction strainers due to the buildup of debris and subsequent pressure drop. Based on these events, the NRC issued NRC Bulletin 93-02 in May 1993, which requested PWR and BWR licensees identify fibrous air filters and other temporary sources of fibrous material in the containment not specifically designed to withstand a LOCA, and to remove the material and ensure the functional capability of the ECCS.

As a result of these occurrences in Europe and the United States, the NRC initiated a study of BWR strainer blockage based on plant surveys. Findings from European experiences were used to identify possible deficiencies in the suction strainers employed in U.S. BWRs. In September 1993, as a result of the initial study, the NRC undertook a plant-specific study using a BWR/4 reactor with a Mark I containment. The results of this plant specific study were documented in *Parametric Study of the Potential for BWR ECCS Strainer Blockage due to LOCA Generated Debris* (Zigler et al. 1995).

In August 1994, a draft of NUREG/CR-6224 was released for public comment. Based on the lack of relevant experimental data available during the preparation of the draft NUREG/CR-6224, the NRC sponsored a series of experiments (Brinkman and Brady 1994, Rao and Souto 1995) to investigate the behavior of debris in the suppression pool and obtain debris bed pressure drop data. The bulk of the experimental work used NUKON^{TM} (a fiberglass insulation) as the fibrous debris material. Particulate material consisted of simulated BWR sludge composed primarily of iron oxide. The new experimental data and revised models for debris transport and pressure drop were presented in the final NUREG/CR-6224 (Zigler et al. 1995). NUREG/CR-6224 concluded that debris blockage could result in a rapid loss of available net positive suction head (NPSH) for most postulated occurrences of pipe breaks.

In 1996, the NRC established *Generic Safety Issue (GSI) 191, Assessments of Debris Accumulation on PWR Sump Performance* (NRC 1996) to identify, prioritize, and resolve concerns regarding the blockage of PWR sump screens following a LOCA. Specifically, GSI-191 deals with the possibility that, during a LOCA within the containment of a PWR, thermal insulation and other materials (e.g., coatings and concrete) may be damaged and dislodged. Dislodged material (debris) may subsequently be transported and accumulate on the sump screens for the ECCS and CSS pumps. Over time, a debris bed could form that progressively blocks the screen, inducing a head loss that could reduce the available net positive suction head below that required for these pumps. Excessive debris bed head loss will reduce the flow rate and discharge pressure of the pumps, potentially terminating the flow of coolant water if the blockage is sufficiently severe.

As part of NRC's efforts to resolve GSI-191, RES contracted with Los Alamos National Laboratory (LANL) to perform additional experiments to determine the pressure drop associated with debris beds on sump screens. LANL was tasked with evaluating the performance of the head loss correlation derived in NUREG/CR-6224 for NUKON and iron oxide particulate on debris beds containing calcium silicate. The test results from LANL are presented in NUREG/CR-6874, *Experimental Studies of Loss-of-Coolant-Accident-Generated Debris Accumulation and Head Loss with Emphasis on the Effects of Calcium Silicate Insulation* (Shaffer et al. 2005).

The NRC's Advisory Committee on Reactor Safeguards (ACRS), Thermal-Hydraulic Subcommittee raised concerns regarding the application range of the NUREG/CR-6224 methodology for calculating head loss through debris clogged sump screens (Bonaca 2004). In September 2004, the RES staff was also provided two documents written by Graham Wallis, the Chairman of the ACRS: *NUREG/CR-6224 Head Loss Correlation*, dated Sept. 3, 2004, and *Flow Through a Compressible Mat: Analysis of the Data Presented in Series 6 Test Reported by LANL in LA-UR-04-1227, dated* Sept 3, 2004, which reviewed and critiqued the head loss correlations presented in NUREG/CR-6224. These documents criticized the NUREG/CR-6224 head loss equation and the associated compression relation for the debris bed. The ACRS indicated that the head loss calculation method should not be based on variances in the specific surface area of the debris and should not use a "thin bed" effect, which was not theoretically based. These documents further indicated that the NUREG/CR-6224 compression relation for the debris bed was inconsistent with the limited test data available and that additional test data were needed.

As a result of the ACRS' technical comments, the RES staff concluded that the existing head loss methodology should be redeveloped and correlated with additional test data. To assist in this task, RES contracted with PNNL to fabricate a test loop and obtain experimental data of the pressure drop across debris beds as a function of approach velocity and temperature. During the experimental effort, data was transmitted to RES staff as it became available. Using these data, RES revised the method for calculating head loss across a debris bed. The revised methodology and comparative results are presented in NUREG-1862 (Krotiuk 2006).

1.2 Objectives

The primary objectives of this task were to:

- Obtain experimental data characterizing the pressure drop associated with debris deposition on sump screen material to be used by RES to develop a methodology for predicting pressure drop for flow through a compressible porous medium debris bed composed of fiberglass and calcium silicate (CalSil) particulate.
- Characterize the head loss as a function of debris composition, loading, and thermal-hydraulic conditions.
- Design experiments for measuring the debris bed pressure drop that have controllable conditions that
  - Minimize the experimental uncertainty
  - Assess the true variability associated with debris bed formation for a given debris composition and loading.
  - Maximize the repeatability of debris bed pressure drop measurements.

To accomplish theses objectives, PNNL performed the following activities:

- Fabricated a test loop for generating debris beds and taking pressure drop measurements for approach velocities of 0.02 to 2 ft/sec (0.01 to 0.61 m/s) at temperatures between 68° and 185°F (20° and 85°C).
- Developed debris preparation procedures and defined metrics for assessing the degree of debris preparation (disassociation of fibrous material).

- Developed a system for taking in situ debris bed height measurements as a function of approach velocity.
- Conducted experiments in which debris beds were generated from vendor provided insulation and coating materials; steady state pressure drop measurements were taken as a function of approach velocity. The following sets of debris beds were evaluated.
  - Eleven tests were conducted for particulate-only (CalSil) debris for target debris loadings of 1451 to 4350 g/m^2.
  - Eighty-six tests were conducted for fibrous-only (NUKON) debris for target debris loadings of 105 to 1681 g/m^2 with debris bed thicknesses measured between 0.11 to 0.63 inches.
  - Thirty-nine tests were conducted for debris beds generated with a combination of particulate and fiber. The target total debris loadings ranged from 135 to 2421 g/m^2. The target mass ratio of particulate to fibrous material ranged from 0.25 to 1.25. The measured debris bed thicknesses ranged from 0.04 to 0.36 inches.
  - Three tests of coating chips were conducted with Ameron's Amercoat 5450 alkyd topcoat (ALK) for a target debris loading of 1400 g/m^2.
  - One test of coating chips was conducted Ameron's Dimetcote 6 inorganic zinc primer with Amercoat 90 epoxy topcoat (ZE) for a target debris loading of 1400 g/m^2.

1.3 Report Outline

An overview of the test setup and instrumentation is contained in Section 2. Schematics of the two head loss test loops constructed are included. Detailed drawings of the test loop are contained in Appendix B.

Section 3 describes the development of the debris preparation procedure and associated metrics used to verify the process for specific debris mass loadings. This section defines the criteria used for establishing the debris preparation process. The results of testing to evaluate the effects of debris preparation on the debris bed pressure drop are included. The description of the preparation and characterization of the coatings materials tested is contained in Section 4.

Section 5 contains the test matrix for the large-scale loop tests and an overview of the test procedures and approach. The test matrixes for the tests completed in the benchtop loop are included in Appendix C.

Phenomenological results for the effect of parameters associated with initial conditions on the measured pressure drop are presented in Section 6. These parameters are potential sources of variability in the results and were investigated to aid in the development of the test matrix and test procedures. These parameters include debris preparation, screen material, debris loading sequence, and flow history.

The results of the pressure drop tests are included in Section 7, and the associated discussion of these results is presented in Section 8. Section 9 presents the discussion and conclusions of the entire test effort. All references for the report are included in Section 10.

Details of the test setup are included in Appendices A and B. The instrumentation and data acquisition system details are provided in Appendices C and D. Appendix E contains the debris preparation procedures and results from the benchtop test loop are included in Appendix F. The Quick Look reports used to transmit the data from individual tests to the NRC are provided in Appendices G through K. The benchmark test plan used by PNNL and ANL to conduct comparative tests is in Appendix L. The test matrices completed in the benchtop test loop for NUKON only and NUKON/CalSil debris beds are contained in Appendices M and N, respectfully. Photographs for the characterization of the coatings debris are included in Appendix O.

2.0 Test Setup

This section provides an overview of the test setup, measurements, and instrumentation used for obtaining the experimental measurements. Two test loops, the benchtop and the large-scale, were constructed for obtaining pressure drop measurements across a debris bed. The benchtop and large-scale loops are described in Sections 2.3 and 2.4, respectively.

The original and final design requirements are discussed in Section 2.1. The specifications for the test screen materials and how they were incorporated into the test loops are presented in Section 2.2. The instrumentation and associated measurements taken during the test program are described in Section 2.5.

2.1 Design Requirements

The original specifications provided by the NRC for performing the tests included:

- Data should be recorded at steady state flow conditions for screen approach velocities from 0.1 to 2 ft/sec (0.03 to 0.61 m/s)
- Screen diameter between 8 and 12 in. (20.3 and 30.5 cm)
- Accommodate and measure debris bed thicknesses of 0.25 to 8 in. (0.6 to 20.3 cm)
- Debris bed pressure drop measurements up to 34 ft H_2O (14.7 psi)
- Water temperature from 68° to 185°F (20° to 85°C).

After procurement and construction of the large-scale test loop had been initiated, the specified screen diameter was reduced to 6 in. (15.2 cm). Preliminary testing conducted in the benchtop loop provided insight as to the range of pressure drops, debris bed thicknesses, and associated approach velocities that would be required to achieve the initial proposed test matrix provided by the NRC. The preliminary benchtop tests indicated the following:

- Debris bed thickness would be less than 1 in.
- For the range of debris loadings evaluated, pressure drops in excess of 14.7 psi, which would be an upper-bound limit for typical plant pumps (not possible to draw a suction from less than -14.7 psig), were measured at approach velocities less than 1 ft/sec (0.3 m/s). Therefore, a maximum approach velocity of 1 ft/sec (0.30 m/s) would be sufficient for conducting the tests.
- Discontinuities and crevices in the main-line flow path should be minimized to reduce the settling and accumulation of debris material in the test loop.

Based on the PNNL test approach, the following additional design criteria for the large-scale test loop were specified:

- The maximum loop pressure should be 100 psig. Increasing the loop static pressure aids in maintaining dissolved gas in solution, thus ensuring single-phase fluid flow through the debris bed with no holdup of gas within the debris bed.
- To allow fully developed flow to be established, 20 length/diameters (L/Ds) of straight, constant diameter piping should be provided upstream of the test screen.

- To ensure the downstream pressure tap is located in a region with a fully developed velocity profile, 10 L/Ds of straight, constant-diameter piping should be provided between the test screen and the downstream pressure tap.
- The entire test section should have a constant diameter with no obstructions or discontinuities.
- The test screen material should extend to the pipe wall with no support lip or collar protruding into the flow stream.
- The test section immediately upstream of the debris bed should be transparent to allow for direct viewing, taking in situ debris bed height measurements, and photography. It was preferred but not mandatory that the test section immediately downstream of the test screen be transparent to make observations associated with debris material passing through or being extruded from the test screen and to determine if gas was coming out of solution in the flow discharged from the debris bed.
- The debris injection system should produce a repeatable process that yields similar debris beds.
- The debris injection system should have the capability to introduce debris constituents separately so there is no mixing of the constituents prior to introduction into the loop.
- The debris bed should be able to be removed from the test loop while still on the screen and within a section of piping (i.e., undisturbed).
- The loop should have sufficient filtering capability to remove suspended debris material under test condition flow rates.

2.2 Test Screen Materials

The primary goal of the project was to characterize the differential pressure across a debris bed formed on sump screen material as a function of approach velocity. Two screen materials were tested, 5-mesh wire cloth and perforated sheet metal with 1/8-in. openings. Table 2.1 provides the specifications of the screen materials tested.

Table 2.1. Characteristics of Sump Screen Materials Tested

Tested Screen Geometries (304-Stainless Steel)					
Type	**Pattern**	**Thickness (in.)**	**Penetration Size (in.) and Shape**	**Hole Pitch (in.)**	**Flow Area (%)**
Perforated Metal (perforated plate)	Hexagonal	0.063 plate	0.125 ID round	0.188	40
Wire Cloth (5-mesh screen)	Orthogonal	0.072 wire interwoven (total thickness x 2)	0.128 square	0.20	41

The 5-mesh wire cloth (woven wire) represents one configuration of screen material that has been employed at PWRs. The material was selected as the closest fit to the description of the screen material used for previous debris bed tests at LANL (obtained via email from Bruce Letellier of LANL, May 24, 2005). The 5-mesh wire cloth will be referred to as 5-mesh screen. The 1/8-in.-opening perforated metal sheet was selected by the NRC staff as a representative configuration of what may be installed in PWRs following the resolution of GSI-191. The perforated metal will be referred to as perforated plate.

For the benchtop loop, test screens consisted of a 6-in.-diameter circular piece of the screen material cut from stock sheets using an abrasive water jet. The circular pieces were sandwiched between two annular rubber gaskets with inner diameter (ID) equal to that of the test section. The screen and gaskets were then secured between two PVC pipe flanges bolted together.

For the large-scale loop, screen assemblies were fabricated by securing the screen material between two stainless steel annular rings. The screen material was tack welded to the annular rings and then the outside of the screen assembly was seal welded. The ID of the annular rings was the same as for Schedule-40 6-in. pipe, 6.065 in. (15.4 cm). The screen assemblies were fabricated to avoid distortion of the screen during testing and handling. Custom-cut Gorlock® gaskets were used to secure and seal a screen assembly within the transparent test section (see Section 2.4.2). Figure 2.1 contains photos of the two screen materials and a wire-mesh screen assembly. Refer to Appendix A for details on the geometry and fabrication of the test screens.

For a pressure drop of 14.7 psi (101.3 kPa) across a debris bed, the 6.065-in.- (15.4-cm-) diameter screen would be subjected to a total load of approximately 425 lb (1890 N). Because in situ debris-bed height measurements were to be taken, the deflection of the 5-mesh material in a screen assembly was evaluated under load.

During the deflection test, the screen assembly was uniformly supported by the stainless steel annular rings by placing the assembly over a 6-in. pipe flange. The screen assembly was marked such that the load would be applied to the same side each time. A pad of 1/16-in silicone gasket material was placed over the screen material followed by a circle of 3/8-in.-thick plywood to distribute the test load and prevent point loads. The test loads were applied to the top of the plywood circle.

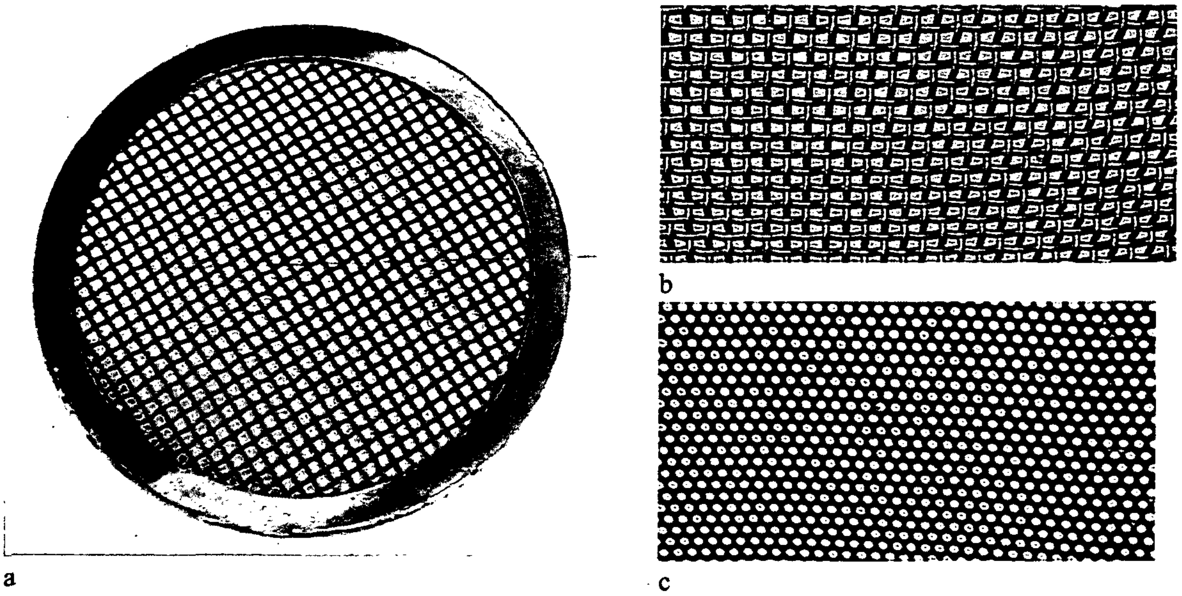

Figure 2.1. Screen Materials Used for Testing: a) screen assembly for large-scale loop with 5-mesh woven wire, b) 5-mesh woven wire material, c) perforated plate material

The test was conducted by adding the desired load, waiting 5 minutes, removing the load, measuring deflection and inspecting for damage. Table 2.2 contains the results of the deflection tests. The perforated plate was much stiffer material and no deflections were measured for the test loads applied.

Table 2.2. Observed Deflections in 5-Mesh Screen Assembly After Applying Distributed Load

Applied Load (lb)	Observations Following Removal of Load
25	No observed or measured change
75	No observed or measured change
125	No observed or measured change
175	One region of screen shows deflection of approximately 0.12 in.(3.2 mm)
225	Depressed region still approximately 0.12 in. (3.2 mm) but larger in diameter.
275	Approximately 40% of screen area is depressed 0.12 in. (3.2 mm). Depressed region is not symmetrical about center of screen and appears shifted to one side.
325	Approximately 40% of screen area is depressed 0.12 in. (3.2 mm). Depressed region is not symmetrical about center of screen and appears shifted to one side. About the same as observations made for 275 lb load except a visually obvious ripple/dimple effect where the screen is not uniformly deformed.
375	No change from 325 load observations
425	Approximately 50% of screen area is depressed 0.12 in. (3.2 mm). Some individual wires indicate a deflection of 0.25 in.

2.3 Benchtop Loop Setup

The benchtop loop was fabricated prior to the large-scale loop to meet the following objectives:

- Evaluate holdup of debris material within the test loop under various operating scenarios. Results and observations from these tests were used to improve the design of the large-scale test loop.
- Develop a debris introduction system and debris bed formation procedure that was controllable, yielded relatively repeatable results, and satisfied the debris bed formation criteria (see Section 3.1.1).
- Aid in developing a debris preparation process and investigate the effects of debris introduction and preparation on debris bed pressure drop.
- Provide feedback on the design of the large-scale test loop by providing test experience associated with debris introduction, debris bed formation, data acquisition, and debris bed retrieval.
- Provide insight into the trends, range of pressure drops, and debris loadings required to form complete debris beds that could be expected during tests in the large-scale loop. Results and observations obtained in the benchtop loop were used to refine the test matrix and prioritize test conditions.
- Develop, evaluate, and refine the test procedures for the large-scale loop.

Because a major objective of the benchtop loop was to assist in developing the final design and procedures for the large-scale loop, the benchtop loop had several modifications incorporated during the test program. The description of the benchtop loop is for the final configuration of the loop. Two additional benchtop loops were used to evaluate debris introduction, debris material holdup, filtration requirements, and CalSil particle size information. These loops did not contain debris screens and no detailed descriptions are provided.

The benchtop loop contained no heating capability or cover gas for increasing the static pressure. Therefore, all tests in the benchtop loop were performed at ambient temperature. With no cover gas system, the static pressure of the loop could not be raised to maintain gas in solution. Therefore, at increased pressure drops across the debris bed, the potential existed for gas bubbles to be generated.

The filter installed in the benchtop loop was not used during testing; therefore, the potential existed for debris to be added to the debris bed throughout a test. The potential sources of additional mass were suspended debris that passed through the debris bed or resuspended debris that had previously settled within the loop. As the approach velocity is increased following the initial test debris bed formation, the debris bed compresses and becomes more efficient at filtering suspended material from the flow. The increased approach velocity also has the potential to resuspended debris that may have settled within the test loop at the lower approach velocities used for the test debris bed formation.

The intent of the benchtop loop was to obtain comparative results for evaluating trends associated with changes in test parameters or procedures. When comparing pressure drop measurements from the benchtop loop with test data from the large-scale loop or other test programs, two limitations of the benchtop loop should be considered.

- The configuration of the test loop piping did not ensure a fully developed flow profile upstream of the test screen.
- The taps used to obtain pressure drop measurements across the debris bed were not located at ideal positions.

An overview of the benchtop loop description is presented in Section 2.3.1. The test section containing the test screen is described in Section 2.3.2.

2.3.1 Benchtop Loop Description

The benchtop loop was assembled on the minus-12-ft level of the 336 Building at PNNL. The test section containing the test screen for the benchtop loop is 4 in. in diameter (see Section 2.3.2 for details). The loop is fabricated mostly of 2-in. flex hose interconnected by Camlock quick-disconnect fittings and Schedule-40 pipe fittings. Kuriyama Tigerflex Series WH, a transparent PVC suction hose, made up the majority of the hoses. The loop is configured for closed-loop testing. The total length of the benchtop loop pipe run is approximately 53 ft, and the volume of the main line is approximately 13 gal.

A 3-hp pump driven by an electronic variable frequency drive (VFD) provides motive power for the test fluid. A combination of the pump VFD and a throttle valve (2-in. gate valve) control the flow rate through the test section. The maximum flow rate of the loop is approximately 50 gpm, which provides a maximum approach velocity of approximately 1.3 ft/sec (0.4 m/s).

Two parallel pipe runs, which bypass the main-line throttle valve, exist for introducing debris material into the loop and are referred to as the debris injection lines. Each 1-in.-diameter injection line includes a Coriolis flow meter and a throttle valve (1-in. gate valve) at the upstream end so that the flow through the individual injection lines can be controlled and monitored. Each injection line contains a section of 1-in. transparent flex hose downstream of the throttle valve that can be removed from the system and loaded with debris material. The two debris injection lines are connected to the main line using pipe crosses. The main-line throttle valve is located between the upstream inlet to the injection lines and the downstream discharge of the injection lines. This configuration allows adjustment of the main line throttle valve to generate a backpressure sufficient to cause flow through the injection lines. The transparent flex hoses allow the debris to be observed during the injection process to ensure the debris is distributed throughout the length of the injection line and is not clumping or settling.

Between the discharge of the test section and the inlet of the pump, two alternative flow paths were plumbed. One of the alternative paths was added for reducing entrained gas bubbles. The flow passed through a small tank exposed to the ambient air. The open tank and reduced velocity allowed gas bubbles to rise to the surface. The flow was passed through the degassing loop prior to debris injection and after the bed formation had been completed. The second alternative path included a filter for polishing the test loop water prior to debris injection. Filtration was not performed during test operations. Figure 2.2 is a simplified schematic of the benchtop loop.

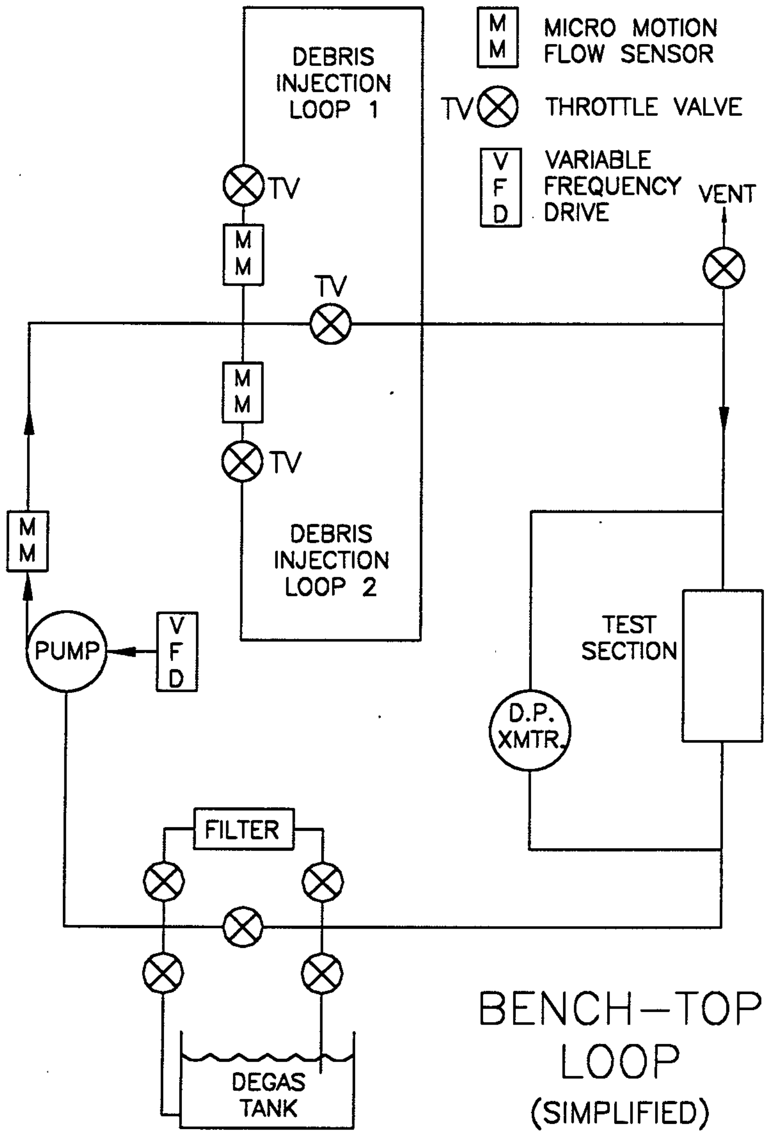

Figure 2.2. Simplified Schematic of the Benchtop Loop

While the benchtop loop could not be pressurized or heated like the large-scale loop, the duration of tests and associated cleanup and turn-around time was much less. Thus tests were conducted, data were provided to the NRC, and decisions were made regarding large-scale testing fairly quickly.

2.3.2 Benchtop Test Section Description

The test section of the benchtop loop was fabricated from 4-in. Schedule-40 transparent PVC pipe glued into 4-in. PVC pipe flanges in the form of pipe spool pieces. Two of these spool pieces form the test section, which has an overall length of 41.5 in. (Figure 2.3).

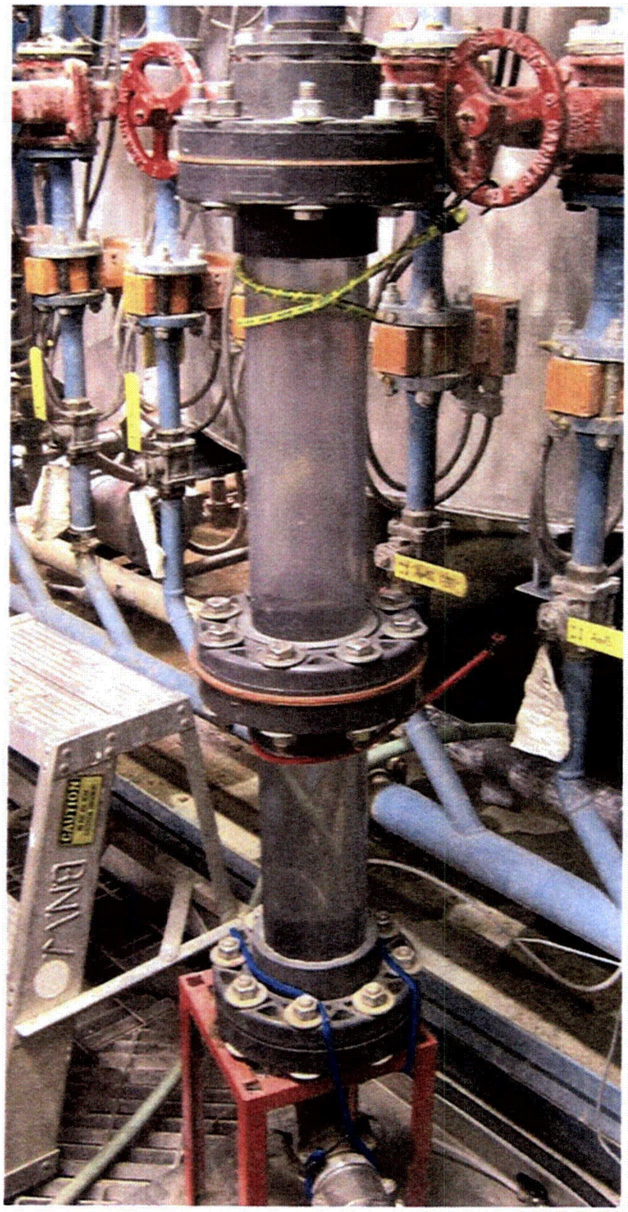

Figure 2.3. Photo of the Benchtop Loop Test Section. The test screen is sandwiched in the center set of pipe flanges.

Ninety-degree pipe elbows exist at the inlet and discharge of the test section. Due to the relatively short length (5.2 pipe diameters) and the proximity of the pipe elbows, fully developed flow is not ensured just upstream of the test screen. The taps used to obtain the pressure drop measurements across the debris beds are located upstream and downstream of the 4-in test section, which are not ideal locations. The locations of the pressure taps are shown in Figures 2.4 and 2.5.

The screen materials and geometries tested in the benchtop loop were the same as those used for the large-scale loop described in Section 2.4. For the benchtop loop, the cut screen material is sandwiched between the flanges of the two spool pieces forming the test section. The screen material contains no annular support ring, is sealed with silicone rubber gaskets custom cut to fit, and is held in place by tightening the bolts of the PVC pipe flanges. This configuration results in the screen material penetrating the test section wall and creates no discontinuity in the test section cross-sectional area, such as with a ledge or other protruding support structure.

The upstream (inlet) pressure port is 10.5 in. (26.7 cm) above the top gasket of the test section assembly. The downstream (outlet) pressure port horizontal "T" run is 11.5 in. (29.2 cm) below the bottom gasket of the test section assembly.

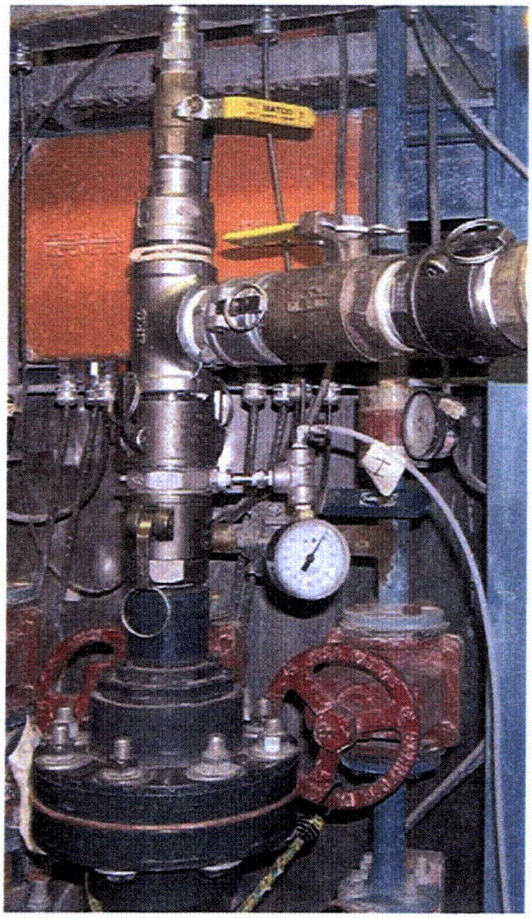

Figure 2.4. Upstream Portion of Benchtop Test Section Showing Pressure Tap Location

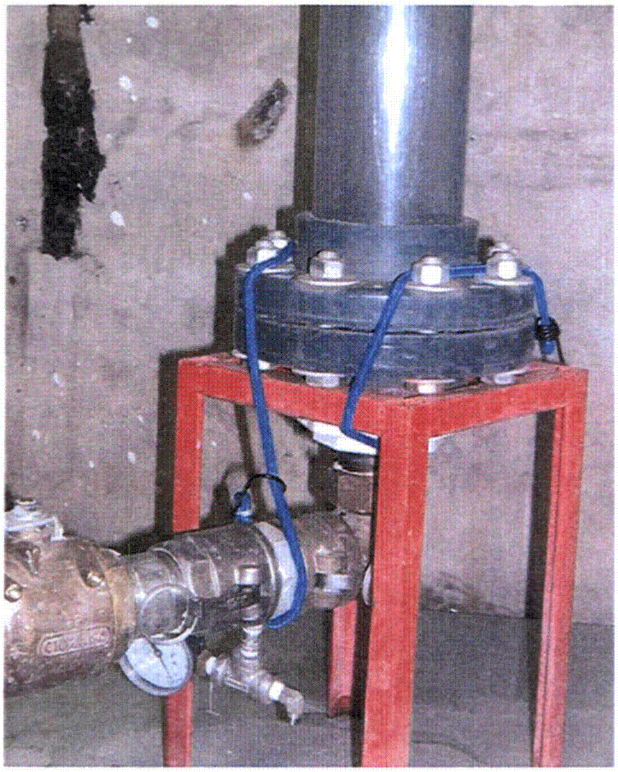

Figure 2.5. Downstream Portion of Benchtop Test Section Showing Pressure Tap Location

2.4 Large-Scale Loop

The large-scale test loop was designed and fabricated to facilitate testing of larger diameter screens than possible in the benchtop loop and to include the following features:

- Temperature control (heating) from ambient to 194°F (90°C).
- Loop pressurization to 100 psig (689 kPa) to maintain gas in solution.
- Filtering at test condition flow rates.
- Fully developed flow upstream of the test screen.
- Sufficiently long test section to allow pressure taps to be placed in ideal locations.
- In situ debris bed height measurements.

This loop was assembled on the main floor level of the 336 Building high bay. The overall height of the test loop is 36 ft. The loop is accessible at four levels.

An overview of the large-scale loop design is presented in Section 2.4.1. The test section containing the test screen and pressure taps is described in Section 2.4.2, and the debris injection system is described in Section 2.4.3.

2.4.1 Large-Scale Loop Description

The initial specifications for the large-scale test loop included a 10-in.- (25-cm-) diameter test screen and a maximum screen approach velocity of 2 ft/sec (0.6 m/s), which would have required a flow rate of 490 gpm (3.1E-2 m^3/s). After design and procurement activities for the test loop had been initiated, the NRC made changes in loop performance specifications. The final requirements specified a test screen diameter of 6 in. (15 cm) and a maximum screen approach velocity of 2 ft/sec (0.6 m/s), which requires a flow rate of 180 gpm (1.1E-2 m^3/s). The initial flow rate requirements specified were used to size the large-scale loop lines so 3- and 4-in. lines were used to fabricate the main line. For the 6-in. test section, smaller line sizes could have been used. This would increase the velocity in the horizontal runs and reduce the potential for of debris settling.

The final design had a test section ID of 6.065 in. (15.405 cm), matching that of 6-in. Schedule-40 pipe. The test section is described in detail in Section 2.4.2. The maximum flow rate of the system was not determined due to the range selected for the mass flow meter. A flow rate of 240 gpm (1.5E-2 m^3/s) was achieved with just the test screen in place and no debris material. A 25 hp (19 kW) centrifugal pump driven by an electronic VFD provided motive power for the loop. The pump was located on the ground level at the lowest point in the system. The pump had a 3-in. inlet and a 1.5-in. discharge. Immediately downstream of the pump discharge, the discharge line expanded to 3-in. pipe.

Other than the 6-in. piping of the test section, the main loop consisted of 3- and 4-in. piping and 3- and 4-in. flex hose. All piping was 304-stainless steel. Main loop flex hoses were Goodyear Flexwing™ White, Hi-Temp (FDA-3A), with 3-in. (8 cm) and 4-in. (10 cm) ID, chosen for its pressure and temperature ratings. Fittings were stainless steel, aluminum, or brass.

Observations and measurements made during preliminary testing in the benchtop loop indicated that debris was readily deposited in any small crevices or behind discontinuities in the pipe wall. Negligible quantities of debris were observed to settle in or adhere to continual lengths of piping or hose. The deposited material was an issue at joints and couplings. The deposited debris was not readily resuspended or flushed from the system; therefore, the design of the large-scale loop attempted to reduce available locations for debris deposits. Most of the pipe fittings were butt-welded, and where flanges were required, custom-cut Gorlock gaskets were used.

Several 3-in, full-port ball valves were installed for isolating various portions of the loop. These ball valves are manipulated during filling, draining, and debris bed retrieval operations. During test operations, the three valves used to control flow through the filter unit and by-pass line were manipulated as needed to either the "full-open" or "full-closed" position. The ball valve just downstream of the pump was maintained in a partially closed position to provide additional backpressure to the pump to eliminate cavitation. All of the other main-line ball valves remained full open during testing.

Downstream of the pump discharge was a 4-in. stainless steel pipe vertical riser with clamshell band heaters attached. The band heaters provided a maximum output of 32 kW. Heater control was via a Chromalox 1601E temperature controller and a Chromalox 10100 over-temperature controller mounted in a cabinet, which were controlled by means of the time-proportional on-off method.

The 4-in. vertical riser transitioned to horizontal pipe via 4-in. flex hose at the top of the test loop where the debris injection lines were located. The debris injection lines are described in Section 2.4.3. The upper horizontal portion of the loop was a combination of 4-in. pipe and flex hose and contained the expansion tank and main-line throttle valve, a 4-in. neoprene pinch valve. The water flow rate through the test screen was controlled by varying the output frequency of the VFD and/or by throttling the 4-in. pinch valve. The pinch valve allowed throttling without any internal parts that may collect debris material.

The expansion tank allowed for fluid expansion and contraction and was connected to the highest point of the loop. Static line pressure in the loop was controlled by means of adjusting the headspace pressure in the expansion tank using an argon cover gas. The argon cover gas was used to reduce the dissolved gas in the working fluid.

The downstream side of the upper horizontal portion of the loop connected to the vertical test section fabricated from 6-in. Schedule-40 pipe. The transparent portion of the test section containing the test screen was accessible from the first level. At the discharge of the vertical test section, the line size reduced to 3-in. piping, which contained the main loop flow meter. A Micro Motion CMF-300 Coriolis flow sensor measures mass flow rate and density in the main line.

Downstream of the flow sensor was a filter with a bypass loop. The filter unit contained an 8-in.-diameter filter bag housing with 4-in. pipe flanges. The filter housing was connected to the main line with custom machined blank flanges to reduce potential crevices; 10-μm filters were used in the filter housing. The bag filters were dried at 194°F (90°C) and then weighed prior to installation in the loop. Following test operations, the bag filters were removed and dried to determine the mass of debris filtered from the loop. During formation of the debris bed, the filter was "valved-out" of the loop to allow debris to circulate and be captured by the test screen. Following the formation of the debris bed, the flow was increased to 0.2 ft/sec (0.06 m/s) and passed through the filter to remove suspended debris. Filtering the flow after bed formation reduced the amount of debris that could be added to the debris bed after steady-state measurements were initiated. The filter unit was also used to polish the test fluid before initiating a test.

No filters existed in the loop during the Series-1 tests; the discharge of the flow meter was connected via 3-in. flex hose directly to the pump inlet. The filter unit and associated by-pass line were installed prior to the Benchmark tests.

Between the discharge of the test section and the inlet of the pump, several drain ports are provided for filling and draining the loop. Figure 2.6 is a schematic of the large-scale test loop.

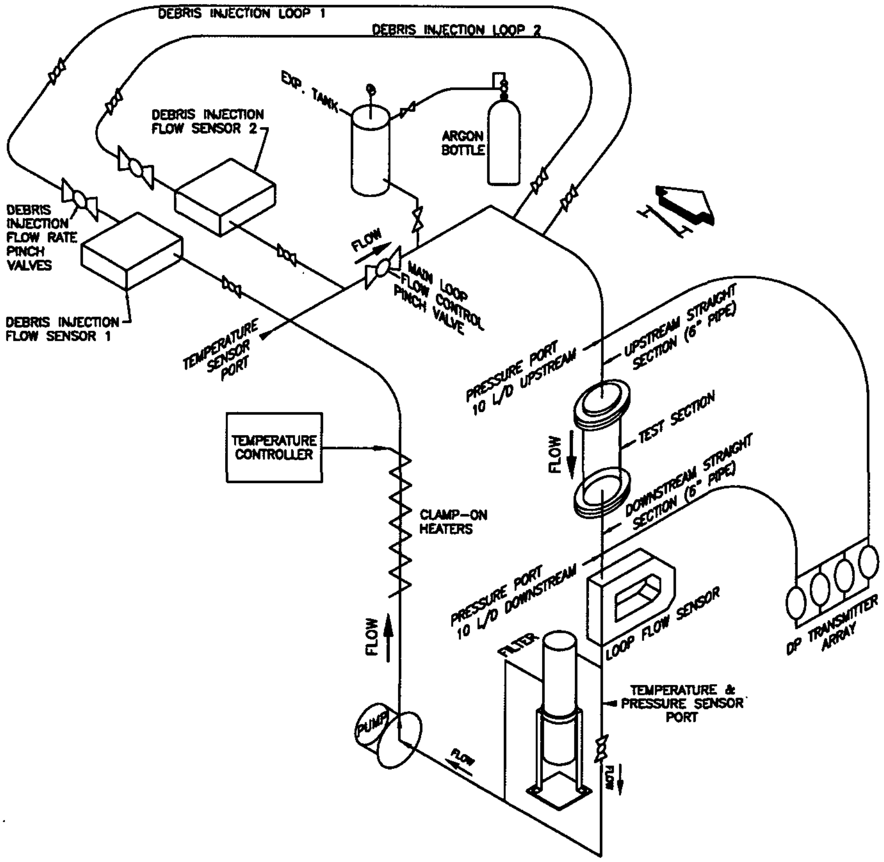

Figure 2.6. Large-Scale Test Loop Schematic (see Appendix B for detailed drawings of the large-scale loop configuration)

2.4.2 Test Section

The test section consisted of the entire vertical run of 6-in. pipe and contained the upstream section, the transparent test section (TTS), which housed the test screen, and the downstream section. The upstream and downstream sections were fabricated from seamless Schedule-40, 6-in., 304-stainless steel pipe. Inside flange welds were butt type with no annular gaps or protrusions to disrupt flow or collect debris material.

The upstream straight section was 9.7 ft (2.96 m) long, allowing for at least 20 L/D of straight pipe to allow a fully developed flow profile to exist upstream of the test screen. The downstream section was 5.6 ft (1.71 m) long, allowing 12 L/D of straight pipe prior to a reduction in pipe size.

The TTS was machined from 8-in. round stock of polycarbonate. The ID was machined to match that of Schedule-40, 6-in. pipe. The test section was designed for operations at 150 psi (1034 kPa) and 200°F (93°C), resulting in a wall thickness of 0.87in. (2.21 cm). Three TTSs were fabricated, allowing the entire section to be removed from the test loop with the debris bed intact and another clean unit to be installed immediately.

The TTS consisted of two parts, an upstream portion and a downstream portion, which cradled the test screen assembly in a socket in the top of the downstream portion. The two halves of the TTS were clamped together by threaded studs and nuts, securing two modified 6-in., 150# blind flanges. These flanges also mounted the TTS assembly to the upstream and downstream straight pipe sections. Photos of the large-scale TTS are presented in Figure 2.7, and the dimensions and assembly details are presented in Figure 2.8.

To obtain pressure drop measurements across the debris beds, ports were drilled and tapped for 1/8-in. national pipe thread (NPT) in the upstream and downstream test sections. At axial locations for the pressure ports. a port was drilled and tapped on each side of the pipe to form a set. The ports were then connected as needed to the manifold for the pressure transmitter array. In the upstream section, ports existed at locations of 2, 5, and 10 L/D upstream of the test screen. Initially it was anticipated that debris beds several inches thick would be generated. To allow pressure measurements to be taken 2 L/D upstream of the debris bed surface, five additional sets of ports were located at 2-in. (5.1-cm) increments upstream of the port located 2 L/D from the surface of the test screen for a total of eight sets of ports upstream of the test screen. In the downstream section, the ports existed at locations of 5 and 10 L/D downstream of the test screen.

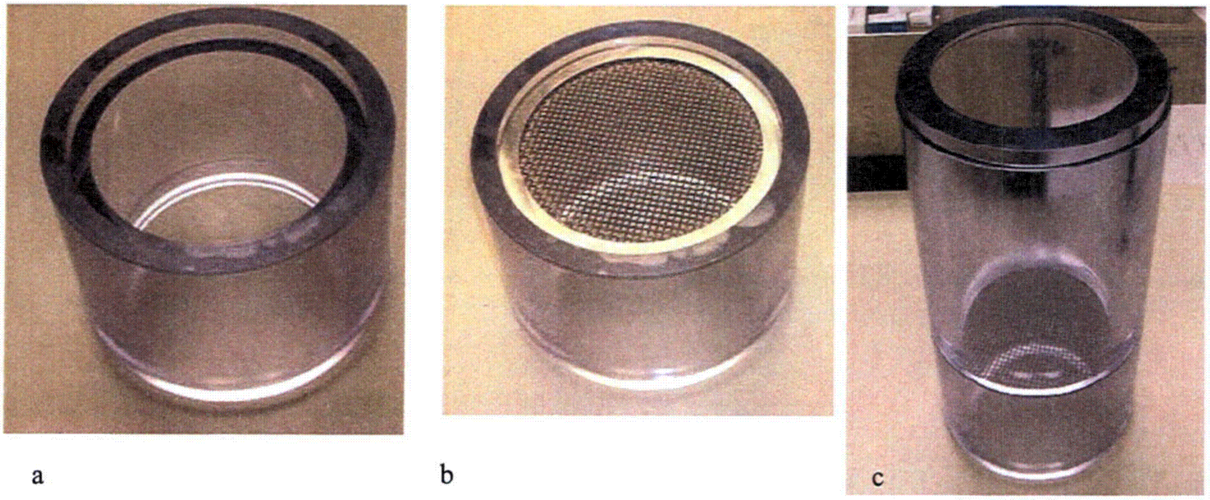
a b c

Figure 2.7. Large-Scale Transparent Test Section: a) downstream (bottom) section with no screen assembly, b) downstream (bottom) section with screen assembly installed, c) assembled test section.

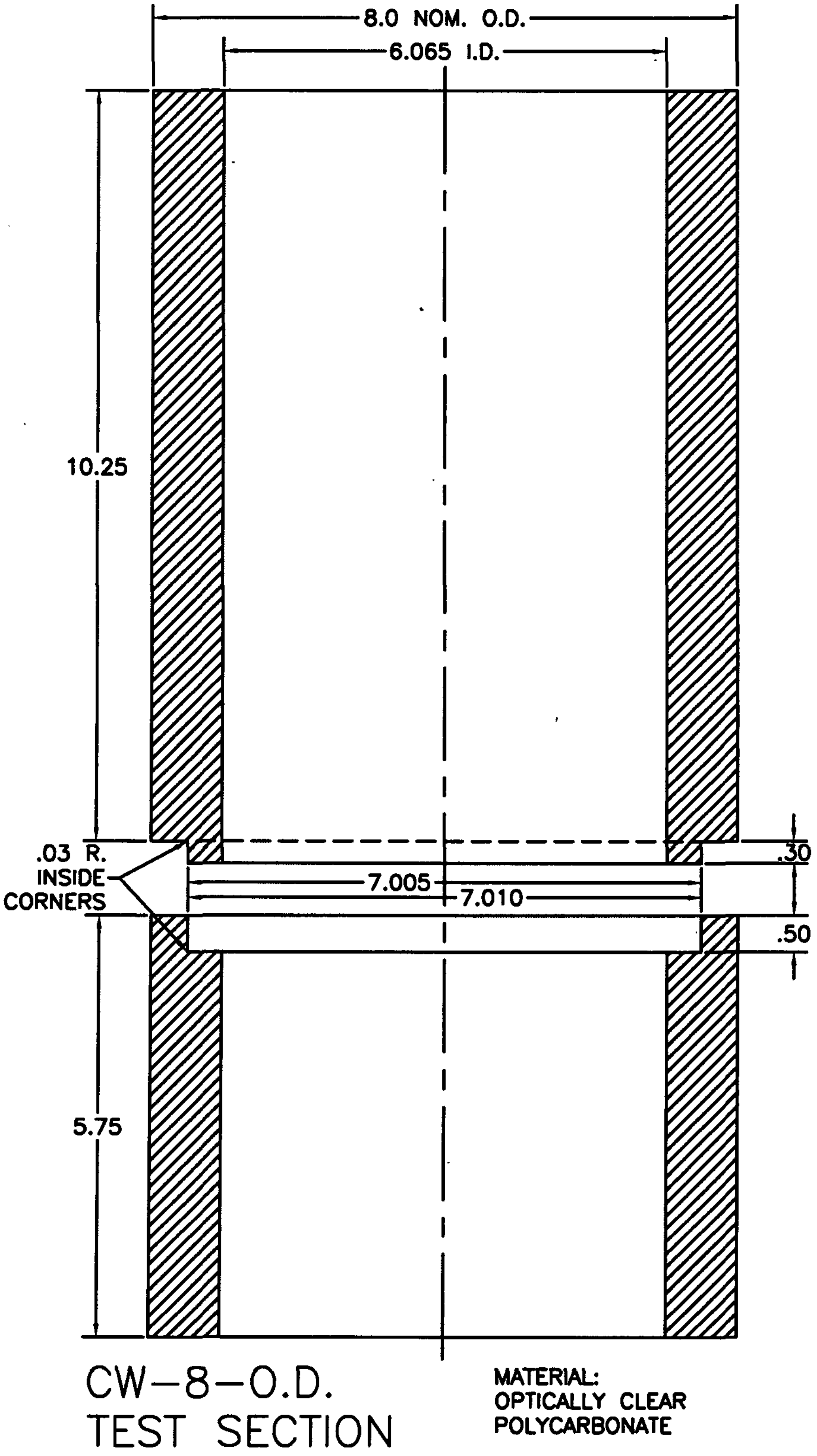

Figure 2.8. Schematic Detailing the Dimensions of the Transparent Test Section

2.4.3 Debris Injection System

To reduce the variability associated with debris bed formation, a debris injection system was developed for introducing debris material into the loop in a manner that could be controlled and repeated. The debris injection system was also designed with the option to introduce debris constituents separately so that they did not mix until after they had been introduced into the test loop. The debris injection system and associated procedure (Section 5.3.1) were developed concurrently.

Significant factors that were taken into consideration in designing the debris injection system included:

- The consistency of the rate at which debris material was introduced into the test loop. The objective was to introduce the debris into the loop at a relatively constant rate to avoid highly concentrated slugs of debris material reaching the test screen. The main reason to avoid slugs of high debris concentration is the difficulty associated with reproducing the flow of debris to the screen from one test to the other. The concentration at which the debris arrives at the test screen may also affect the formation of the debris bed and its resulting structure.
- The ability of the debris injection system to deliver all of the prepared material to the loop. It was desired that no residual debris be left in the injection system.
- No agglomeration of debris in the injection system. Initial work with NUKON demonstrated that if prepared debris was allowed to settle the material would clump, changing its behavior.
- Maintaining debris concentrations in the debris injection system of less than 7.4 g of debris per liter of water (personal communication from BC Letellier, LANL, to CW Enderlin and F Nigl, PNNL, June 17, 2005, providing guidance for concentrations of debris used for blending during debris preparation and debris introduction into the loop).

The final method of debris injection consisted of filling a transparent flexible hose with prepared debris and then connecting the flexible hose to a line that bypassed the main throttle valve. By diverting a portion of the main-line flow through the injection line, the debris material was introduced into the main line. This type of system was originally developed for the benchtop loop and proved very successful in generating debris beds that yielded repeatable head loss test results.

The debris injection system consisted of two parallel, identical lines located on the third level, 29.5 ft above the main floor. Two loops facilitated simultaneous or phased injection of two different debris recipes. The upstream end of an injection line was 1-in. piping and contained in series a Micro Motion CMF 100 Coriolis mass flow sensor, a 1-in. ball valve, and a 1-in. pinch valve. Downstream of the injection-line pinch valve was a 2-in. ID, 13.3-ft- (4.1-m-) long transparent flex hose connected to the loop via isolation valves (1-in. ball valves) and Camlock quick-disconnect fittings. The transparent hose was Kuriyama Tigerflex^{TM} Series WH PVC hose with a rated working pressure of 35 psig (241 kPa) at 68°F (20°C). The schematic of the large-scale test loop shown in Figure 2.8 includes the debris injection lines.

The mass flow sensors installed in each injection line allowed precise monitoring of the injection line inlet mass flow rate. The original design had the mass flow sensors located at the discharge of each debris injection line to monitor the rate at which debris entered the test loop. However, testing of this configuration in the benchtop loop demonstrated that the flow path through the smaller range mass flow sensors could result in the accumulation of debris and even plugging. Therefore, the mass flow meters were located at the upstream end of the injection lines to monitor the inlet flow rate.

Testing in the benchtop loop determined that a fluid velocity of 0.8 ft/sec (0.2 m/s) through the injection line hoses was sufficient to mobilize the debris for the range of NUKON/CalSil loadings prescribed in the proposed test matrix.

The main-line pinch valve was used to adjust the flow rate through the debris injection lines. The main-line pinch valve was partially closed to generate backpressure to drive flow through the injection line. The main-line and injection-line pinch valves were adjusted in combination to obtain the desired debris bed formation velocity at the screen and the desired velocity through the injection lines. The ball valves allow the injection line to be isolated when the flexible hose was disconnected.

The size and length of the flexible hose was selected based on:

- The physical location of the upstream and downstream connections to the main line. The space limitations of the platform dictated the configuration of loop components, which generated a minimum distance that had to be spanned by the debris injection line hose.
- The need to produce a velocity of 0.8 ft/sec (0.2 m/s) in the injection line while generating a screen approach velocity of 0.20 ft/sec (0.06 m/s) during debris bed formation (the debris bed formation velocity was later reduced to 0.10 ft/sec (0.03 m/s) by the NRC, as discussed in Section 5.3).
- Ensuring that a maximum debris concentration of 7.4 g of debris per liter of water was not exceeded for any case in the test matrix.

The flexible hose could be manipulated manually to disperse the debris within the hose and prevent the material from settling between the time of loading and the time flow was initiated (usually only several minutes). The transparency of the hose allowed the following:

- Observation to ensure the debris was distributed throughout the length of the hose.
- Determination of whether settling or clumping of the debris was occurring and if additional agitation was required.
- Determination of the time at which the debris was completely discharged from the injection line.

Because of its low temperature and pressure ratings, the transparent hose was isolated prior to increasing the static pressure of the loop or heating the loop. For the tests conducted with the debris injected at an elevated temperature, 2-in. Goodyear Flexwing^{TM} White, Hi-Temp (FDA-3A) hose replaced the transparent hose.

2.5 Instrumentation and Measurements

Experimental data were obtained from manual measurements, digital readouts, electronic outputs captured on a data acquisition system (DAS), post-test analysis of digital photographs, and scanning electron microscopy (SEM). The DAS and electronic instrumentation connected to the large-scale loop are described in Section 2.5.1, and the instrumentation connected to the benchtop loop is described in Section 2.5.2. Additional instrumentation used to support the experimental loops is discussed in Section 2.5.3. Section 5.4 presents post-test measurements and the analysis associated with optical triangulation to determine in situ debris bed heights, ion selective probe readings to determine the mass of CalSil within debris beds, and SEM to assess the debris bed structure. Refer to Appendix C for the detailed project measurement and testing equipment (M&TE) listings.

2.5.1 Large-Scale Test Loop Instrumentation and Data Acquisition

The DAS recorded the following large-scale loop measurements to an electronic file:

- Specific gravity of the main-line flow
- Mass flow rate through the test screen. The mass flow rate and fluid density were used to calculate the screen approach velocity.
- The pressure drop across the debris bed/test screen.
- Fluid temperature
- Mass flow rate entering each debris injection line
- Specific gravity of the flow entering each debris injection line.
- The main line pressure
- Ambient temperature
- Temperature of the differential pressure (DP) manifold tube bundle for assessing temperature corrections.

The DAS computer and associated hardware are presented in Section 2.5.1.1 and the instruments connected to the DAS in Section 2.5.1.2. Large-scale M&TE are listed in Appendix C.

2.5.1.1 Large-Scale Test Loop Data Acquisition System

A personal computer (PC)-based DAS with a standard Dell tower model GX280 was used for the project. The operating system was Microsoft Windows XP® Professional.

Signals from instrument sensors were first fed to industry-standard 5B analog signal conditioning modules mounted on motherboards designed to accept them. Specific versions of 5B modules were available for input voltage, current, thermocouple (TC), and resistive temperature device (RTD) signals. 5B32-02 modules were used for signals transmitted on standard 4~20 mA current loops. All sensors except the three TCs used 4~20 mA loops. Type J TC signals were handled by 5B47J-02 modules. All 5B modules used in the system output in the 0~5V range, which was linearly proportional to the input range of the module. Voltage signals from the 5B modules were fed to the PC-based DAS. The analog-to-digital (A/D) converter circuit board was a Measurement Computing PCI-DAS6402-16. This 16-bit peripheral component interconnect bus board could handle up to 64 analog input channels.

The DAS software was DasyLAB 7, a flexible, graphical user interface based system. Individual signals were sampled by the 6402 board at a 100-Hz rate. Each input signal was run through a running 1-second average and scaled to engineering units. Signals were displayed on meters or charts, run though specific calculations, and logged to an ASCII text data file that facilitated post-processing and analysis using Microsoft Excel® and other software. Appendix D contains screen prints of the worksheet layout.

The DAS software was also used to perform real time calculations to assess the data with respect to meeting the steady-state criterion (see Section 5.3.). The value of the acceptance criterion was displayed on a DAS meter and could be readily evaluated by the test operators.

2.5.1.2 Large-Scale Test Loop Instrumentation

The mass flow rate and specific gravity were measured using Micro Motion Elite series Coriolis mass flow (CMF) sensors. A CMF 300 sensor measured flow in the main loop downstream of the test section, and a CMF 100 sensor in each of the two debris injection loops measured the injection line inlet mass flow rate and specific gravity. Transmitters for these sensors were Micro Motion model RFT 9739. An Ametek 88F005A2SCSSM pressure transmitter sensed the line pressure at the lower elevation of the loop.

Four Rosemount 115-series DP transmitters were connected to a DP valve manifold that facilitated quickly valving in or out (bring on- or off-line) individual transmitters based on the magnitude of the pressure drop across the test screen or flushing gas bubbles from the DP manifold and associated tubing. The array of DP transmitters had ranges of 5, 30, 150, and 750 in. of H_2O.

Temperature sensors monitored temperature in the top and bottom of the loop, ambient air temperature near the top of the loop, and the temperature of the bundle of DP lines near the DP manifold. The upper loop sensor was an RTD, while the others were Type J TCs. Further details for the large-scale instrumentation can be found in the M&TE listing in Appendix C.

2.5.2 Benchtop Test Loop Instrumentation

The same DAS used for the large-scale test loop was also used for the benchtop loop. Different analog input channels were allocated for the large-scale and benchtop loops. Two versions of DasyLAB worksheet or setup files were produced, one to acquire and process the benchtop instrument signals and the other for the large-scale instruments. Appendix D portrays the graphical layout of the benchtop DAS worksheet. Benchtop instruments connected to the DAS were:

- Micro Motion D100 Coriolis mass flow sensor sensing main loop flow rate and fluid density
- Micro Motion DH03S Coriolis mass flow sensor sensing debris injection loop-1 flow rate and fluid density
- Micro Motion DH025S Coriolis mass flow sensor sensing debris injection loop-2 flow rate and fluid density
- Honeywell Y41104 DP transmitter with a span of 1000-in. H_2O sensing DP across the test screen
- Type J TC sensing loop fluid temperature.

Each of the Micro Motion sensors was connected to Micro Motion RFT9739 transmitters that perform calculations and produce 4~20 mA analog outputs.

2.5.3 Additional Instrumentation and Equipment

To conduct the tests and evaluate the debris material and debris beds, additional instrumentation that was not connected to the DAS computer was used. This section provides an overview of the instrumentation and equipment that is not discussed in other sections.

Several laboratory benchtop digital scales were used for taking general mass measurements such as mass of debris constituents and dry debris beds. The Sartorius BP 3100 S was the most frequently used scale for debris preparation.

Manual measurements of the debris bed under flow conditions in the large-scale loop were made with a tape measure fastened to the outside of the test section. The zero of the scale was aligned with the top of the screen assembly ring. More substantial in situ bed height measurements were taken using optical triangulation (Section 2.5.4.1). Post-test measurements of the debris bed height were made using a commercially available ruler with centimeters and millimeter graduations. With the retrieved debris bed in the TTS, a straight edge was placed across the top of the test section and the measurements made by lowering the ruler into the test section until it touched the debris bed. Section 5.3 contains details of the post-test bed-height measurements.

Relative moisture content measurements of the debris beds were taken using a Delmhorst BD-2100 moisture content probe (property No. 35519). These measurements were taken for managing the drying of the debris beds and to obtain comparative measurements. These measurements were taken and recorded for indication only and are not reported.

Particle size analysis was performed with an S3000 Microtrac particle size analyzer (ID No. N830468) per PNNL Waste Treatment Plant procedure TPR-RPP-WTP-222, Rev. 2 (2005). A variable-speed recirculating pump setting of 45 was used for the measurements. An Ultrameter II 6P Serial No. 6203236 was used to monitor the conductivity of the large-scale test loop water.

To prepare the debris materials, blenders and a 3-in. ceramic mortar and pestle were used to disassociate or break up the debris material from its as-received condition. Four blenders were used in the course of the test program; three Waring (7011HS Model HGB2WTS3) commercial blenders and one Kitchen Aid (Model KSB50B4). The blenders were not interchangeable. The Waring blenders were designated 1, 2, and 4 (see Appendix C). Section 3.2 contains a discussion of the blender effects on debris preparation.

Still and video digital cameras were used to photograph various aspects of testing including debris bed formation. Appendix C shows details.

2.5.4 Supporting Post-Test Measurements

Following the completion of tests and the drying of debris beds, additional evaluations were performed on selected debris beds. This section describes the three main activities of:

- Obtaining in situ debris bed height measurements using optical triangulation. Following the Series-1 tests, a system was developed and installed as part of the large-scale transparent test section that allowed digital pictures to be taken with an array of spaced lines projected across the surface of the debris bed. Post-test analysis of the pictures allowed the bed height and topography of the debris bed to be determined. The test procedures, Section 5.3, called for taking the optical triangulation pictures at each steady-state test condition. However due to cost constraints, post-test analysis was only conducted on a limited set of photos. Section 2.5.4.1 explains the methodology used to obtain the bed height measurements, and Section 7.0 presents the results.
- Assessing the CalSil mass contained in debris beds consisting of both NUKON and CalSil. A procedure was developed for dissolving the debris beds and determining the mass of CalSil retained

in the bed based on relative measurements of CalSil performance standards (mixtures containing known masses of CalSil) obtained with a Ca^{++} ion selective electrode (ISE). An overview of the method is discussed in Section 2.5.4.2.

- To assess the structure of debris beds formed under selected conditions, these retrieved beds were prepared and sectioned for imaging by SEM. Section 2.5.4.3 discusses the preparation and scanning of the debris bed sections.

2.5.4.1 Debris Bed Height Measurements Using Optical Triangulation

The NRC wanted debris bed heights to be measured as a function of velocity throughout the test without disrupting the flow upstream of the debris bed. Optimally, this objective would involve measuring the topography of the debris bed. The transparent test section allowed manual measurements to be made by visually sighting across the top of the debris bed and estimating the elevation using a scale fixed to the pipe wall. However, manual measurements were complicated by the existence of a raised rim of deposited debris material that formed at the wall of the test section around the entire outer edge of the debris bed. The fluid velocity profile across the test section along with the characteristics of the fiber debris contributed to the formation of a raised rim. For debris beds of smaller mass loading with less pronounced rims, the position of the interface between the two halves of the TTS and the associated gasket interfered with manual measurements.

PNNL investigated using ultrasonic and optical methods and had the greatest success using optical triangulation, which is an established method to determine the position of an object. A schematic describing the technique is presented in Figure 2.9. A light beam shines on a surface and is imaged onto a detector array. As the surface position (i.e., debris bed thickness) changes, Δz, the image of the reflected beam, moves on the detector, Δx. The light beam could be a white light source or a laser beam and can be a dot, a line, or an array of dots or lines, depending on the item to be measured. The detector array can be a linear detector or a two-dimensional array (video camera). The sensitivity of the technique depends on the angle between the input beam and the detector, the size of the pixels in the array, and the focal length of the imaging lens.

For the tests performed in this study, a series of light and dark lines on a grid (50 lines per inch) was projected onto the test bed through the TTS. The detector was a video camera. The camera detector array was 3264 x 2448 pixels. Figure 2.10 is a diagram of the test setup, and Figure 2.11 presents pictures of the system installed on the test bed. The light source and digital camera were attached directly to the test section to reduce any relative motion of the debris bed and camera. In the course of the testing, several changes had to be made to the setup. For example, the camera position had to be moved back and made more secure so it would not be in the way during loading and unloading operations. Also, the light source had to be raised to minimize the shadow of the rim on the test bed. The position of the camera was changed to minimize the obscuration of parts of the debris bed due to the support posts.

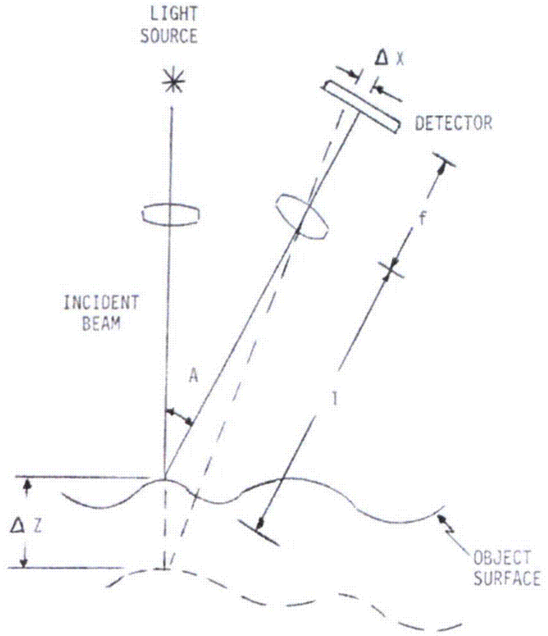

Figure 2.9. Schematic of the Optical Triangulation Technique

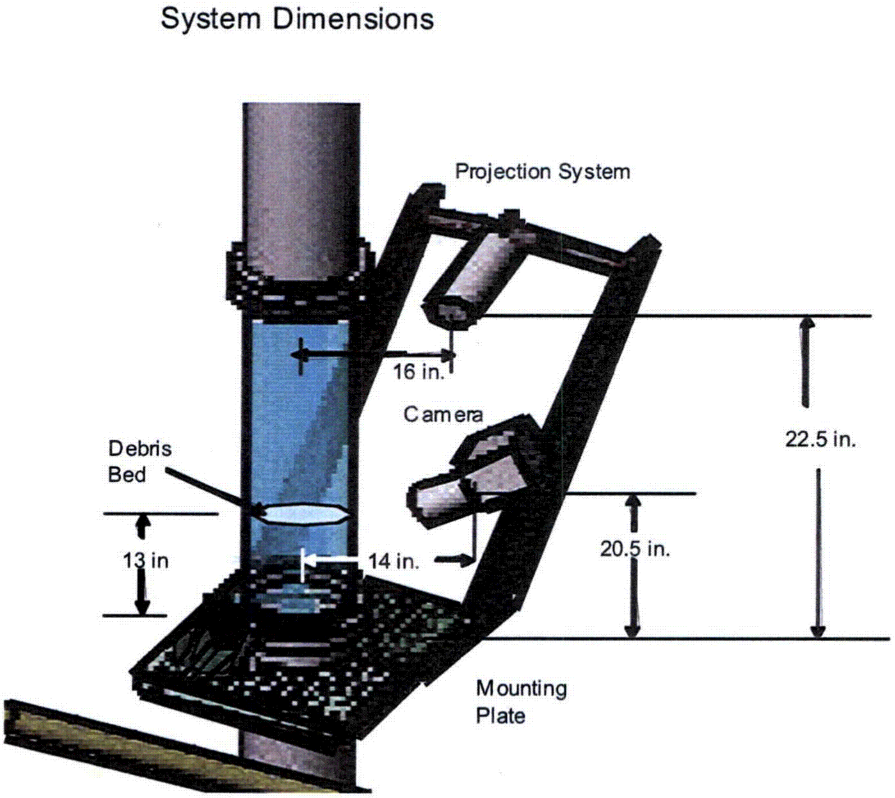

Figure 2.10. Schematic of Plan View Setup of Optical Triangulation System for Large-Scale Test Loop

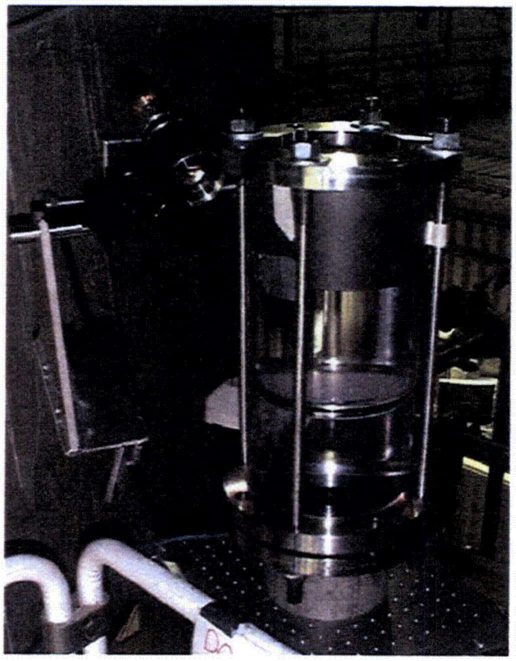


Figure 2.11. Photos of Optical Triangulation System Installed on the Large-Scale Test Loop

To determine the thickness of the debris bed, it was necessary to calibrate the system. A calibrated step wedge, shown in Figure 2.12, was placed in the system, and a picture was taken with the same setup as was used when the actual unknown debris beds were measured. From this calibration, the amount of movement (in camera pixels) that corresponds to a certain height of the debris bed can be correlated. Additional reference points were provided by a line placed on the inside of the TTS at a measured height of 1.6 in. (40 mm) above the screen and the interface 0.4 in. (10 mm) above the screen where the top and bottom pieces of the TTS meet. When possible, the rim height from the manual measurements was also provided as an additional reference. These values allowed a calibration constant to be determined over a wide range of thicknesses. Based on this calibration wedge, the resolution of the system was determined to be 0.025 in. (0.63 mm).

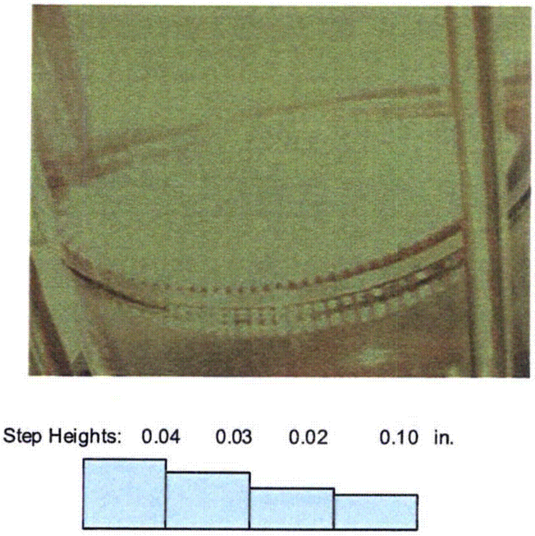

Figure 2.12. Calibration Wedge Used for the Optical Triangulation System

To measure the bed height, digital photos of the debris bed with the set (grid) of lines projected across the bed surface were taken at each test condition after a steady-state pressure drop had been achieved. The distance from the edge of the debris bed to the reference elevations on the inside of the pipe wall were determined (in camera pixels) and then translated through the calibration constant to an edge height. Similarly, the distance to the edge of the bed plane (flatter area of the bed surface inside the outer rim) was determined. By using the projected grid lines, one could determine the change in bed height from the edge to any point on the bed.

The analysis could not be performed if the complete surface of the debris bed was not in focus. Occasionally, changes in lighting or suspended debris caused a change in focus, resulting in some photos being corrupted with respect to the optical triangulation analysis.

2.5.4.2 Assessment of CalSil Mass in Debris Beds

The CalSil mass in debris beds was assessed using chemical dissolution and calcium ISEs. The CalSil insulation material used for testing was primarily composed of calcium silicate. By dissolving the entire debris bed in hydrochloric acid (HCl), the concentration of the calcium ions was detected by the ISE probe. The potential (millivolts) measured by the probe were correlated to a CalSil concentration.

Probe readings are not fixed in relation to Ca^{++} concentration. The readings may vary with time, temperature, and probe usage. Thus, the Ca^{++} concentration readings of unknown CalSil masses in debris bed samples were compared to a performance curve, which was a curve fit of Ca^{++} concentration readings to CalSil masses of performance curve samples. The performance curve samples consisted of known CalSil masses. Because of the potential shift of the performance curves with changes in time, temperature, and probe usage, the performance curve standards were generated at approximately the same time that the debris beds were dissolved. The ISE readings for the performance curve samples were taken each time readings were made of debris bed samples.

Before taking measurements using the ISE probe, the dissolved CalSil and debris bed solutions were diluted in deionized (DI) water, the pH was adjusted to 7, and ionic strength adjuster (ISA) was added. The dilution, pH adjustment, and ISA were added to obtain better results with the ISE probe.

2.5.4.3 Debris Bed Sectioning

To perform SEM analysis of a debris bed, the bed must first be dried, impregnated with an epoxy resin, and sectioned. The sectioned sample is then polished to provide a uniform smooth surface for SEM analysis. For this process the debris bed was not removed from the screen, and the screen material was also sectioned.

After a debris bed was retrieved from the test loop, it was dried in an oven at 194°F (90°C) until constant mass readings were obtained. For impregnating the debris bed with epoxy, a rubber mold was fabricated to hold the debris bed and test screen. Because of the weak structure of the debris bed, care was taken not to distort it while adding the epoxy. The epoxy was poured into the mold and degassed by placing it in a vacuum chamber to remove as much air as possible. The debris bed was then carefully lowered into the mold, taking care to not disturb the bed or entrap additional air in the epoxy. The epoxy filters into the debris bed and was then allowed to set at room temperature, which required several hours.

After the epoxy was set, forming a solid disk, the disk was cut using a circular saw with a silicon carbide abrasive disk. The bed was cut along two lines running through the center of the bed: one along the center wire of the 5-mesh woven-cloth screen (Section 2.2), and the other cut along a diagonal with respect to the screen grid. A thin section was taken from along each cut and mounted. Because of the fragile nature of the debris bed, the entire bed could not be placed in a vacuum chamber to remove all of the trapped air. Therefore, the surface of the slice was examined to find a section with no or minimal air pockets. The surface was then polished and examined.

A JEOL GSM-5900LV SEM was used to obtain detailed images of the debris bed structure and identify any distinct regions. The technique used was backscattered imaging at 20 kV and 100X magnification. Images were also taken at higher magnification as needed to examine the detailed structure of regions of interest. A series of images was taken traversing the height of the debris bed and along the top surface for each sample. The images in each series were relatively evenly spaced. The preliminary analysis performed on the selected images is presented in Section 6.5.

3.0 Test Debris Preparation

Debris bed head loss testing at PNNL was conducted using both NUKON and CalSil insulation. To introduce the debris to the test loop, NUKON and CalSil slurries were prepared. The target NUKON and CalSil slurry criteria, characteristics, quantification methods, and associated evaluations are elucidated in this section. The proposed test matrix specified target debris loadings in terms of mass of debris constituent per unit area of screen. The target mass loading was used to determine the amount of material to introduce to the test loop. Because all of the debris material was not necessarily retained on the screen, the target mass loadings generally differ from the retained mass loadings.

The debris material received for the formal testing conducted by PNNL was the following:

- NUKON material received from Performance Contracting Inc., Lot No. 09/06/5ND5, BS-4813, shipped on 10/8/05. The vendor/manufacturer subjected the NUKON to a 12- to 14-hr heat-treating process and then shredded the material in a wood chipper prior to shipment. G. Hunter, of Performance Contracting Inc., described in phone conversations to Carl Enderlin of PNNL the heat-treating process and "average effective fiber diameter." The fiberglass "blankets" were placed in direct contact with a hot plate surface that was maintained at approximately 600°F. During the heat-treating process only one side of a blanket was brought in direct contact with the heated surface. The average effective fiber diameter of the NUKON had been measured by Performance Contracting Inc. at 2.6e-4 in. for virgin material and 2.8e-4 in. for fiber with the binder applied. The effective diameter was determined for a "fiber pack" via an air resistance test to an uncertainty of ± 2E-5 in. and does not necessarily match the physical diameter of the individual fibers.
- CalSil material received from Johns Manville, Lot No. 017-276, BS-4823, shipped on 9/28/05. The CalSil material was not subjected to any heat treatment and was in the form of 3 x 12 x 48-in. blocks.

The debris material used for the preliminary PNNL testing conducted to evaluate the debris preparation methodology as described herein was ordered in June 2005 from the vendors listed above. The initial order of CalSil was from Lot No. H 14 RP. The initial order of NUKON was received in two forms; the 3-in.-thick sheets (blankets) of material were from Lot No. 03/30/4ND5 BS-4700, and the shredded material was not from a specific lot but was made up of leftover materials saved by the vendor for shredding. The material may have been from two to four lots of material.

In Section 3.1, the target slurry criteria and defining characteristics are identified. Testing results for the formation criteria and techniques to quantify these characteristics are presented in Section 3.2, and the debris preparation techniques are summarized in Section 3.3.

3.1 Debris Bed Formation Criteria and Target Characteristics Identification

The debris bed head loss testing at PNNL was conducted to provide data useful for developing and validating a head loss correlation that can be applied in safety basis-type applications for varying debris-loading conditions. To obtain data useful to the development of a correlation, the debris preparation process should produce debris material with an initial condition that can be verified (characterized) and repeated. Failure to do so makes it difficult to determine whether differences in the test results should be attributed to variations in the test parameters or variations in the initial condition of the debris. In Section 3.1.1, the PNNL-defined NUKON and CalSil slurry-generated debris bed criteria are listed.

Guidance for the target characteristics, as defined by previous related work, is discussed in Sections 3.1.2 and 3.1.3 for NUKON and CalSil debris material, respectively. These criteria and target characteristics were agreed to by NRC staff and NRC contracted national laboratories [LANL and Argonne National Laboratory (ANL)].

3.1.1 Debris Bed Formation Criteria

The current debris bed head loss correlation, as presented in NUREG/CR-6224 (Zigler et al. 1995), assumes that the debris bed is uniform in thickness as well as composition. To assess possible accident scenarios, conditions should be created for different debris loading scenarios to provide statistically significant and repeatable results. Additionally, given the safety aspects of the applications of the developed correlations, evaluated conditions should consider the effect of slurry preparation on the resulting debris bed head loss.

The objective of this experimental task was to study debris conditions that form a complete (entire screen covered with debris with no channeling present) debris bed. Obtaining pressure drop measurements for incomplete or partial debris beds was outside the scope of this effort. Elevated pressure drops are present only if a complete debris bed was formed. Consequently, the tested debris beds should have certain standard characteristics that provide repeatable data for developing a method for calculating the pressure drop. Actual debris beds formed in a nuclear plant following a LOCA may not possess these standard characteristics; however, a calculational method can address only known, specified debris bed conditions. Variations from non-standard bed conditions may be handled using probability techniques. The five NUKON and CalSil debris bed formation criteria for the debris beds generated and tested at PNNL are listed below:

1. Material should form a complete debris bed on the specified metal screen or perforated plate.
2. Debris beds should be uniformly thick and internally as homogeneous as possible in the radial direction.
3. Uniform debris beds should be formed over the range of debris loadings specified by the NRC proposed test matrix (NRC 2005).
4. The debris beds generated for a given composition and target debris loading should yield repeatable physical and performance characteristics.
5. The debris beds should meet NRC specifications for debris bed composition and criteria for head loss measurements (e.g., formed at specified bed formation velocity and temperature).

3.1.2 NUKON Slurry Target Characteristics

The target NUKON slurry characteristics provided by investigators from previous related work (Shaffer et al. 2005) were approximately defined by specifying the slurry preparation conditions. These slurry preparation conditions were obtained through personal communications with previous investigators such as B.C. Letellier of LANL. The NUKON slurry preparation was performed using vendor-supplied NUKON material. G. Hunter of Performance Contracting Inc., the supplier of NUKON, stated that the preparation of the shredded NUKON was achieved by passing NUKON "blankets" through a commercially available wood chipper. Mr. Hunter stated that shredded NUKON previously supplied to investigators had been created by passing the blankets through a leaf shredder.

The preparation of the shredded NUKON was defined by previous LANL investigators as follows: 25 g of shredded NUKON and 1,000 mL of water were added to a Black and Decker blender (550W BL6000) operated at the "middle" setting for 10 minutes.

To establish baseline characteristics, PNNL prepared a slurry consisting of 25 g of wood-chipper-shredded NUKON and 1,000 mL of water in a Waring commercial blender (model 31BL41, 840 W) operated for 10 minutes on the "low" setting. The slurry was poured through an 8-in.-diameter 5-mesh screen. The material retained on the screen as well as the collected material that passed through the screen were dried and weighed separately. The required blender preparation time and NUKON mass/water volumes were subsequently evaluated.

The results of the preliminary NUKON slurry preparation tests are presented in Table 3.1. In this table, as well as in all subsequently presented results of Section 3, the practice of maintaining the significant digits in numerical values is not followed.

Table 3.1. Preliminary NUKON Slurry Preparation Tests

Test	Initial NUKON Mass (g)	Water Vol. (mL)	Prep. Time (min)	Blender Speed	Dried NUKON on Screen (g)	Dried NUKON Through Screen (g)	R1	R2	R3
NS2	25	1000	10	low	18.03	4.83	0.72	0.19	0.27
NS3	25	1000	3	low	18.64	4.69	0.75	0.19	0.25
NS4	12.5	500	10	low	7.72	3.4	0.62	0.27	0.44
NS5	12.5	500	3	low	8.99	1.86	0.72	0.15	0.21
NS6	12.5	500	3	high	8.82	2.8	0.71	0.22	0.32

Test NS2 used the same debris concentration, water volume, and blender time in an attempt to mimic, as closely as possible, the NUKON slurry preparation definition provided by LANL investigators, and replicate the baseline test.

Although no metrics were provided from the previous work for characterizing the prepared debris material, the current results were quantified by measuring the mass after drying of both the NUKON on the screen and the mass that passed through the 5-mesh screen. Visual observations showed that test NS2 produced an apparent homogenous slurry with no clumps. It was expected that a homogeneous slurry would support Criterion 2 from Section 3.1.1. The measured quantities were related to the initial NUKON mass of the test as well as to each other by computing the following ratios:

$$R1 = \frac{dried\ NUKON\ mass\ on\ screen}{initial\ NUKON\ mass} \tag{3.1}$$

$$R2 = \frac{dried\ NUKON\ mass\ through\ screen}{initial\ NUKON\ mass} \tag{3.2}$$

and

$$R3 = \frac{dried\ NUKON\ mass\ through\ screen}{dried\ NUKON\ mass\ on\ screen} \tag{3.3}$$

Before drying, liquid was decanted from the material that had passed through the screen. Thus, the sum of defined parameters R1 and R2 may yield results less than unity due to the loss of suspended fines with the decanted liquid.

Following test NS2, test NS3 was conducted to determine whether shorter preparation times could achieve similar results. It was determined by a comparison of the computed mass ratios in Table 3.1 that the shorter preparation time produced similar slurry and consequently also matched baseline conditions.

The range of debris loadings specified by the proposed test matrix dictated that a lower NUKON mass would be needed. Therefore, test NS4 evaluated the effect of a lower initial NUKON mass. (A secondary consideration for evaluating a reduced amount of slurry was the working capacity [volume] of the blender). A 10-minute blender-operation time (referred to as preparation time) was used, and the ratio of the initial NUKON mass to the water volume was held constant. A lower R1 with higher R2 and R3 values, neglecting the possible loss of fines, indicated that more material passed through the screen; the slurry had changed characteristics (more fines were possibly produced). It was therefore determined that the preparation time was too long to replicate the baseline results, and a reduced preparation time (same as for test NS3) was evaluated in test NS5.

Although metric results similar to the baseline test NS2 were achieved with test NS5, it was determined from R2 and R3 (again neglecting possible decanted fines) that the amount of NUKON that passed through the screen was low (possibly fewer fines were produced), and the "high" preparation speed in the blender was thus considered for test NS6. Metric results for NS6 were determined to be reasonably similar to those for baseline test NS2. The procedure to produce the slurry of test NS6 was therefore chosen as the preliminary procedure to evaluate the potential to achieve Criteria 1 through 5 listed in Section 3.1.1. In subsequent tests in the benchtop loop, this preparation procedure was indeed shown to form and produce uniform debris beds on a 5-mesh screen. Thus, 12.5 g of NUKON and 500 mL of water prepared for 3 minutes on "high" in a Waring commercial blender (model 31BL41) was selected as the baseline slurry to be evaluated in the benchtop loop.

To facilitate slurry preparation and development, a simple metric was developed to relate the slurry preparation to that of test NS6. The metric used wet conditions, relating the NUKON and water mass retained on an 8-in.-diameter 5-mesh screen immediately after the slurry was poured through the screen to the initial dry NUKON mass or

$$R4 = \frac{NUKON\ and\ water\ mass\ on\ screen}{initial\ NUKON\ mass} \tag{3.4}$$

Excess water was removed from the screen before the mass was measured by tapping the screen five times on the rim of the collection container, rotating it 90° counter-clockwise, and then tapping five more times. When pouring the slurry through the 5-mesh screen, care was taken to ensure that the operator continually moved the pour across the screen such that the material was continually poured onto an unused (clean) portion of the screen. After the bulk of the slurry was poured out, sufficient water was added to the blender (on the order of 100 mL) to flush all of the debris material out and through the screen. The R4 procedure is presented in detail in Appendix E.

The value of R4 was determined for the Test NS6 NUKON slurry preparation to establish a baseline criterion. The conditions of Test NS6 were reproduced two times, resulting in R4 values of 11.8 and 10.6. The specifics for these tests are reported in Table 3.2.

Table 3.2. NUKON Slurry Preparation Test NS6 R4 Results

Condition/Debris Loading (g/m^2)	**Initial NUKON Mass** (g)	**Water Volume** (mL)	**Prep. Time** (min)	**Blender Speed Setting**	**Mass of NUKON and Water on Screen** (g)	**R4**
Baseline	12.5	500	3	high	147.11	11.8
Test NS6	12.5	500	3	high	132.66	10.6

3.1.3 CalSil Slurry Target Characteristics

As with the NUKON characteristics (Section 3.1.2), the target CalSil slurry characteristics for previous related work (Shaffer et al. 2005) were approximately defined by specifying the slurry preparation conditions obtained through personnel communication with previous investigators such as B.C. Letellier of LANL. The CalSil debris preparation procedure was defined as using a mortar and pestle to completely disassociate the particulate CalSil from the fibrous binder material.

The simple R4 metric developed for the NUKON slurry preparation (Eq. (4)) was used to provide a rapid means of approximate quantification of the CalSil slurry preparation. Visual observation of the prepared CalSil material was also made such that it appeared to be relatively homogenous with no clumps. The disassociated fibrous material was visually observable. As with NUKON, homogeneity was expected to support Criterion 2 from Section 3.1.1.

To establish a baseline criterion, an R4 value was determined for CalSil material that was first disassociated by using a mortar and pestle and then wetted. Particle size distribution (PSD) analyses were subsequently conducted on the debris after being further fragmented in a blender. Evaluations of the effects of CalSil debris preparation techniques have also been made using various sieves. The baseline preparation conditions as well as results from the additional analyses are presented in Section 3.2.2.

3.2 Target Characteristics and Formation Criterion Testing

NUKON and CalSil materials were prepared to meet the target characteristics defined in Section 3.1. These prepared materials were then evaluated in regards to meeting the five criteria listed in Section 3.1.1. Actual debris masses for all target debris loadings presented herein correspond to the 4-in. test section of the PNNL benchtop loop. In Section 3.2.1, target characteristic testing of the NUKON slurry is discussed. CalSil debris preparation is discussed in Section 3.2.2. In Section 3.2.3, the prepared slurries are tested against the five debris bed criteria. Testing against these criteria was conducted in the PNNL benchtop loop. Note that the benchtop loop does not have the degassing capability of the PNNL large-scale loop; the quantity of gas in the test section was visually observed to vary to some degree between the test cases. The instrumentation in the benchtop loop had greater uncertainties and less resolution compared to the instrumentation of the large-scale loop. Data from the benchtop loop was recorded electronically. However, the data presented within Section 3 were obtained from manual recordings taken from the DAS screen meters.

3.2.1 NUKON Slurry Preparation Characteristic Testing

The test NS6 slurry R4 values were used to develop slurry preparation procedures for NUKON-only debris loadings. Relative homogeneity of the prepared NUKON debris was also confirmed by visual observation. The R4 metric is a function of the preparation time, blender and associated speed setting used, initial debris mass, and the added water volume. The initial condition of the NUKON may also impact the preparation time required to reach a specific R4 with all other parameters held constant. Additionally, the R4 metric can be shown to have a range of NUKON masses and dilution ratios in which it is most applicable. Subsection 3.2.1.1 has an explanation for this phenomenon.

3.2.1.1 R4 Metric Applicability

The 5-mesh screen used for the NUKON slurry R4 tests was 8 in. in diameter, which allowed for all of the slurry (within the 1-L blender operational limit) to be poured through an unused (clean) portion of the screen, as specified in Section 3.1, with no overflow (such that no liquid or slurry flowed beyond the edge of the screen). The mass of the material retained on the screen is

$$m_{SM} = NUKON + water\ retained\ in\ NUKON + water\ retained\ on\ screen \tag{3.5}$$

For a constant water volume, it may be expected from Eq. (3.5) that slurries with different R4 values and NUKON masses may in fact have similar slurry characteristics. The reverse may also be true because the water retained on screen will have a comparatively more significant effect on the R4 ratio for lower NUKON masses. Tests were thus conducted to evaluate this effect. Four cases were considered:

1. Constant water volume (800 mL) with no blender operation
2. Constant dilution ratio of 0.025 g/mL (NUKON mass per water volume) with no blender operation
3. Constant dilution ratio of 0.015 g/mL with no blender operation
4. Constant water volume (800 mL) with 1-minute preparation time.

Within the relative grossness of the R4 metric itself, the test case results presented in Figure 3.1 suggest that the effects of the mass of the "water retained on the screen" are reduced for tests with at least approximately 10 g of NUKON (see subsection 3.2.1.2.1 regarding R4 variability for repeated tests). Thus, a rough applicability range of the R4 metric can be defined such that the NUKON mass should be greater than 10 g. The R1, R2, and R3 metrics are not affected by water retained on the screen. They do, however, require extended evaluation times to obtain dry masses.

The R4 data shown in Figure 3.1 may also be considered in terms of the dilution ratio (grams of NUKON per mL of water). For Cases 1 and 4, with a constant water volume of 800 mL, the possible limit of 10 g translates to approximately a 0.01 g/mL dilution ratio, suggesting that the water retained on screen dominates at lower dilution. However, from Figure 3.1, R4 may also be observed to approach a relatively constant value only after the mass is increased for the constant dilution ratio tests (Cases 2 and 3). Therefore, for the evaluated R4 tests, it appears that both the mass of the NUKON and the dilution ratio provide similar applicability limits; nominally greater than 10 g and 0.01 g/mL, respectively. For dilution ratios on the order of 0.01 g/mL and lower and the 1 L capacity of the blenders, the mass of the NUKON is the critical parameter.

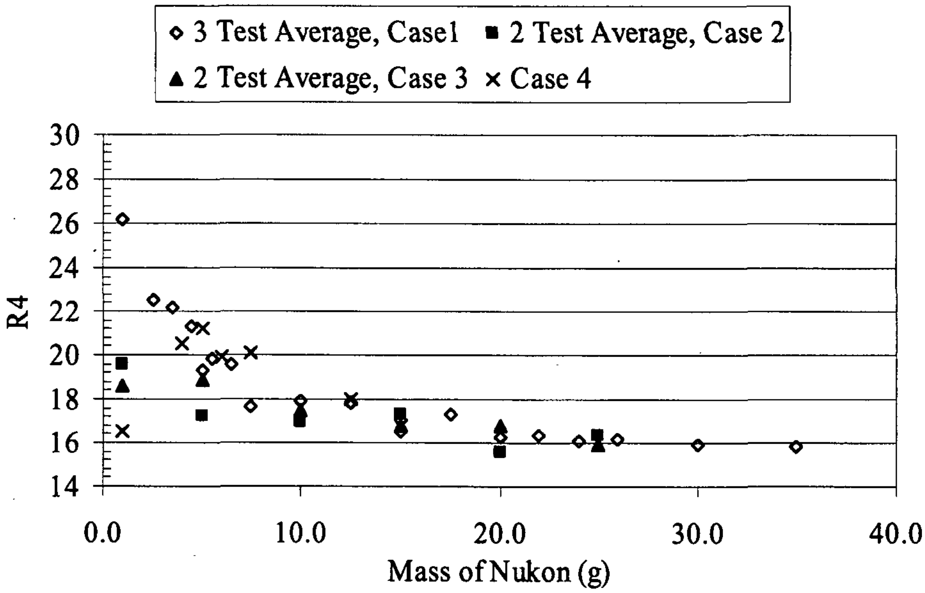

Figure 3.1. R4 as a Function of NUKON Mass

The proposed test matrix specified that NUKON be prepared in quantities less than 10 g (NRC 2005). Therefore, with the possible 10-g applicability limit, it may be suggested that (1) the R4 metric is not useful or (2) the effect of NUKON mass on the R4 value as indicated by Figure 3.1 should be accounted for in the slurry preparation determination. However, the intent of the metric is to provide a rapid, simple, and repeatable means whereby slurry that meets the five debris bed criteria in Section 3.1.1 may be produced. Therefore, although the water retained on the screen issue presented by Eq. (3.5) is acknowledged, reliance is placed on the slurry characteristic testing for debris bed formation (see Section 3.2.3), and the indicated R4 metric applicability range is ignored in light of this testing.

3.2.1.2 Effect of Preparation Conditions on the R4 Metric

The R4 metric has been shown to be a function of the blender preparation time, water volume added, debris mass (see subsection 3.2.1.1), and blender and associated operating speed used. Thus, slurry preparation for the target R4 value should be evaluated for each new condition (including different blenders of the same make and model or for a blender that may have aged due to use).

3.2.1.2.1 Preparation Time (Blender Operation Time)

Figure 3.2 illustrates R4 as a function of blender preparation time for a debris loading of 1449.5 g/m^2 (corresponding to 11.75 g of NUKON in the PNNL benchtop loop) with 470 mL of water in a Waring commercial blender (model 31BL41) operated on the high setting. For the cases evaluated, R4 decreases with increases in the preparation time (see Figure 3.2).

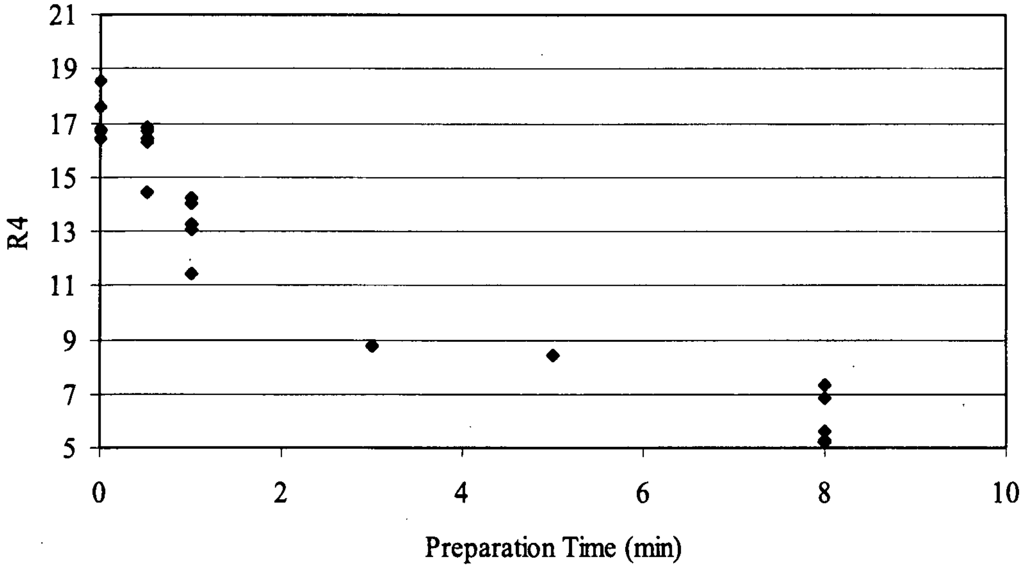

Figure 3.2. R4 as a Function of Blender Preparation Time for Constant 1449.5 g/m^2 Target Debris Loading

The repeatability of the tests depicted in Figure 3.2, as determined by the standard deviation, is similar for all the tests (see Table 3.3). Distinction between the R4 values as a function of blender preparation time is also apparent. For the tested conditions, the only overlap for maximum and minimum values is between the 0- and 0.5-minute preparation times. Given the visually observable difference in the NUKON slurry (see Sections 3.2.3.1 and 3.2.3.3), this apparent overlap is not considered to render these slurries similar in terms of the debris bed criteria listed in Section 3.1.1. The NUKON slurry with no blender preparation is primarily made up of up to 1-in.^{3} chunks or clumps of NUKON fiber, while the NUKON slurry with 0.5-minute blender preparation time has no chunks larger than about 0.25 in.^{3}. Relatively long fibers are apparent in the former. This indicates that the blenders may be chopping (reducing in size) some of the fiber as well as separating the fibers (disassociation).

Table 3.3. Repeatability of R4 Values with Different Preparation Times

Statistical Properties for Sets of Repeated Tests	Blender Preparation Time (min)			
	0	0.5	1	8
Median	16.78	16.39	13.26	5.63
Average	17.20	16.14	13.19	6.04
Maximum	18.57	16.81	14.24	7.33
Minimum	16.41	14.45	11.41	5.18
Standard Deviation	0.88	0.97	1.11	0.97
Data Points	5	5	5	5

The apparent distinction of R4 with blender preparation time was confirmed by analyzing R1 (see Eq. 3.1 in Section 3.1.2) for three distinct nominal R4 values. A distinction in the R4 values is also apparent in the R1 values for the non-boiled and boiled tests (see below), Table 3.4.

Previous investigations of NUKON debris bed head loss (Shaffer et al. 2005) have prepared the debris by boiling it for 10 to 15 minutes before introducing it to the loop. Other researchers have subjected the debris material to a presoak, which consists of soaking the material in 140°F water for 30 minutes before placing it into the loop. The 30-minute presoak is intended to simulate the approximately 30-minute delay between the occurrence of a LOCA and the start of the circulation pump. The soaking of NUKON material in the water at an elevated temperature is predicted to affect the characteristics of the NUKON's binder. PNNL investigated the effect of boiling the NUKON material both before and after blender preparation to determine if this would affect R4 results. The target debris loading tested was 1681.4 g/m^2, and the NUKON material was boiled for 10 minutes.

Testing was conducted to repeat the middle of the three blender preparation times (median R4 of 10.6) of the non-boiled tests shown in Table 3.4. In Table 3.4, BPP denotes boiling the as-received material for 10 minutes, oven drying at 194°F (90°C) until constant mass was reached (within the accuracy of the scale), resaturating it, and then blender preparing it for the R4 tests. Boiled after preparation (BAP) means that the material was first prepared in the blender, boiled for 10 minutes, and then the R4 test was conducted immediately. The variability of the R4 values between the boiled and non-boiled tests does not exceed that typical of repeated R4 tests (Tables 3.3 and 3.4), although a trend of lower R4 values may be indicated from non-boiled to BAP to BPP. The apparent opposite trend in R1 values from non-boiled to BAP may suggest that more water was retained on the screen (Eq. 3.5) for the non-boiled test (lower R1 values indicate less NUKON mass is retained on the screen (Eq. 3.1).

Table 3.4. Distinction in R4 and R1 Values and Boiling Effect (1681.4 g/m^2 target debris loading)

Test ID (blender prep. time in minutes, boiling distinction)	R4	R1
0.25	14.34	N/A[(a)]
0.25	14.82	N/A
0.25	14.20	0.88
0.25	13.96	0.89
0.75	10.02	N/A
0.75	11.10	N/A
0.75	10.68	0.76
0.75	10.59	0.75
0.75, BPP[(b)]	8.63	N/A
0.75, BPP	9.26	N/A
0.75, BPP	8.10	N/A
0.75, BAP[(c)]	9.73	0.77
0.75, BAP	10.15	0.81
0.75, BAP	9.85	0.79
1.75	6.85	N/A
1.75	6.01	N/A
1.75	7.15	0.62
1.75	6.52	0.55

(a) N/A: Not available.
(b) BPP: boiled prior to preparation.
(c) BAP: boiled after preparation.

However, the BAP tests were conducted by preparing the material, immediately boiling the slurry and then pouring the slurry through the screen while it was still hot. Thus it may be argued that the water mass is lost through accelerated evaporation. This argument may not be made for the BPP results, however, because the NUKON debris was first boiled and then dried prior to resaturation and preparation. Therefore, although boiling has not been demonstrated to significantly alter the R4 test results with regard to the anticipated variability, there is some indication that boiling the material may alter the prepared slurry's physical properties.

3.2.1.2.2 Water Volume for Blender Preparation

Data relating to the effect of the water volume used for blender preparation is illustrated in Figure 3.3 for a target debris loading of approximately 363 g/m^2 (corresponding to 1.76 g of NUKON in the PNNL benchtop loop). A Waring commercial blender (model 31BL41) operated on the high setting was again used. Within the variability of the R4 measurements themselves and the limited data, it appears that the R4 value decreases with increasing water volume. Also apparent from Figure 3.3 is the effect of blender preparation time on the R4 value. The results indicate that changes in the water volume and associated ratio to debris mass should be accompanied by an evaluation of the R4 metric.

3.2.1.2.3 Blender Effects

Differences in R4 values for NUKON slurries with similar debris loading (1449.5 to 1541.8 g/m^2) prepared in different blenders with the same preparation time (3 minutes) and ratio of NUKON mass to water volume (Section 3.1.2) are illustrated in Figure 3.4. Blenders 1, 2, and 4 are the same make and model, and blender 4 differs from blenders 1 and 2 only in that the blades may have been dulled due to extensive intermediate use with an alternative potentially abrasive material. Based on the observed results, consideration should be given to periodically assessing the R4 for a given slurry with continued use of a blender or if a change in blenders is made.

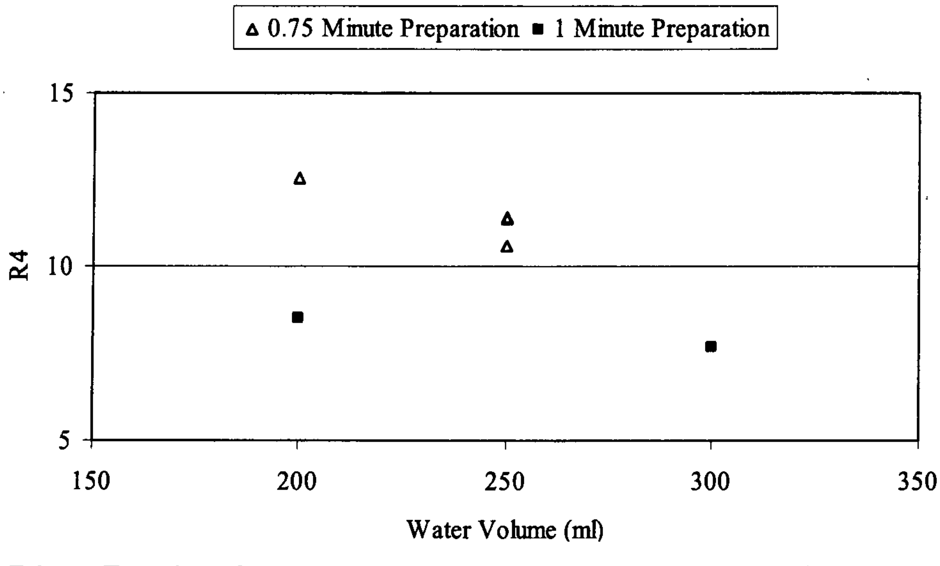

Figure 3.3. R4 as a Function of Water Volume Used for Blender Preparation for Blender Preparation Time s of 0.75 and 1.0 minutes. Constant target debris loading is 363 g/m^2 (1.76 g of NUKON in the PNNL benchtop loop).

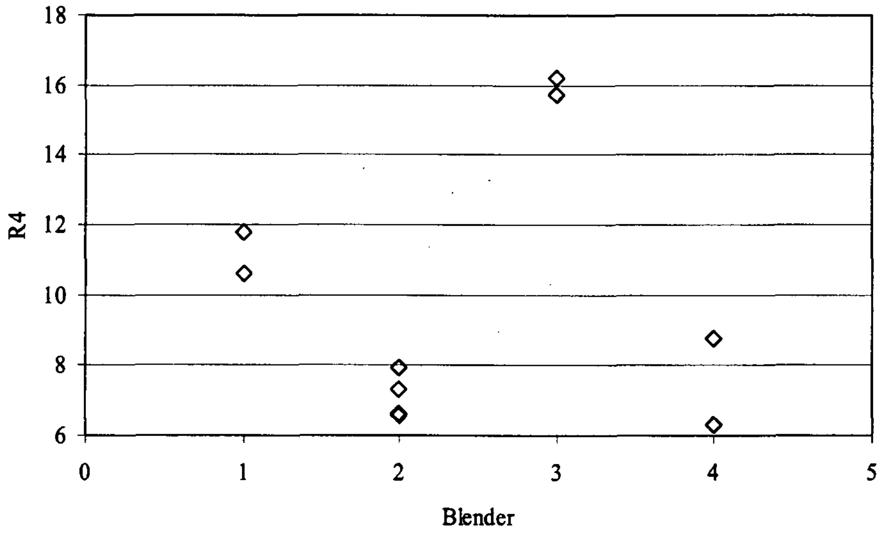

Figure 3.4. R4 as a Function of the Blender Used for Target Debris Loading of 1449.5 to 1541.8 g/m^2 in the Benchtop Loop (3-minute blender preparation time)

3.2.1.2.4 Visual Observation of Homogeneity

When evaluating/determining a slurry preparation technique using the R4 metric, visual observation of the slurry consistency should be considered. As described in Section 3.1.2, visual confirmation of slurry homogeneity (no clumps) may be desirable to meet the specified (Section 3.1.1) debris bed criteria. It has been observed that similar NUKON slurry R4 values from different blenders may produce slurries with different visually observable characteristics. That is, although the same amount of material is retained on a 5-mesh screen during a "pour-through" test, visual observation of the slurry condition indicates a different consistency.

The variation of R4 results with blender preparation time for a potentially altered blender is used for illustration. Before potentially dulling the blades of a specific blender, a preparation time of 0.75 minutes at "high" was used for the 1449.5 g/m^2 target debris loading to achieve the desired R4 value. Increasing the preparation time to 1 and 3 minutes resulted in lower R4 values, as shown in Figure 3.5. The "non-dulled" case is denoted by "Blender A" in the figure.

The variation in the R4 value with blender preparation time for the altered blender (blades were potentially dulled over time due to abrasiveness of the debris material), denoted by Blender B, is also shown in Figure 3.5. Operating Blender B for 0.75 minutes produced similar R4 values, but the response of R4 to various mixing times was different. The slurry from Blender A appeared to be uniform, while in Blender B clumps were observed for the same R4 values (approximately 10–12) until the mixing time was increased to 1.25 minutes. Visual observation of the homogeneity of the slurry should therefore be considered.

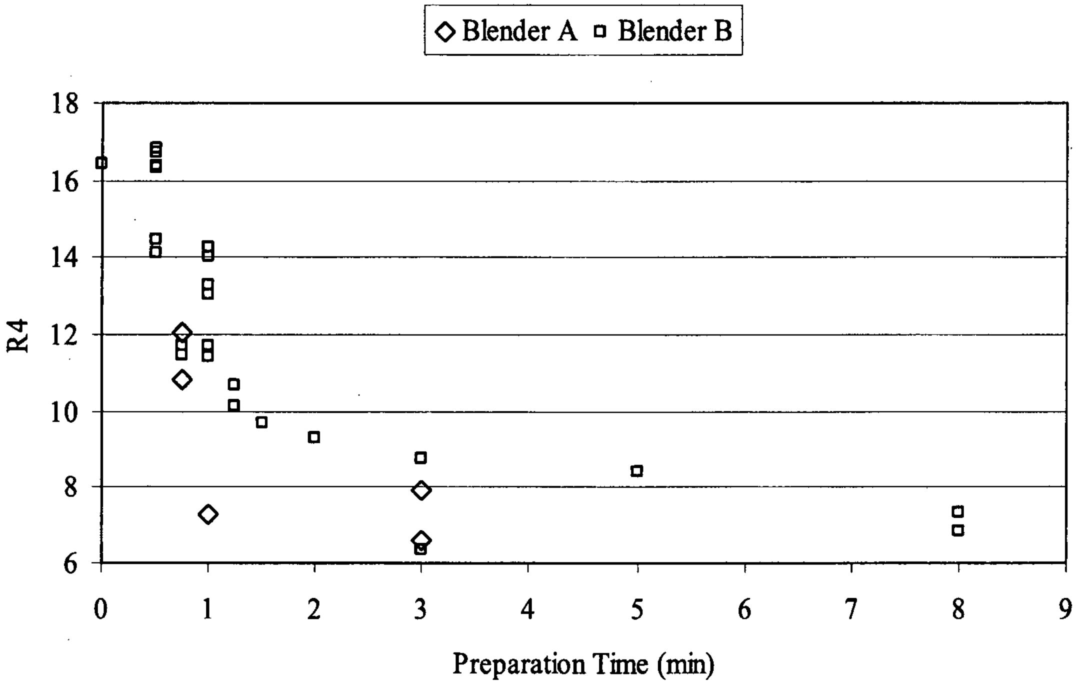

Figure 3.5. Effect of Mixing Time on R4 Values for 1449.5 g/m^2 NUKON Debris Loading Case

3.2.2 CalSil Slurry Preparation Characteristic Testing

The target CalSil slurry characteristics for previous related work (Shaffer et al. 2005) were approximately defined by specifying the slurry preparation conditions. The simple R4 metric developed for NUKON slurry preparation (Eq. 3.4) was used to provide a rapid means of approximate quantification of the CalSil slurry prepared by completely disassociating the particulate CalSil from the fibrous binder material using a mortar and pestle. The prepared CalSil material was also processed until visual observation showed it to be relatively homogenous with no clumps.

For initial evaluation, a relatively large target debris loading for CalSil of 725 g/m^2 was chosen from the proposed test matrix. For the PNNL large-scale test loop, this debris loading equates to 13.22 g. Material was separated from the as-received CalSil blocks using a saw. Irregularly shaped chunks of approximately 0.2 to 0.8 in. (5 to 20 mm) in diameter were broken off from the separated material with pliers until the desired mass was obtained.

To establish the CalSil baseline for criterion 2 (see Section 3.1.3), a mortar and pestle were used to completely disassociate the particulate from the fibrous binder material. The prepared fibrous binder and CalSil particulate were then diluted with 530 mL of water (arbitrarily chosen to match the 12.5-g debris to 500-mL water dilution ratio for the NUKON) (Section 3.1.2), and the resulting slurry was poured through an 8-in.-diameter 5-mesh screen to obtain a value of R4 (Eq. 3.4). Minimal debris was observed retained on the screen. The bulk of the retained material consisted of the fiber material added to the CalSil during manufacturing to provide structural integrity of the formed shapes (e.g., sheets, pipe shells). Particulate was held up in this fibrous material as well as on the screen mesh itself. Relatively repeatable R4 values were achieved over three tests with a median value of 1.82. As expected from the debris preparation procedure, no clumps of particulate were observed. This visually observable relative homogeneity was used as the primary guideline for CalSil material preparation. The R4 metric, given the lack of significant quantities of debris on the screen, was used as a secondary consideration.

Testing showed that blender-prepared (no mortar and pestle preparation) CalSil with a median R4 value less than approximately 1.55 is relatively homogeneous, while CalSil slurries with R4 values greater than a median value of approximately 1.82 have clumps and chunks of undisturbed CalSil particulate. (The equivalence of the mortar-and-pestle-prepared median R4 with that of the blender-prepared median R4 with clumps and chunks was considered coincidental and not investigated further.)

Data were also taken that suggested that longer blender preparation times may alter the CalSil particulate from that expected using a mortar and pestle. CalSil material was ground with a mortar and pestle to disassociate the fibrous material from the particulate. The bulk material was then separated by sieving through a 212-µm-opening screen mesh, which was visually observed to segregate the CalSil particulate from the fiber. Three separate samples of 13.22 g from this visually inspected fiberless CalSil particulate were diluted with 530 mL of water. The first sample was the as-prepared material. The second was prepared for 0.75 minutes in a KitchenAid blender (Model No. KSB50B4) set to "Liquefy," and the third sample was similarly prepared for 6 minutes. R4 type tests using a 150-µm sieve for the pour-through test were then conducted. The 150-µm sieve R4 results were 1.3, 0.88, and 0.37, respectively, suggesting that extended preparation times can affect the CalSil material's properties.

PSD analyses were conducted on the prepared CalSil material using a MicroTrac S3000 particle size analyzer to determine whether this measurement method could be used to provide quantifiable insight. Instrumentation and configuration, as well as conditions such as particulate/ agglomeration shape, can affect and potentially distort PSD results. Given the presence of fibrous material in the CalSil and sampling effects, the PSD results should not be considered highly accurate. However, the PSD results provide an understanding of the relative distribution of the particle size and insight into the possible effect of varying the blender preparation time. Three cases of blender-prepared CalSil were generated for a constant mass loading with one case having a blender preparation time of 1 minute and the other two cases a preparation time of 3 minutes. The cases were evaluated to:

- Determine the effectiveness of using PSD analysis to characterize the CalSil debris
- Evaluate the repeatability of the CalSil debris preparation process
- Evaluate the distinguishability between blender preparation times.

The results are presented in Figure 3.6. There was no discernable definitive trend in the PSD-determined CalSil particulate size with preparation time (Figure 3.6) for the limited cases evaluated.[1]

In practice, a minimum preparation time in the KitchenAid blender of approximately 0.5 minutes was required for 13.22 g of the as-received bulk CalSil in 530 mL of water to achieve an R4 value of

---

[1] Aliquots of prepared CalSil slurry were taken form the bulk sample for the preparation-time PSD analysis using a pipette. For some aliquots, the visually observed fibrous material plugged the pipette, causing the samples to be redrawn. For other aliquots, the observed fibrous material did not plug the pipette. Thus, fibrous material is present in the analyzed samples and the amount of fibrous material may not be constant from aliquot to aliquot.

nominally less than 1.55 on a 5-mesh screen and visually exhibit no chunks. The minimum preparation time was desired to reduce the potential blender effects on the particulate. CalSil slurry preparation was therefore roughly standardized by visually determining the minimum mixing time required to produce a homogeneous slurry using the maximum R4 value as a guideline.

PSD analyses were conducted for the upper and lower range of the target CalSil debris loadings specified in the proposed test matrix, 135 and 724 g/m^2 (Section 5.1). The blender preparation time for the CalSil debris was determined based on the criteria:

- An R4 value of nominally less than 1.55 for a 5-mesh screen
- Blender operations continued until visual observation of slurry indicated no chunks present.

The results for the two cases are plotted in Figure 3.7. While PSD by itself was not conclusive, no discernable difference was identified for the two conditions presented in Figure 3.7, indicating that the level of debris fragmentation was similar. The blender preparation time used for generating the CalSil debris associated with the data in Figure 3.7 was determined as the point at which chunks were no longer visually observed, while the blender preparation time for the CalSil used to produce the data in Figure 3.6 exceeded this time.

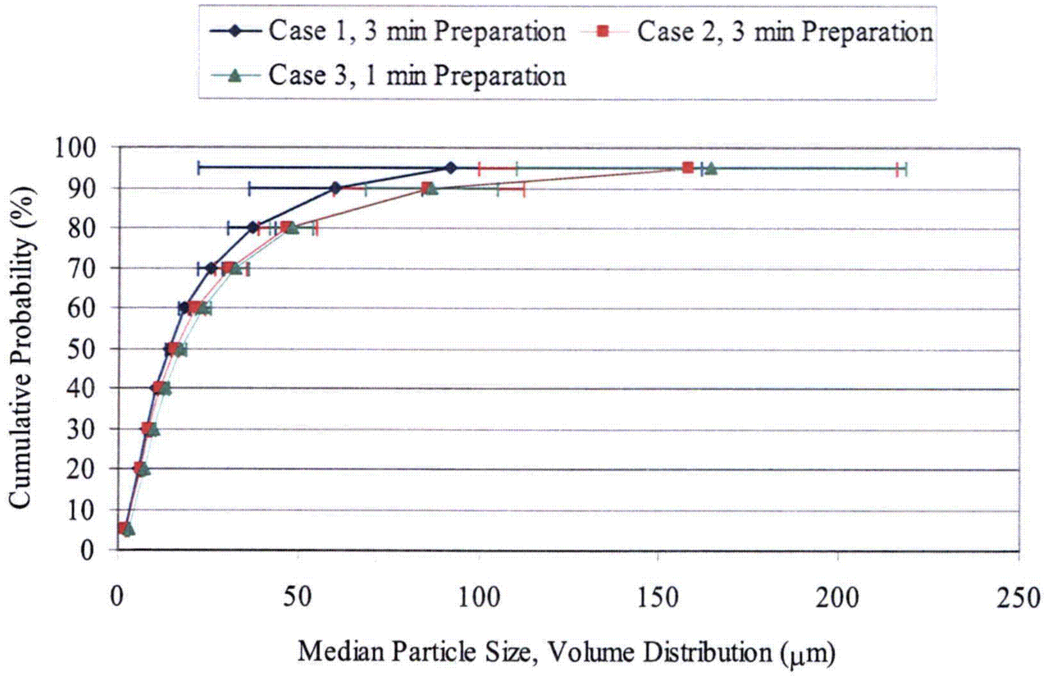

Figure 3.6. PSD Results for Blender Prepared CalSil Slurry for Blender Preparation Times of 1 and 3 minutes (median of at least 5 repeated samples; error bars indicate ±1 standard deviation; results are comparative and do not represent actual particle size)

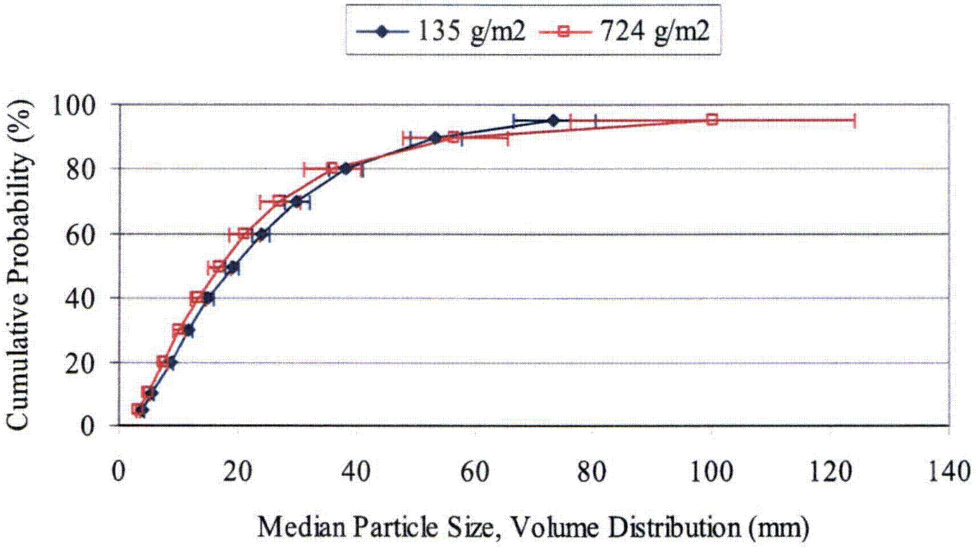

Figure 3.7. PSD Results for Blender Prepared CalSil Slurry. Blender preparation time determined from visual observation of "no chunk" condition (median of three repeated samples; error bars indicate ±1 standard deviation; results are comparative and do not represent actual particle size)

3.2.3 Debris Bed Criteria Testing

Five specific debris bed criteria are listed in Section 3.1.1. The PNNL benchtop loop was used to determine the applicability of debris prepared to these criteria, as described in Sections 3.2.1 and 3.2.2.

3.2.3.1 Debris Bed Formation Criteria 1–3

As shown in Figure 3.8, NUKON debris prepared to the test NS6 R4 conditions (R4 ~ 11, see Table 3.2) forms a complete debris bed (Criterion 1) when introduced into the PNNL benchtop loop. When the debris preparation process is altered for the same target debris loading to produce higher R4 values, the surface uniformity is lost, as observed for debris beds in Figures 3.9 (R4 ~ 17, no blender preparation) and 3.10 (R4 ~ 16, 0.5-minute blender preparation time). Each of these debris beds had a target debris loading of 1449.5 g/m^2 and was formed at an initial screen approach velocity of 0.2 ft/sec. NUKON debris beds for a target debris loading of 1449.5 g/m^2 at R4 ~ 11 were formed at varied screen approach velocities (0.07 to 0.36 ft/sec). At a lower target debris bed loading, 107.3 g/m^2, the ability to form a complete debris bed (0.2 ft/sec screen approach velocity) as well as debris bed surface uniformity were lost at higher (R4 ~ 20, no blender preparation) and lower (R4 ~ 6) R4 values (Figures 3.11 and 3.12, respectively). Examples of complete uniform debris beds formed for an R4 value of approximately 11 and debris loadings of 107.3, 217.4, and 724.7 g/m^2 are shown in Figures 3.13 through 3.15, respectively.

Visual comparison of the NUKON debris beds shown in Figures 3.8 and 3.13–3.15 demonstrate the achievement of Criterion 1, produce a complete debris bed on the screen; Criterion 2, uniform thickness; and Criterion 3, uniform debris beds over the specified debris loading range. The NUKON debris beds shown were formed at the same nominal screen approach velocity of 0.2 ft/sec on a 5-mesh screen. Formation of these beds has been shown to be repeatable based on visual observation and debris bed height (Section 3.2.3.2).

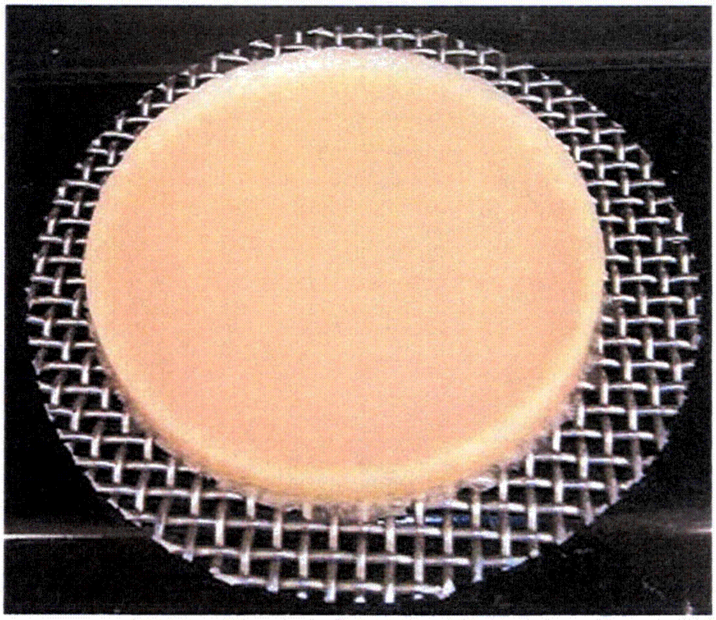

Figure 3.8. NUKON Debris Bed for 1449.5 g/m^2 Target Debris Loading (R4 ~ 11)

Figure 3.9. NUKON Debris Bed for 1449.5 g/m^2 Target Debris Loading
(R4 ~ 17 as-received material/no blender preparation)

Figure 3.10. NUKON Debris Bed for 1449.5 g/m^2 Target Debris Loading (R4 ~ 16)

Figure 3.11. NUKON Debris Bed for 107.3 g/m^2 Target Debris Loading (R4 ~ 20, no blender preparation)

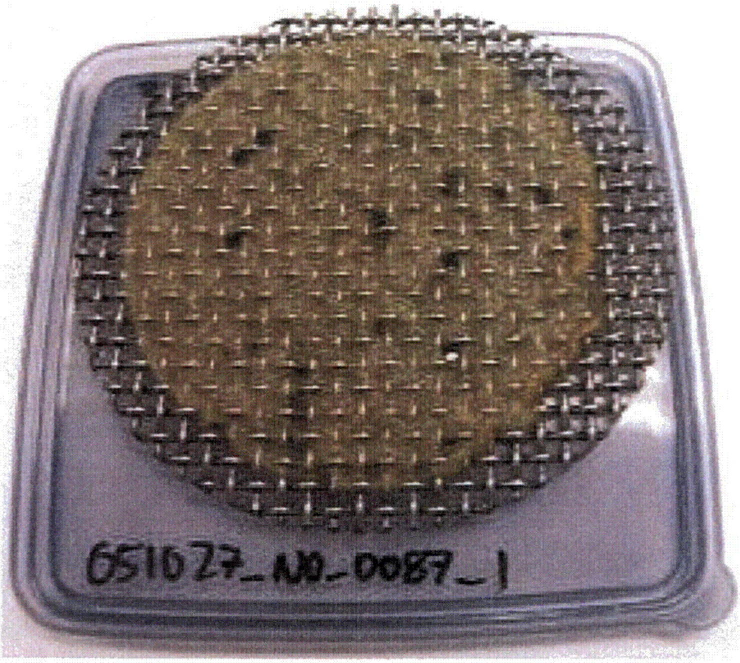

Figure 3.12. NUKON Debris Bed for 107.3 g/m^2 Target Debris Loading (R4 ~ 6)

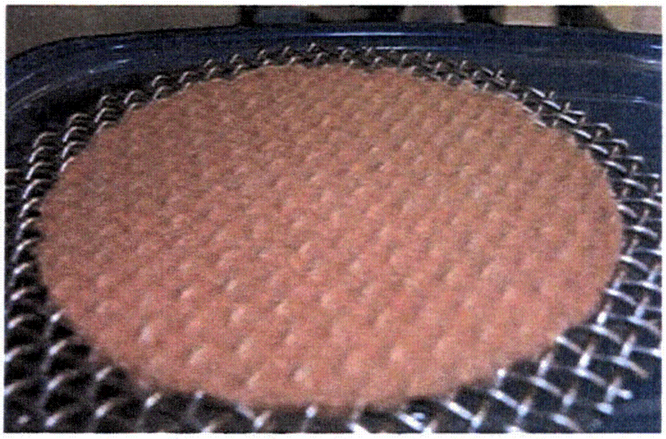

Figure 3.13. NUKON Debris Bed for 107.3 g/m^2 Target Debris Loading (R4 ~ 11)

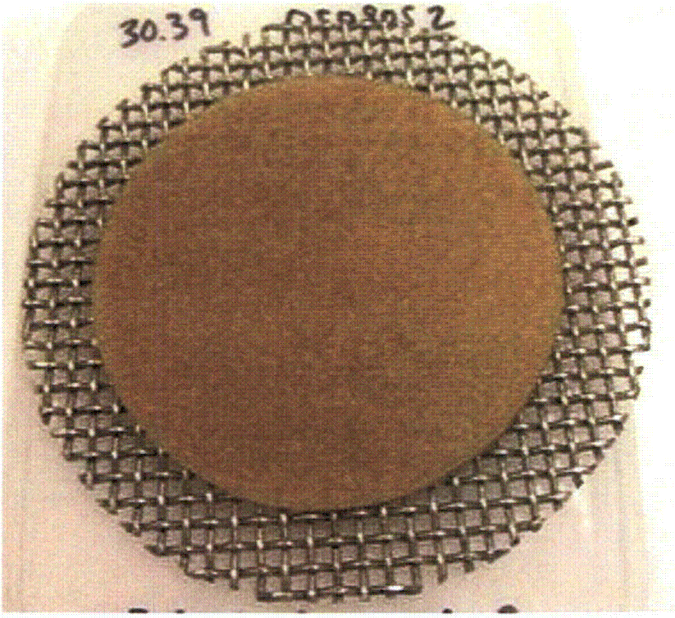

Figure 3.14. NUKON Debris Bed for 217.4 g/m^2 Target Debris Loading (R4 ~ 11)

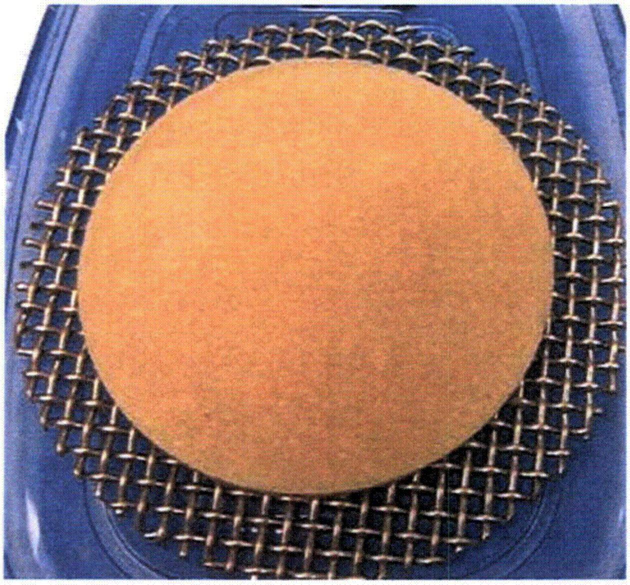

Figure 3.15. NUKON Debris Bed for 724.7 g/m^2 Target Debris Loading (R4 ~ 11)

The visually uniform NUKON and CalSil (referred to as NUKON/CalSil) debris bed shown in Figure 3.16 was formed at an initial screen approach velocity of 0.2 ft/sec. Uniform NUKON/CalSil debris beds were formed at screen velocities of 0.1 ft/sec as well. Additional photos of the debris beds can be seen in the "Quick Look" reports in Appendixes H through K and in the discussion of debris loading sequences in Section 6.3. The NUKON and CalSil slurries prepared to the guidelines presented in Sections 3.2.1 and 3.2.2 produced complete debris beds (Criterion 1) that were uniform in thickness (Criterion 2) over the specified debris loading range (Criterion 3). Criteria 1 through 3 were satisfied for

Figure 3.16. NUKON and CalSil Debris Bed for 1811.9 g/m^2 Target Debris Loading (NUKON R4 ~ 11, CalSil R4 < 1 = 1.55) (see Section 3.2.2)

both methods of debris injection; premixed (NUKON and CalSil slurries mixed together just prior to introduction into the test loop) and independent introductions (the CalSil and NUKON are introduced via separate injection lines and do not come in contact until they are in the main line of the test loop).

Investigation of the internal uniformity of debris beds (second part of Criterion 2) was made via sectioning of a limited number of the debris beds (see Section 6.5). Visual observation of the sectioned beds does not provide compelling evidence that this requirement has not been met. Observation of the sectioned beds using SEM provided a more definitive assessment with regard to this requirement than visual observation alone.

3.2.3.2 Debris Bed Formation Criterion 4

Determination of the achievement of Criterion 4 (the formed debris beds should yield repeatable physical and performance characteristics) is made by examining a representative debris bed height, surface appearance, and head loss history for debris beds of equivalent target debris loading and the same debris preparation procedure. Based on the results presented in Section 3.2.3.1, NUKON and CalSil debris slurries were prepared to achieve R4 ~ 11 and R4 ≤ 1.55, respectively (Sections 3.2.1 and 3.2.2). All debris beds formed under these preparation conditions exhibited a uniform surface appearance.

Representative retrieved NUKON debris bed heights are relatively repeatable at a target debris loading of 1449.5 g/m^2 (Figure 3.17). All debris beds for this evaluation were formed at an initial screen approach velocity of 0.2 ft/sec. The debris bed body measurements (plane area of the bed, not the outer rim; see Figure 3.8 for example) are inferred from a 1-mm-increment ruler placed vertically beside the debris bed. (The measured debris bed heights are referred to as representative because of the limitations of the described measurement technique. This gross technique is only employed for the benchtop evaluations and provides a qualitative means of comparison.) The reported debris bed heights are taken post-retrieval and thus represent no-flow conditions. Different methodologies were employed for obtaining the heights of debris beds formed in the large-scale test loop.

The observable variations in the approximate heights are deemed appropriate for the different time at flow (the debris beds were subjected to varying numbers of circulations, 4 to 103), as evidenced by the recovery fraction. The recovery fraction shown in Figure 3.17 for target NUKON debris loading of 1449.5 g/m^2 is computed from the dry retrieved debris bed mass divided by the initial mass added to achieve the target debris loading. The observed debris bed height variation is deemed reasonable given the measurement technique. Aside from a single outlier, similar variation is observed for NUKON/CalSil debris beds formed with a target debris loading of 1811.9 g/m^2. In summary, the physical characteristics of the debris bed thickness and uniform surface appearance indicate that relatively repeatable debris beds have been produced.

The performance characteristics of debris beds formed from the specified debris preparations were shown to be repeatable as judged by their head loss history. An example comparison is provided in Figure 3.18. The head-loss history is taken from tests of two NUKON debris beds (1681.4 g/m^2 target debris loading) that included incremental cycling of the screen approach velocity. Only the first ramp up from each case is shown for approximately equivalent screen approach velocities (i.e., not all of the test data are plotted). The median difference in head loss was 12%. Additional comparison of the repeatable performance of debris beds was made in the PNNL large-scale loop, resulting in a median difference of 2% for the head

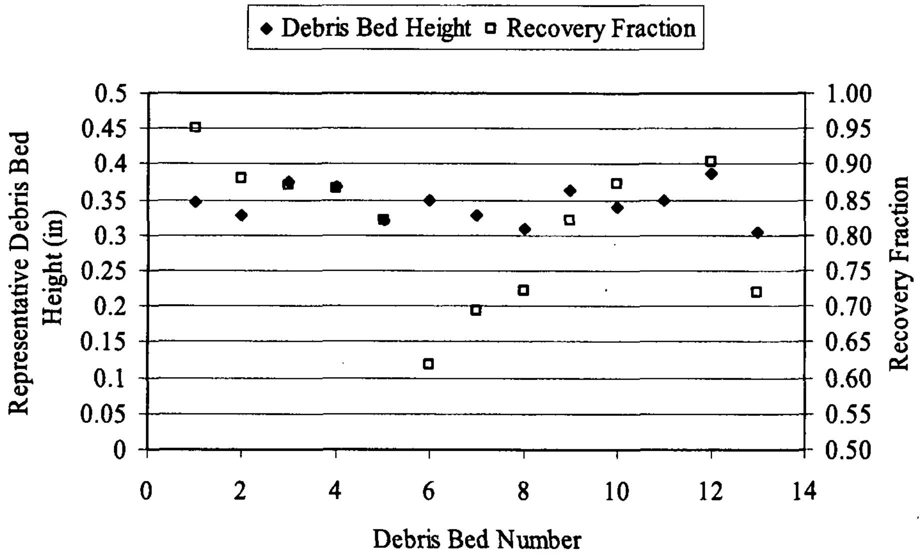

Figure 3.17. Representative Debris Bed Heights and Recovery Fraction (1449.5 g/m^2 target NUKON debris loading)

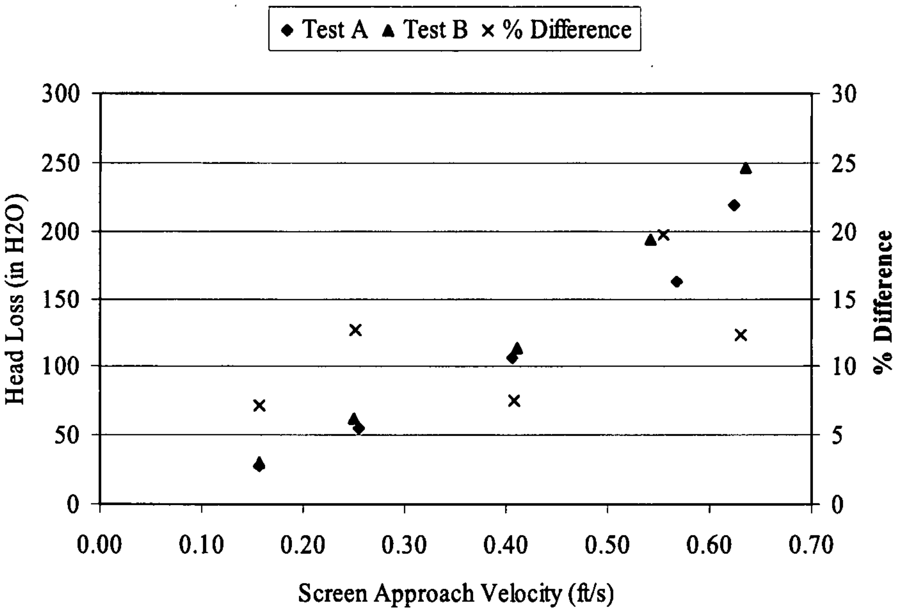

Figure 3.18. NUKON Debris Bed Head Loss as Function of Screen Approach Velocity (1681.4 g/m^2 target NUKON debris loading)

loss measured during the first ramp up. Reasonably comparable results were achieved for the same target debris loading in the benchtop and large-scale PNNL test loops (refer to Quick Look report for PNNL Test 060125_NO_3067_L1 in Appendix H).

The repeatability of the measured head loss as a function of screen approach velocity has been investigated for NUKON/CalSil debris beds generated with the debris prepared as specified. Test results indicate the head loss was strongly affected by the debris loading sequence (i.e., the order in which NUKON and CalSil debris was introduced into the test loop), but carefully controlled similar loading sequences yielded relatively repeatable results (refer to Section 6.3).

3.2.3.3 Debris Bed Formation Criterion 5

Tests have shown that the debris preparation procedure can affect the measured head loss. At a target debris loading of 1681.4 g/m^2, the measured head loss can be doubled depending on the slurry preparation procedure. For the NUKON-only tests depicted in Figure 3.19, the R4 values were approximately 18.6 (no blender preparation) and 10.4. Only the ramp up portions of the tests are shown. The percent difference is computed from the subsequent data pairs, neglecting the apparent screen approach velocity differences; the percent difference is plotted at the pair-averaged screen approach velocity.

At the average debris bed formation velocity, the NUKON debris bed (R4~10.4) had a head loss that was approximately 13% larger than that of the debris bed formed with NUKON with no blender preparation (R4~18.6). A nominal 50% increase in screen approach velocity raised the difference to approximately 28%. The maximum difference observed was almost 60%, corresponding to the maximum tested screen approach velocities for each case (these peak velocities were different, as shown in Figure 3.19). The initial debris bed formation velocity was the same, but the actual screen approach velocity after introducing the NUKON slurry into the loop varied, as depicted in Figure 3.19.

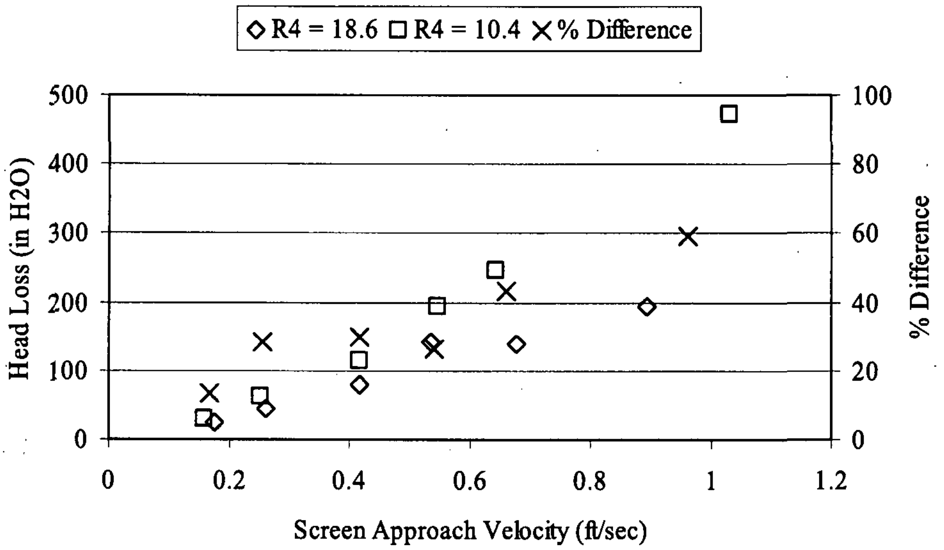

Figure 3.19. Approximate NUKON Debris Bed Head Loss as a Function of Slurry Preparation (target debris loading of 1681.4 g/m^2)

When evaluating Criterion 5, it is important to consider Criteria 1 through 3 as well. If the NUKON slurry is not prepared in a blender, debris bed surface uniformity is markedly reduced (see, for example, Figure 3.9).

Based on the apparent variance in debris bed head loss associated with the slurry preparation procedure presented above, further tests were conducted in which the R4 value for the debris preparation was varied. As suggested in Section 3.1.2, it may be expected that NUKON slurry with no blender preparation will have the highest R4 value, and that successively longer blender preparation times will yield lower R4 values as the debris is disassociated or ground to a finer state. It may also be expected that nonuniform clumping of NUKON in a debris bed will result in a reduced head loss for a given debris loading and flow compared with a uniformly packed debris bed. However, excessively long blender preparation time may produce debris with characteristics insufficient to form a debris bed with significant flow resistance, resulting in a low head loss. Thus, the function relating head loss to R4 can be expected to have a maximum at some intermediate R4 value.

To establish the repeatability of producing debris batches with the same R4 value, multiple debris preparation tests were conducted by different researchers at varied blender preparation times. Tests were conducted with debris masses corresponding to target debris bed loadings of 107.3 and 1449.5 g/m^2 in the benchtop loop (4-in. diameter), which bound the proposed test matrix. The resulting R4 values are presented in Table 3.5. R4 decreases with increasing blender preparation time, as can be observed in Figure 3.2.

The debris bed head loss at various screen approach velocities for NUKON slurries prepared to match the R4 values of Table 3.5 are shown in Figure 3.20 and 3.21 for target debris bed loadings of 107.3 g/m^2 and 1449.5 g/m^2, respectively. At the lower target debris loading, the R4A1 and R4D1 slurries did not produce complete debris beds (see Figures 3.11 and 3.12). The R4C1 debris beds developed ruptures (channeling) as the screen approach velocity exceeded 0.6 ft/sec (0.2 m/s). The ruptures occurred as gas

Table 3.5. Criterion 4 Testing NUKON Preparation

Debris Loading (g/m^2)	Parameters	NUKON Preparation			
107.3	Slurry Name	R4A1	R4B1	R4C1	R4D1
	Preparation Time (min)	0	0.75	1.5	2
	Median R4	20.3	14.5	8.6	5.9
1449.5	Slurry Name	R4A2	R4B2	R4C2	R4D2
	Preparation Time (min)	0	0.5	1	8
	Median R4	16.8	16.4	13.3	5.6

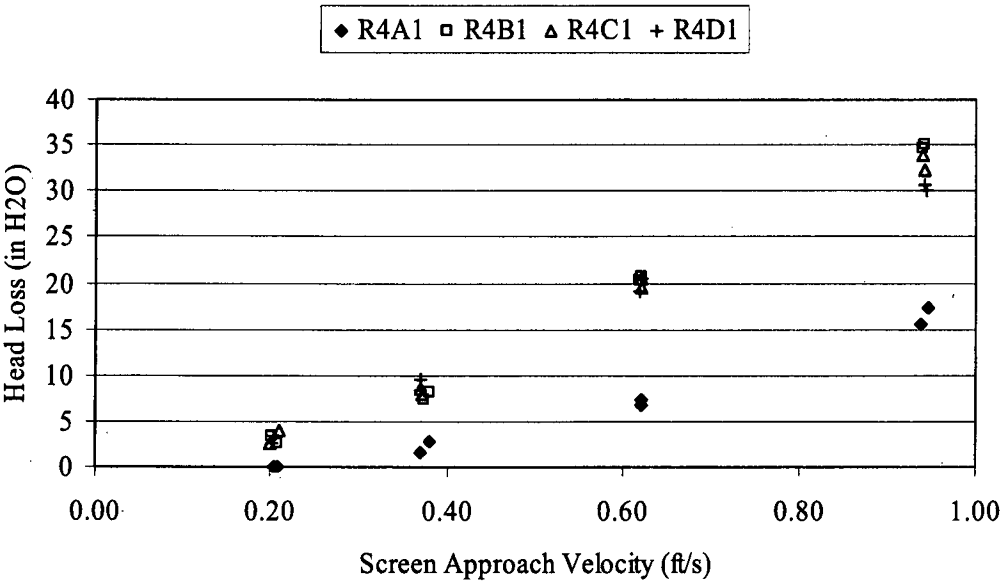

Figure 3.20. NUKON Debris Bed Head Loss as a Function of Screen Approach Velocity (R4 values from Table 3.5; target debris loading of 107.3 g/m^2)

came out of solution and bubbles were formed on and around the debris bed and opened less than approximately 5% of the screen area to flow based on visual observation.

Regardless of the ruptures observed in the R4C1 beds, for each debris loading, the data indicate that the head loss at each screen approach velocity tested is at a minimum for R4A, and at higher velocities appears to peak for values of R4 with less blender preparation time than R4D. A clearer quantitative comparison of the effect of R4 on the debris bed head loss can be made by evaluating a loss coefficient for the debris bed. The head loss produced by the debris bed can be expressed by

$$\Delta H = K\frac{\rho V^2}{2} \tag{3.6}$$

where K is the loss coefficient for the debris bed, ρ is the fluid (water) density, and V is the screen approach velocity. With the data from Figures 3.20 and 3.21, the loss coefficient may be expressed as

$$\frac{K\rho}{2} = \frac{\Delta H}{V^2} \tag{3.7}$$

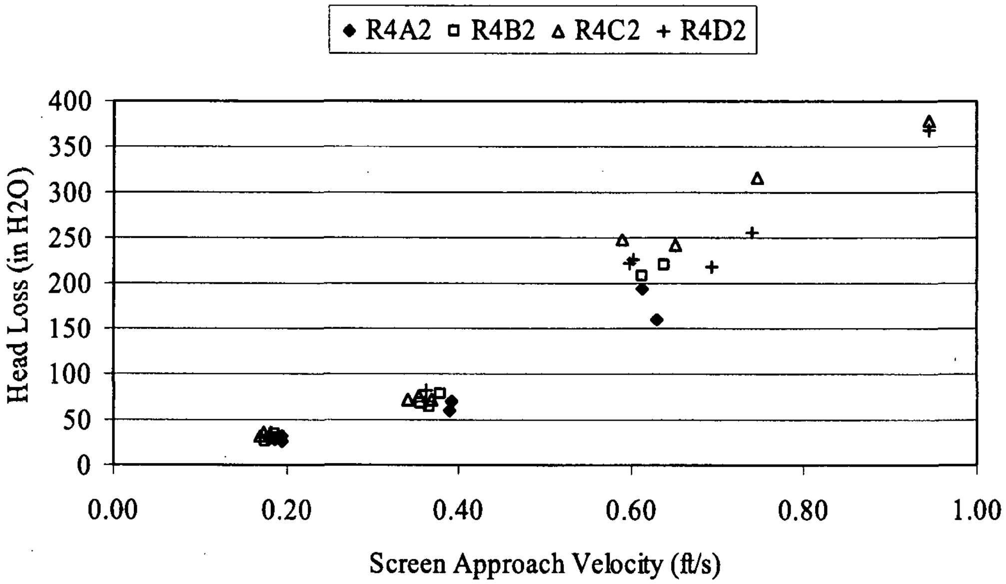

Figure 3.21. NUKON Debris Bed Head Loss as a Function of Screen Approach Velocity (R4 values from Table 3.5; target debris loading of 1449.5 g/m^2)

The loss coefficients (from Eq. 3.7 including ρ and 1/2) for the debris beds of Figures 3.20 and 3.21 are plotted as a function of the screen approach velocity in Figures 3.22 and 3.23. The apparent variation of K with the screen approach velocity is briefly addressed. The indicated transition or decrease from high to low K with increasing screen approach velocity apparent in Figures 3.22 and 3.23 is most likely the result of the potential transition of the flow regime upstream of the debris bed relative to laminar/transitional/fully turbulent flow (Reynolds number dependent) and compression of the debris bed with changes in the screen approach velocity. Another potential factor affecting the loss coefficient with changes in screen approach velocity is the transition of flow regime occurring at the debris bed surface, assuming predominantly laminar flow through the pores in the debris bed.

The increase of K with increasing screen approach velocity for the no-blender preparation cases at 107.3 g/m^2 (R4A1 in Figure 3.22) may be due to the incomplete coverage of the debris bed (see example in Figure 3.11), which allows for a redistribution of the flow through open areas with increasing velocity. The longer fibers and clumped material associated with NUKON debris having no blender preparation may form debris beds with relatively high porosity that undergo a greater degree of compression than the blender prepared material, which could also increase the resistance of flow at higher velocities.

Based on the results observed in Figure 3.23, it is arguably evident that the highest K value (i.e., the highest head loss) was achieved for the debris beds with R4C (for the approach velocities tested). Regardless, in conjunction with achieving Criterion 5 (which at the time the debris preparation process was being developed was assumed to include the maximum head loss), Criteria 1–4 should also be met, as is addressed below.

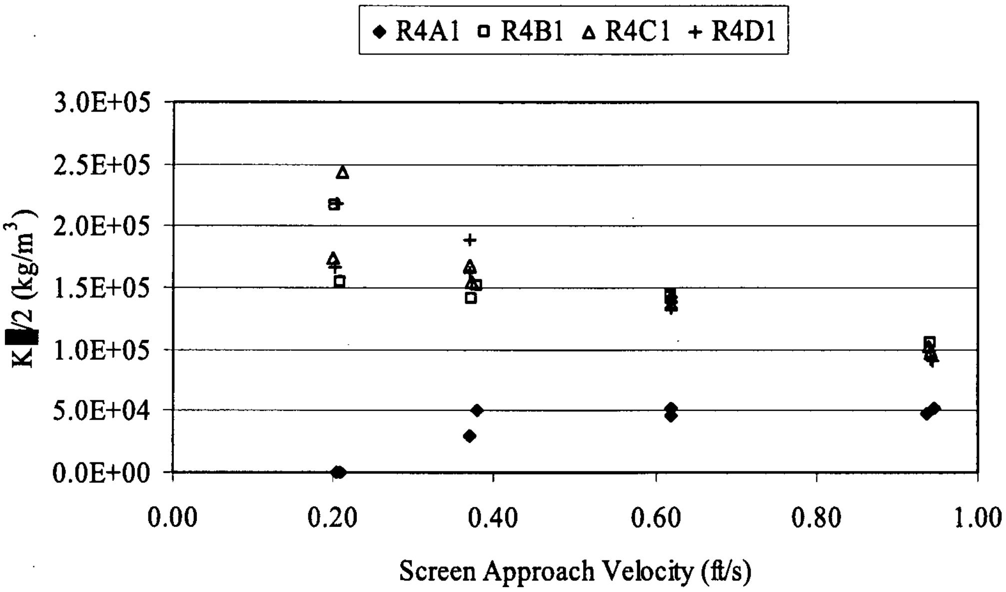

Figure 3.22. **NUKON Debris Bed Loss Coefficients as Functions of the Screen Approach Velocity (R4 values from Table 5; target debris loading of 107.3 g/m²)**

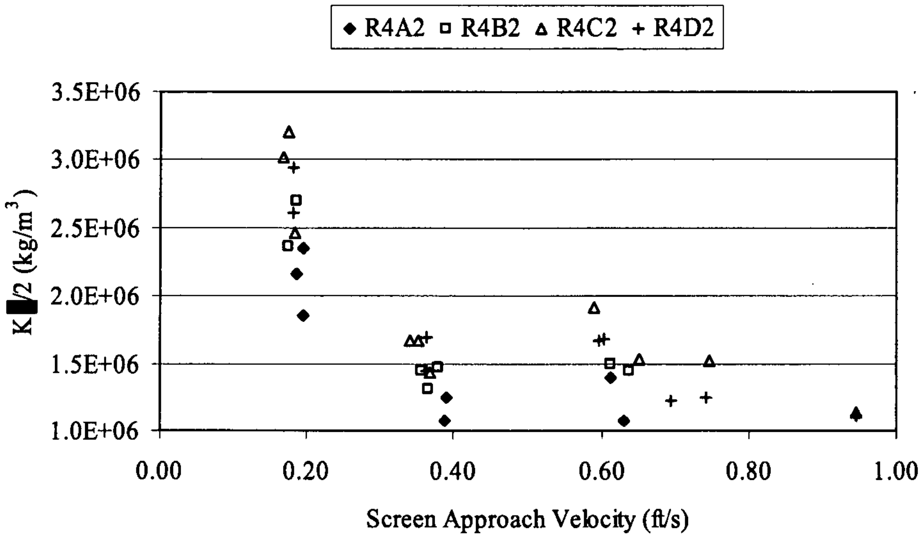

Figure 3.23. **NUKON Debris Bed Loss Coefficients as Functions of the Screen Approach Velocity (R4 values from Table 3.5; target debris loading of 1449.5 g/m²)**

First, however, consider the target debris loading 1449.5 g/m² results with regard to potential contributors other than debris preparation to the apparent head loss differences and whether the differences are due to actual differences in the formed debris bed or to a reduction of actual debris loading of the debris bed. That is, for a given preparation, less mass on a debris bed would be expected to result in a lower measured head loss.

The calculated fraction of the NUKON mass added to the test loop that was retained in selected debris beds is presented in Figure 3.24. The calculated mass fraction trend from R4A to R4C is the opposite of that for head loss. The decrease in the calculated mass fraction from a median of 0.97 to a median of 0.96 for R4C and R4D, respectively, is essentially negligible. These results suggest that the difference in head loss is predominantly due to the different NUKON preparation procedures, which changed the structure of the debris beds.

The Test Set labels in Figure 3.24 refer to the order in which the tests were performed. They are important because the debris beds from Test Sets 2 and 3 were tested for longer durations and at higher flow rates. Thus, the increase in retention of debris on the screen over Test Set 1 is expected. Ideally the ratio of the dry retrieved debris mass to the initial debris mass should not exceed a value of 1.0. However, in practice (Cases for R4A2 in Figure 3.24) some contamination from residual construction materials (e.g., pipe dope) was experienced during early tests in the benchtop loop.

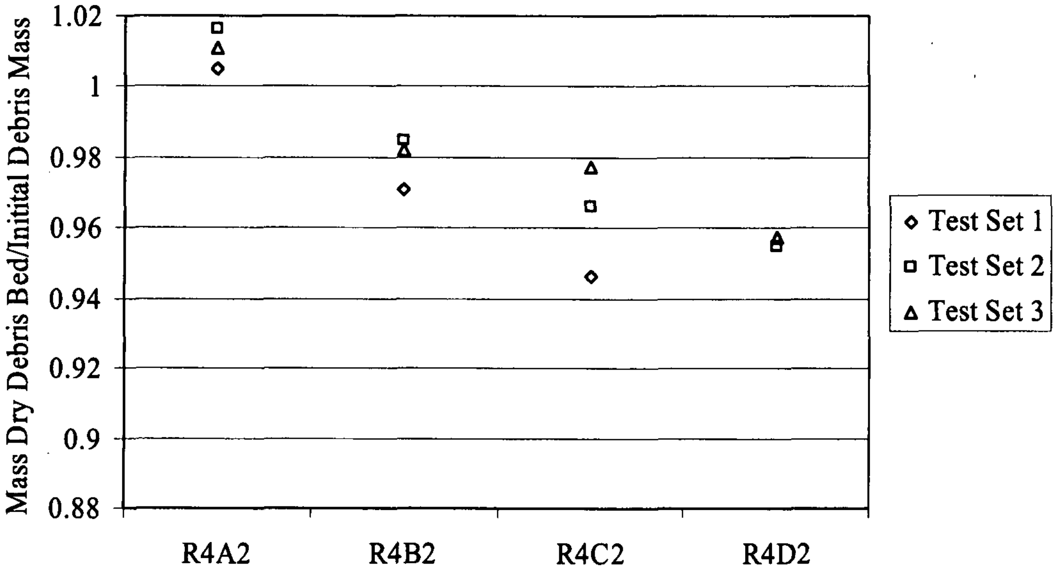

Figure 3.24. Fraction of Initial NUKON Mass Retained in Debris Bed as a Function of R4 (target debris loading of 1449.5 g/m^2)

The negligible decrease in the retained mass fraction of initial NUKON on the debris bed from R4C2 to R4D2 is briefly compared in terms of expected head loss using the NUREG/CR-6224 (Zigler et al. 1995) correlation. Based on the correlation, a 1% decrease in fiber mass results in a 1% decrease in head loss at a screen approach velocity of approximately 0.95 ft/sec (0.29 m/s). Considering the retrieved debris bed mass, the data from Figures 3.21 and 3.24 for R4C and R4D at 0.95 ft/sec (0.29 m/s) indicate that a 1% reduction in mass (0.97 to 0.96) results in a 3% decrease in head loss (379 to 368 in. H_2O) that is not fully accounted for by the correlation. The results of the correlation suggest that the approximately 3% decrease in head loss from R4C2 to R4D2, as observed in Figure 3.21, is due predominantly to differences in the slurry preparation and not to a reduction in the debris-bed mass loading.

In Figures 3.11 and 3.12, Criterion 1 was not satisfied for R4A2 and R4D2 (target debris loading of 107.3 g/m^2). Debris bed formation was not an issue for the 1449. 5 g/m^2 target debris loading in Figures 3.9 and 3.25 (R4A2), 3.10 (R4B2), 3.26 (R4C2), and 3.27 (R4D2)]. It is readily apparent,

Figure 3.25. Example NUKON Debris Bed for R4A (target debris loading of 1449.5 g/m^2)

Figure 3.26. Example NUKON Debris Bed for R4C (target debris loading of 1449.5 g/m^2)

Figure 3.27. Example NUKON Debris Bed for R4D2 (target debris loading of 1449.5 g/m^2)

however, that surface uniformity, Criterion 2, is reduced for R4A and, to a much lesser extent, for R4B (Figure 3.10). The surface uniformity of an R4D2 debris bed was affected after being subjected to higher screen approach velocities. The screen surface (pattern) was telegraphed through the debris bed (Figure 3.28).

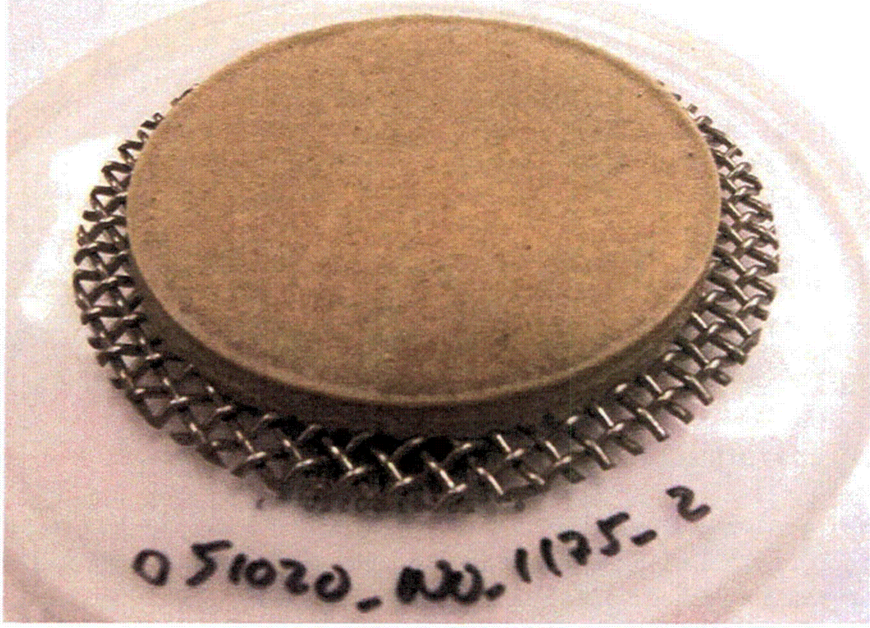

Figure 3.28. NUKON Debris Bed for R4D2 Subjected to 0.29 m/s Screen Approach Velocity (target debris loading of 1449.5 g/m^2; screen pattern perceptible on surface)

The representative debris bed height (see Section 3.2.3.2) was also affected by varying the R4 metric. For discussion, the debris beds having a target debris loading of 1449.5 g/m^2 are considered. Not surprisingly, the NUKON with no blender preparation (R4A2) resulted in the thickest debris bed, as shown in Figure 3.29. The thickness reported for R4A2 and R4B2 debris beds are the visually observed "average" heights; surface irregularities up to 1.2 and 0.2 in., respectively, were observed.

Based on the discussions in Sections 3.2.3.1 through 3.2.3.3, a NUKON debris preparation procedure that achieves an R4 of approximately 11, similar to test NS6, appears to be the best candidate to meet the debris bed criteria specified in Section 3.1.1.

The effect of debris preparation procedures on head loss for NUKON/CalSil debris beds has only been directly considered with regard to the NUKON preparation procedure as discussed above. CalSil preparation has only been indirectly examined based on a single test with the actual particulate content of the material altered, not the subsequent debris preparation. It is deemed reasonable to expect that the trend of the individual constituents, as presented for the NUKON debris, will dictate the combined debris bed response. Further, as described in Sections 3.2.3.2 and 6.3, the debris loading sequence appears to have a dominant effect on the resulting debris bed head loss. Therefore, the potential for debris preparation interaction to significantly affect the head loss of the NUKON/CalSil debris beds was not evaluated further.

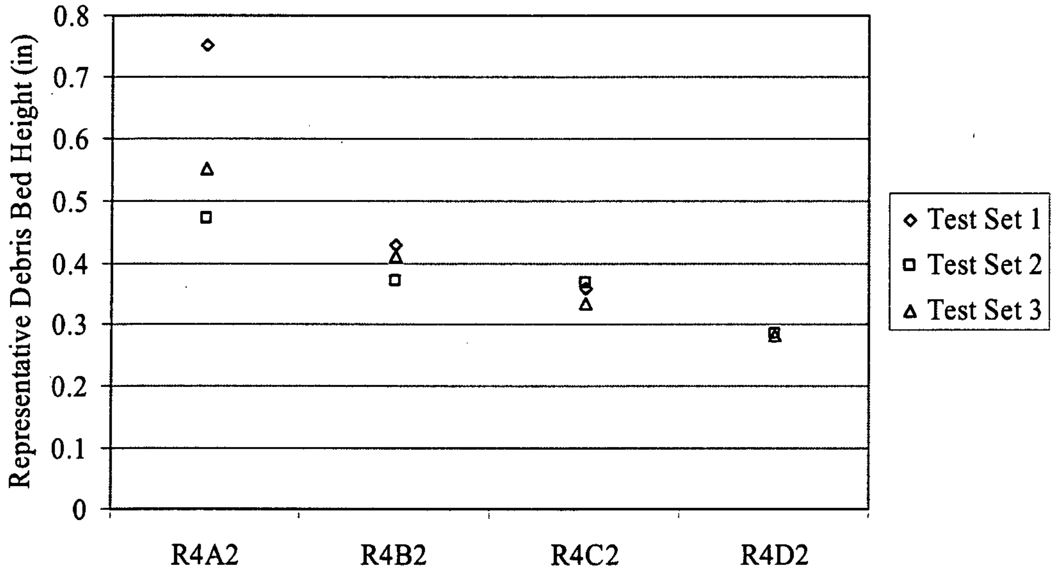

Figure 3.29. NUKON Debris Bed Height as a Function of R4 (target debris loading of 1449.5 g/m^2)

3.3 Debris Preparation Summary

The debris preparation techniques, procedures, and associated criteria developed and tested at PNNL (Sections 3.1 and 3.2) are summarized in this section. NUKON debris is addressed in Section 3.3.1, and CalSil debris is addressed in Section 3.3.2.

3.3.1 NUKON Debris Preparation

The as-received NUKON debris material was subjected to a 12- to 14-hr heat-treating process and shredded in a wood chipper by the vendor/manufacturer prior to shipment (Section 3.1). The following steps have been developed to prepare the as-received NUKON for testing. The NUKON preparation procedure is included in Appendix E.

1. Dry a quantity of as-received NUKON in an oven at a nominal temperature of 194°F (90°C) until a constant mass (within the uncertainty of the scale) is reached.
2. Select the required mass for testing from the dried material of step 1.
3. Based on a dilution ratio of 12.5 g of NUKON to 500 mL of water and the blender volume limits, and considering the indicated applicability range of the R4 metric (Section 3.2.1.1), determine the mass of NUKON to be prepared and its associated water volume. Multiple preparations of sub-batches may be required to reach a target debris loading.
4. Determine the debris preparation time necessary to achieve the desired R4 value (Section 3.1.2) and establish repeatability. To meet the debris bed criteria listed in Section 3.1.1, testing has established that the target R4 value should be 11 ±1. The resulting slurry should be observed to have a homogeneous consistency. The procedure for conducting the R4 test is provided in Appendix E.
5. The necessary blender preparation time should be reevaluated for each blender used. Additionally, the required blender preparation time should be periodically reevaluated for a given blender.

3.3.2 CalSil Debris Preparation

The as-received CalSil material was not subjected to any heat treating and was in the form of 3 x 12 x 48-in. blocks. The following steps have been developed to prepare CalSil for testing. The CalSil preparation procedure is included in Appendix E.

1. Separate material from the as-received CalSil blocks using a saw.
2. Dry the CalSil from step 1 in an oven at a nominal temperature of 194°F (90°C) until a steady mass (within the uncertainty of the scale) is reached.
3. Break off irregularly shaped chunks of approximately 0.25 to 0.75 in. in diameter from the dried material of step 2 with pliers until the required mass for testing is obtained.
4. Based on a dilution ratio of 12.5 g of CalSil to 500 mL of water and the blender volume limits, determine the mass of CalSil to be prepared and its associated water volume. Multiple preparations of sub-batches may be required to reach a target debris loading.
5. Determine the minimum mixing time necessary to produce a homogeneous slurry using the maximum R4 value of 1.55 as a guideline (Section 3.2.2) and establish repeatability.
6. The necessary preparation time should be reevaluated for each blender used. In addition, the necessary preparation time should be periodically reevaluated for a given blender.

4.0 Coating Characterization and Preparation

PNNL staff prepared Ameron's Amercoat 5450 alkyd topcoat (ALK) and Ameron's Dimetcote 6 inorganic zinc primer with Amercoat 90 epoxy topcoat (ZE) coating to serve as debris for head loss testing. Descriptions of the two tested coatings are presented in Table 4.1. The ALK and ZE coatings purchased by Ameron were applied to plastic sheets during preparation by the vendor. The plastic sheets with the coating materials attached were folded and shipped to PNNL. In Section 4.1, the preparation target slurry requirements and defining characteristics are identified. Like the insulation material, the coatings preparation procedure was referenced to an R4 criterion. Testing results for the criterion and quantification techniques for the characteristics are presented in Section 4.2. A summary of the debris preparation techniques is provided in Section 4.3.

Table 4.1. Description of Coatings Materials Used in PNNL Testing

Designation	Vendor Name/Specification	Description
ALK	Ameron's Amercoat 5450 alkyd topcoat	Single layer low density alkyd topcoat; unqualified nuclear containment coating; manufacturer, Ameron; coating name, Amercoat 5450; density, 1.35 g/cc; thickness, one coat of 1.5 mils[(a)]
ZE	Ameron's Dimetcote 6 inorganic Zn primer with Amercoat 90 epoxy topcoat	Inorganic zinc primer with epoxy-phenolic topcoat; qualified nuclear containment coating; manufacturer, Ameron; coating name, primer, Dimetcote 6; topcoat, Amercoat 90; primer density, 1.5 g/cc, topcoat, 1.75 g/cc; thickness, one primer of 2.5 mils, two topcoats of 4 mils per coat

(a) 1 mil = 0.001 in. (0.0254 mm).

4.1 Requirements and Target Characteristics Identification

ALK and ZE coatings were prepared to conditions specified by the NRC. Unlike the insulation preparation (Section 3), specific performance criteria were not identified. The NRC defined target characteristics for "processed coating" and "coating chips" (sieving process [1/4-in. square coating]).

4.1.1 ALK Coating Preparation

"Processed coating" preparation tests used 6.52 g of ALK (mass corresponds to 0.35 kg/m^2 debris loading in the PNNL large-scale loop) and 260 mL of water prepared in a Waring blender. The coating was peeled from the plastic backing, torn into pieces smaller than 6 in. square, and pressed into the bottom of the blender. Water was then added and the blender operated at low speed for three specific times. R4 tests (see Section 3) were then conducted using an 8-in.-diameter 5-mesh screen (Table 4.2). Duplicate results are provided. Figures 4.1, 4.2, and 4.3 are photographs of the debris on the screen representing each R4 test. As agreed to by the NRC, the ALK processed coating was prepared to an R4 target value of 1.4.

Table 4.2. ALK R4 Test Data

Test No.	ALK Mass (g)	Water Volume (mL)	Blender Preparation Time (sec)	R4
PN1L0	6.52	260	1	3.1
PN1L1	6.52	260	1	3.4
5N1L1	6.52	260	5	2.3
5N1L2	6.52	260	5	2.0
15N1L0	6.52	260	15	1.4
15N1L1	6.52	260	15	1.3

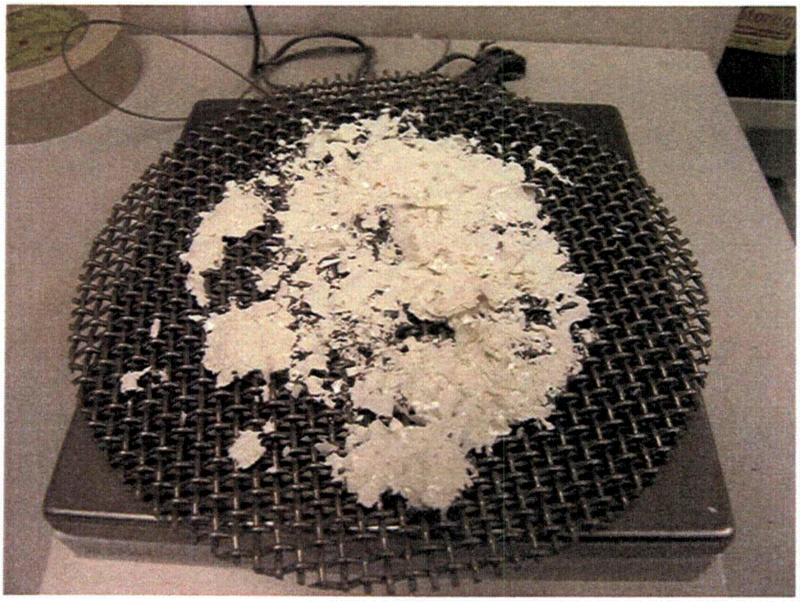

Figure 4.1. ALK Debris Poured onto 5-Mesh Screen for R4 Evaluation, R4 ~ 3.3

R4 testing of prepared ALK coating debris was also conducted for target debris loadings of 0.7 kg/m^2 (corresponds to 13.05 g in the PNNL large-scale loop and 5.68 g in the benchtop loop) and 1.4 kg/m^2 (corresponds to 26.10 g in the PNNL large-scale loop [two batches with 13.05 g ALK each to produce quantity of 26.10 g] and 11.35 g in the benchtop loop). The water volume used for each ALK mass was determined from a constant 500-mL H_2O per 12.5-g debris mass ratio (Section 3). The R4 results are shown to be essentially independent of debris mass (compared to blender preparation time in Table 4.2), as shown in Figure 4.4.

For the 1/4-in.-square coating (paint chips), the ALK coating was peeled from the plastic backing, torn into pieces less than 6 in. square, and pressed into the bottom of the blender. The blender was pulsed on high for 1 second. No water was used. A constant ALK coating mass of 6.52 g was used each time. Coating pieces larger than a 50-cent piece were separated and reprocessed in the blender with a 1-second pulse on high. The bulk coating debris was then passed through a stack of progressively smaller sieves with 0.5-, 0.265-, 0.157-, and 0.111-in. openings. To agitate the material, the sieve stack was dropped from about 2 in. onto a flat surface five times. The resulting coating mass of each size from each sieve and in the bottom receptacle are listed in Table 4.3. Figure 4.5 is a photograph of the prepared coating debris in the range 0.17 to 0.265 in.

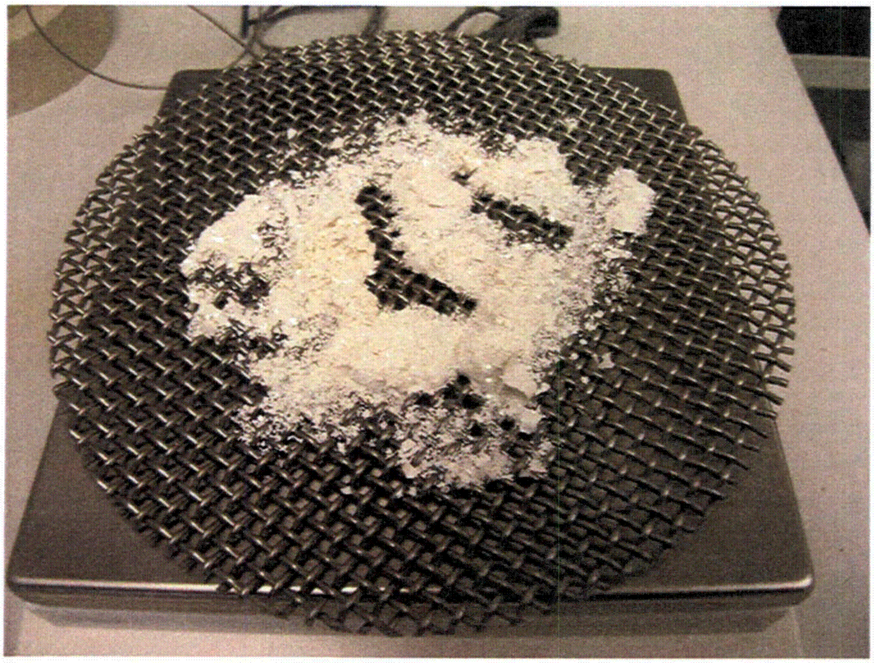

Figure 4.2. ALK Debris Poured onto 5-Mesh Screen for R4 Evaluation, R4 ~ 2.2

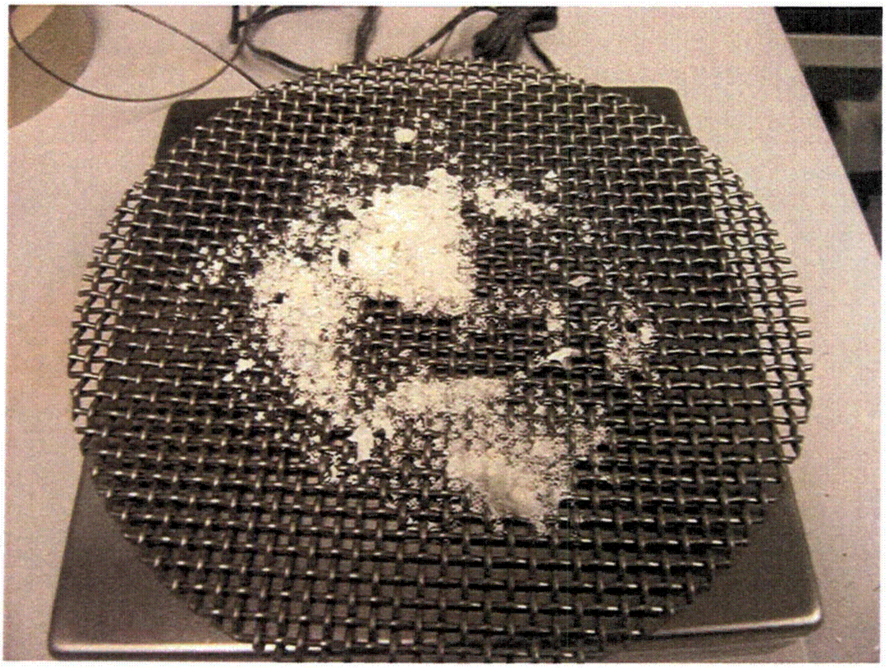

Figure 4.3. ALK Debris Poured onto 5-Mesh Screen for R4 Evaluation, R4 ~ 1.4

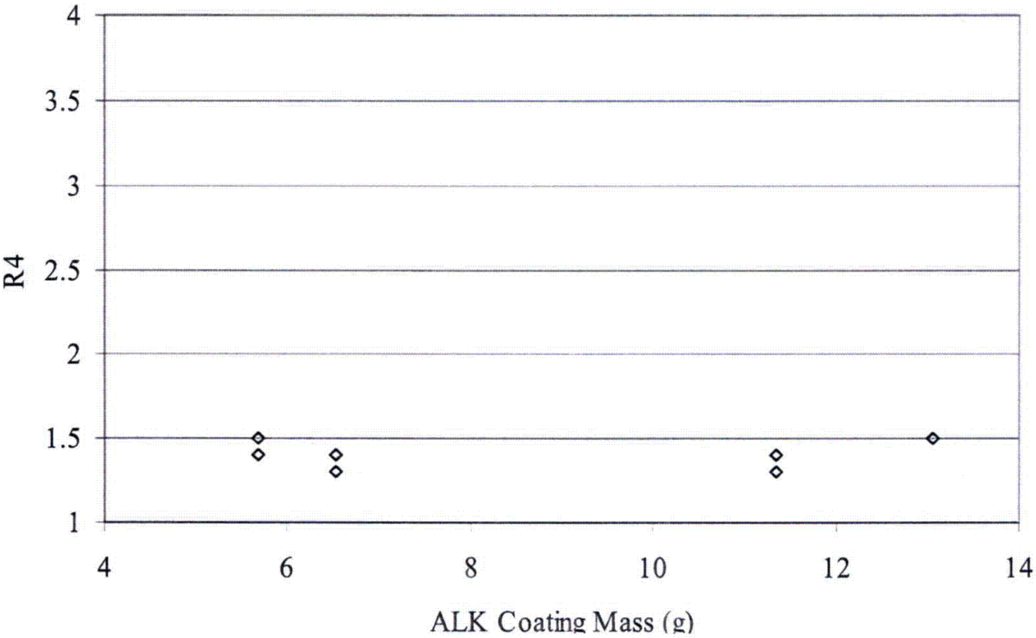

Figure 4.4. R4 as a Function of Initial ALK Coating Mass (constant 15-second blender preparation time and constant dilution ratio)

Figure 4.5. "1/4 in. Square Coating" (paint chips) for ALK Prepared Coating Debris in the Range 0.157 to 0.265 in.

4.1.2 ZE Coating Preparation Results

The "Processed Coating" tests used 13.05 g of ZE (mass equivalent to 0.7 kg/m^2 loading in the PNNL large-scale loop) and 520 mL of water prepared in a Waring blender. The coating typically broke into pieces smaller than 6 in. square when it was removed from its plastic backing. The coating was then placed into the blender, the water added, and the blender operated at low speed for three specific times. R4 tests (see Section 3) were then conducted using an 8-in.-diameter 5-mesh screen (Table 4.4). Photographs of the debris on the screen representing each R4 test are provided in Figures 4.6, 4.7, and 4.8. In agreement with the NRC, the ZE processed coating was prepared to an R4 target value of 0.5.

Table 4.3. Prepared and Sieved ALK Coating Mass by Sieve Size from Two Preparations of 6.52-g Each

Sieve Size (in.)	Mass[(a)] (g)
0.500	1.31
0.265	1.39
0.157	1.09
0.111	0.76
bottom receptacle	8.67

(a) Mass sums to greater than initial amount (13.04 g) due to measurement error associated with segregated samples.

Table 4.4. ZE R4 Test Data

Test No.	ZE Mass (g)	Water Volume (mL)	Blender Preparation Time (s)	R4
PN1L0	13.05	520	1	1.5
PN1L1	13.05	520	1	1.4
5N1L0	13.05	520	5	0.9
15N1L0	13.05	520	15	0.4
15N1L	13.05	520	15	0.6

For the ¼-in. square coating (paint chips), the coating was removed from the plastic backing, placed into a container, and then grasped 10 times with a rubber-gloved hand to break the material into finer chips. No water was used in the preparation. The process was repeated for three separate samples of nominally 25 g ZE coating. The bulk coating debris (75 g total) was then sifted through a stack of progressively smaller sieves of 0.5, 0.265, 0.157, and 0.111-in. openings. To agitate the material, the sieve stack was shaken back and forth 4 times and dropped about 2 in. onto a flat surface. The shaking and dropping sequence was repeated 5 times. The resulting coating masses of each size from each sieve and in the bottom receptacle are listed in Table 4.5. Figure 4.9 is a photograph of the prepared coating debris in the range 0.157 to 0.265 in.

4.2 Coatings Preparation Summary

The processed coating ALK and ZE coatings debris were prepared to attain R4 values of 1.4 and 0.5, respectively. The 1/4 in. square coating ALK and ZE coatings debris were prepared by sieving through progressively smaller sieves. The material in the range 0.157 to 0.265 in. was used for testing. Photos of the four different coatings debris were prepared and sent to Naval Surface Warfare Center (NSWC) for particle size characterization. The prepared photos and associated particle size distributions are included in Appendix O.

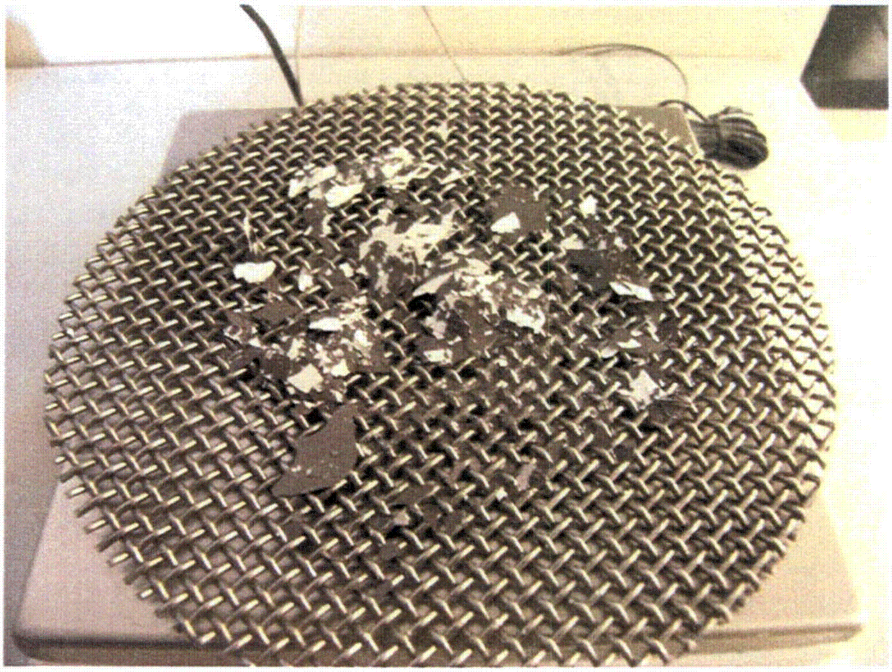

Figure 4.6. ZE Debris Poured onto 5-Mesh Screen for R4 Evaluation, R4 ~ 1.5

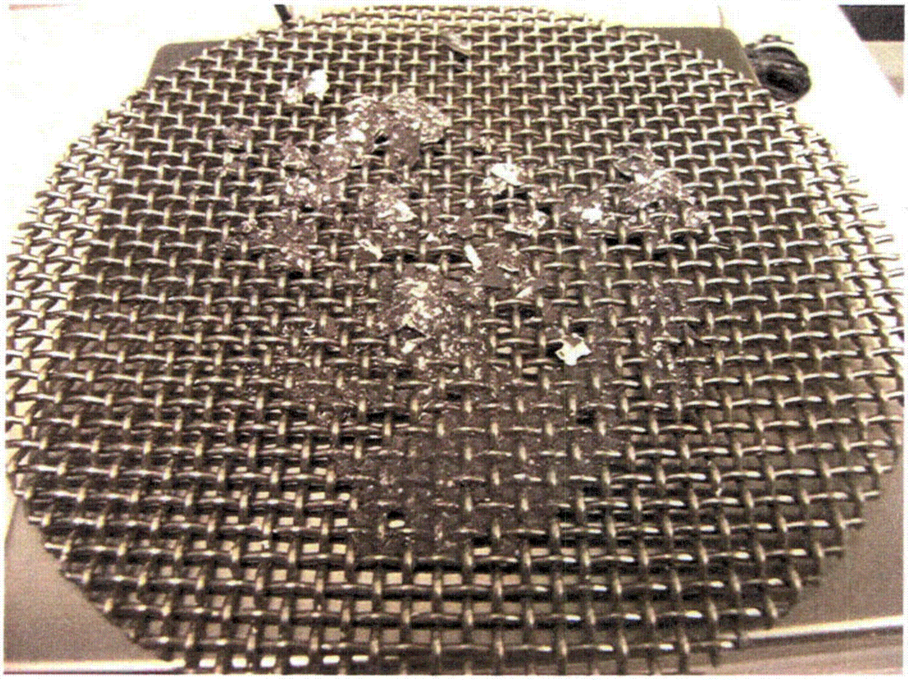

Figure 4.7. ZE Debris Poured onto 5-Mesh Screen for R4 Evaluation, R4 ~ 0.9

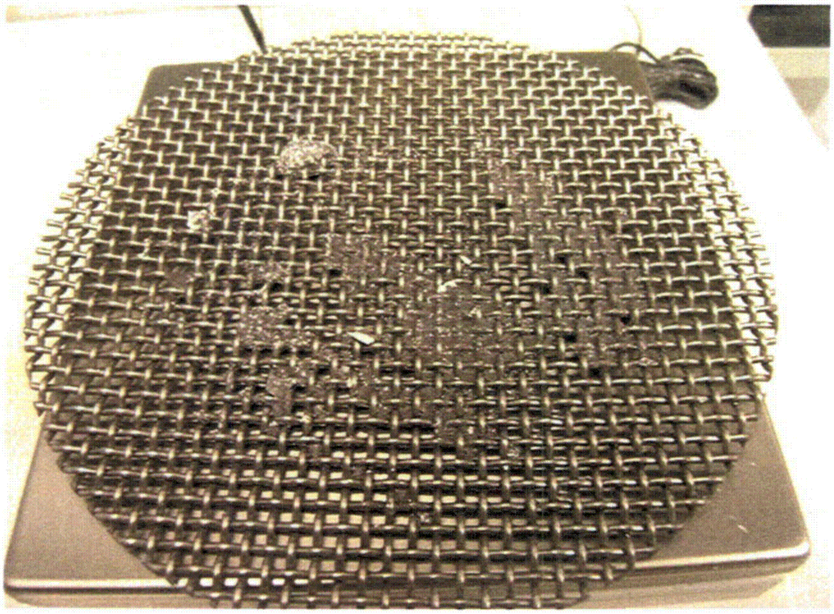

Figure 4.8. ZE, R4 ~ 0.5

Table 4.5. Mass of Prepared and Sieved ZE Coating Debris by Sieve Size from Three Preparations of ~ 25 g each for a Total Processed Mass of 75 g

Sieve Size (in)	Mass (g)
0.500	1.11
0.265	22.58
0.157	23.08
0.111	14.33
bottom receptacle	14.00

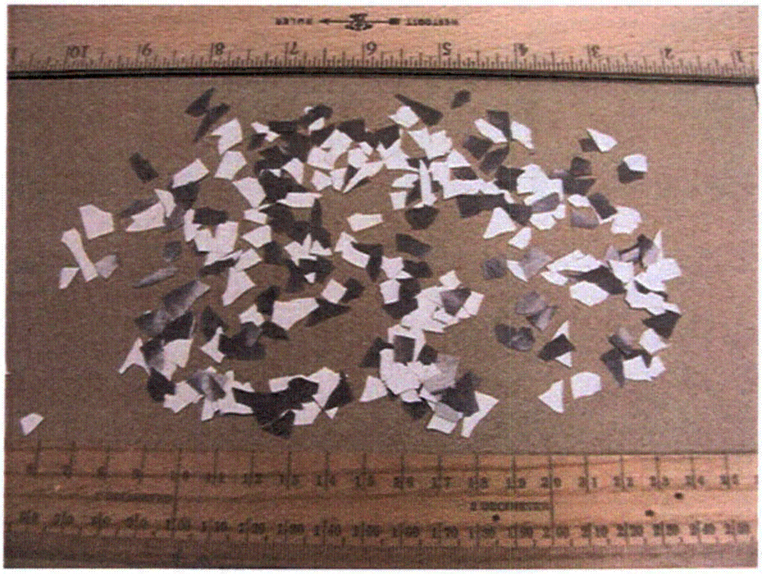

Figure 4.9. ¼-in. Square Coating ZE Coating Debris with Particle Dimensions of 0.157 to 0.265 in.

5.0 Test Matrix and Approach

This section presents the test matrix that was conducted for the PNNL debris bed head loss measurement effort in Section 5.1, discusses key factors considered in developing the test program and test procedures in Section 5.2, and in Section 5.3 provides an overview of the test procedures used to conduct the tests.

5.1 Test Matrix

Testing in the large-scale test loop was performed based on four separate test matrixes, which are referred to as Series 1, Benchmark, Series 2, and Coatings and are presented in Sections 5.1.1, 5.1.2, 5.1.3, and 5.1.4, respectively. In each section, the test matrix is described in tabular form along with a brief description of the associated test program.

In each table describing a test matrix, a test case number, test identification, mass loading for the individual debris constituents, total debris loading, nominal fluid temperature, and the screen material used are listed. The test case number was assigned to each test after the majority of the testing was completed and is intended to provide unified, simple labels that relate the tests from the separate matrixes.

For the test labels, the various test conditions are identified as SO = screen only, PO = perforated plate only, CO = CalSil only, NO = NUKON only, NC = NUKON and CalSil (denoted as NUKON/CalSil), BT = benchtop test, ALK = Ameron's Amercoat 5450 alkyd topcoat, and ZE = Ameron's Dimetcote 6 inorganic Zn primer with Amercoat 90 epoxy topcoat. The test cases are numbered in ascending order of the mass loading for each individual test condition. For the NUKON/CalSil cases (NC) the test cases are numbered according to the ascending order of the NUKON mass loading followed by the ascending order of the CalSil loading.

Some test case numbers end with a lower case letter, indicating that the same debris bed was used to conduct multiple tests. The alphabetical order of the letters indicates the order in which the tests were conducted. Thus those test cases with an "a" were conducted immediately after debris bed formation.

NO6a through NO7b and NC15a though NC17b are exceptions to the numbering order of the test cases. These test cases were added to the Series 2 test matrix after the writing of the report had been initiated, and therefore were provided sequential numbers in the order the tests were completed.

The test identification is the test name created at the time the test was executed. The test identification is the same name given to the electronic DAS file used to record the instrument readings. The associated data sheets and Quick Look reports are labeled with the test identification (ID) number. The test ID number is created from the date of the test, the test condition, the total mass of debris being introduced to the test loop, the test loop being used, screen material installed in the test loop, and the number of the test run for a given day. The test ID is written as *YYMMDD_tc_WWWW_LS#*

where

YY = two digits indicating year. (2005 = 05)
MM = two-digit number of month (August = 08)
DD = two digits representing day of the month

Tc =two-letter designation of the test condition as listed for the test case numbers above with the following exceptions used for the coatings tests:

  - P is used to designate that processed (finer sized coating particles, refer to Section 4) coating is included in the debris
  - Q is used to designate that ¼-inch chips are included in the debris
  - ALK is replaced with a "C" for coating
  - ZE is replaced with a "Z"

WWWW= four digits representing the total dry target material mass in grams being introduced to loop with two digits to the right of the decimal place (e.g., 12.03 g = 1203). Note: this is the sum of the masses for all of the debris constituents being introduced to the test loop.

L = designation of test loop. "L" for large-scale loop and "B" for benchtop loop.

S = screen material. "P" for the perforated plate with 1/8-inch holes and no indication if the 5-mesh woven-wire cloth is installed.

\# = the sequential number of the test being conducted that day: 1 = first test of the day, 2 = second test of the day, etc.

Examples of test identifications used are:

- 051123_NC_2181_L1 – This was the first test, conducted on November 23, 2005. The test was conducted in the large-scale loop with the 5-mesh woven wire cloth installed. A total of 21.81 g of debris containing both NUKON and CalSil debris material was introduced into the test loop.
- 060501_PQC_2609_LP2 – This was the second test, run on May 1, 2006. The test was conducted in the large-scale loop with the perforated plate installed. A total of 26.09 g of debris consisting of both ALK processed and ¼-inch chip material was introduced into the test loop.

The bulk of the tests conducted in the benchtop loop were performed to develop procedures and evaluate trends in the data. However, a number of benchtop loop tests were used for direct comparison to the large-scale results. These benchtop loop tests are listed in Section 5.1.5 and the associated results presented in Section 7.

In Section 7, the results of the large-scale tests are presented in separate sections for each type of test condition (e.g., NO, NC). The test series of a particular test is pertinent because slight changes were made to the test procedures for each series of tests. The variations in the test procedures for each test series are discussed in Section 5.3.

5.1.1 Series 1 Test Matrix

The Series 1 tests are listed in Table 5.1 and were the first suite of tests conducted in the large-scale test loop. The test conditions selected for the matrix were based on conditions used in a previous study of the head loss associated with sump screen debris beds (Shaffer et al. 2005). Both the initial debris loadings and the test velocity sequence from the previous study were matched for the Series 1 tests. Section 5.3 discusses the test procedures unique to the Series 1 tests. Comparisons to the pressure drop measurements obtained in the previous study are not made in this report, but some comparisons have been included in the Quick Look reports of Appendixes H and J. The far right column of Table 5.1 contains the test identification numbers used by the previous study and the Quick Look reports.

Table 5.1. PNNL Series 1 Test Matrix

Test Case No.	Test ID	Target Debris Bed NUKON Loading (g/m^2)	Target Debris Bed CalSil Loading (g/m^2)	CalSil to NUKON Mass Ratio	Total Target Debris Bed Loading (g/m^2)	Target Fluid Temperature (°C)	Screen Material Used[a]	Corresponding Test Case ID from Previous Study[b]
SO1	051114_SO_0000_L1	0	0	N/A	0	21	screen	N/A
SO2	051128_SO_0000_L1	0	0	N/A	0	21	screen	N/A
NO4	051108_NO_3067_L1	1645	0	0.00	1645	21	screen	1a
NO5	060125_NO_3067_L1	1645	0	0.00	1645	21	screen	1a
NC3	051110_NC_0595_L1	213	106	0.50	326	21	screen	6h
NC7	051121_NC_1586_L1	568	284	0.50	851	21	screen	6f
NC11	051123_NC_2181_L1	780	390	0.50	1170	21	screen	6i
NC12	051117_NC_2776_L1	993	496	0.50	1489	21	screen	6e
NC13	051128_NC_2776_L2	993	496	0.50	1489	21	screen	6e2
NC14	051115_NC_4098_L1	1419	780	0.55	2199	21	screen	6b

(a) Screen = 5-mesh woven wire cloth, plate = perforated plate with 1/8-inch holes.

(b) Test conditions were intended to match those from the previous test study conducted at the University of New Mexico under the direction of LANL (Shaffer et al. 2005).

All of the Series 1 tests used the 5-mesh woven wire and were conducted at ambient temperature. The Series 1 tests were the only large-scale tests that did not premix the debris constituents prior to introduction to the test loop. The Series 1 tests used two debris injection lines to simultaneously inject the debris constituents into the main line of the test loop.

5.1.2 Benchmark Series Test Matrix

The three Benchmark test cases listed in Table 5.2 were selected by NRC staff to be run in parallel in both the ANL and PNNL test loops. The results were to be used by the NRC to compare the two loops and evaluate the variability in the pressure drop measurements associated with multiple test loops. The results of the ANL Benchmark tests and a comparison to the PNNL results are included in NUREG/CR-6913 (Kasza et al. 2006). The R4 metric was used by both organizations to determine and monitor the debris preparation for the tests to ensure that similar material consistency was used for both suites of tests.

To match the R4 metric for both tests, ANL conducted R4 tests first and provided data to PNNL. PNNL in turn adjusted the blender mixing time to match the data from ANL. While PNNL was able to match the R4 values produced at ANL, ANL had deviated from the baseline procedure for conducting the R4 tests. The ANL operators used higher dilution rates (2500 mL water) than the base point of 12.5 g NUKON/500 mL water defined by PNNL. After matching the ANL results using 2500 mL of water, PNNL then reevaluated the R4 values immediately after blending operations in 1000 mL of water. For BM-2, the PNNL NUKON preparation provided an R4 ~ 10.8, and for BM-1 and BM-3 the R4 was ~16.4. These results suggest the NUKON preparation for BM-2 was similar to the R4 values used by PNNL for the other test series and that BM-1 and BM-3 were not. However, the debris mass-to-water volume ratio used in the final PNNL evaluations of the Benchmark R4 metric were still significantly different than the 12.5g/500 mL used as the PNNL base point. The results presented in subsection 3.2.1.2.2 indicate the R4 value decreases with increased dilution.

Table 5.2. PNNL Benchmark Series Test Matrix

Test Case No.	Test ID	Target Debris Bed NUKON Loading (g/m^2)	Target Debris Bed CalSil Loading (g/m^2)	CalSil to NUKON Mass Ratio	Total Target Debris Bed Loading (g/m^2)	Target Fluid Temp. (°C)	Screen Material Used[a]	Corresponding Test Case ID from Benchmark Test Plan[b]
NO1	060321_NO_0405_LP1	217	0	0.00	217	21	plate	BM-1
NO2	060313_NO_1349_LP1	724	0	0.00	724	21	plate	BM-2
NC8	060323_NC_1619_LP1	724	145	0.20	869	21	plate	BM-3

(a) Screen = 5-mesh woven wire cloth, plate = perforated plate with 1/8-inch holes.
(b) The Benchmark test plan was used by both PNNL and ANL to conduct the Benchmark tests and is included in Appendix **.

The final evaluations of the R4 values used for the Benchmark tests indicate that the consistency of the NUKON debris for the ANL and PNNL tests should be relatively close within the limits of the R4 metric. However, comparison of the NUKON-debris consistency between the Benchmark tests and the other PNNL test series cannot be quantified with the R4 metric due to the difference in the dilutions used for blender preparations (refer to Section 3 for effect of dilution on R4 metric). It is therefore uncertain whether the NUKON debris preparation of the Benchmark tests matches that of the other PNNL tests. The R1 through R3 metrics (Section 3) were not evaluated for comparing the ANL and PNNL Benchmark tests debris preparation.

The ANL test loop did not contain filters; therefore, the PNNL loop filters were bypassed for the benchmark tests. The far right column of Table 5.2 contains the test identification for the Benchmark tests that is used in the Benchmark test plan of Appendix L and the Quick Look reports in Appendixes H and J.

5.1.3 Series 2 Test Matrix

The Series 2 tests make up the bulk of the PNNL large-scale tests and all of the elevated temperature tests. All Series 2 tests were conducted with the perforated plate installed in the test loop, and the test fluid was filtered after ramp up 1 in the screen approach velocity. Table 5.3 lists all Series 2 tests. The far right column of the table contains the test priority number provided in the NRC proposed test matrix from the "Modification to the Statement of Work," JCN: N6106, for the performance period of 4/1/05 to 12/30/06. Reference is made to the test priority numbers in the Quick Look reports in the appendixes.

For the CalSil-only test condition CO1 (priority 2 +200%), the initial target debris loading proposed by the NRC was 1450 g/m^2. Initial tests in the benchtop loop (Sections 5.1.4 and 7.3) indicated that the original mass loading was insufficient to form a complete debris bed. Therefore, based on the results of the benchtop testing, the mass loading for the CalSil-only test condition was increased by an additional 200% over the original priority 2 mass loading.

5.1.4 Coatings

Table 5.4 contains a list of the Coatings tests, which were conducted the same way as the Series 2 tests except for changes in the screen approach velocity used for debris bed formation. Screen approach velocities as high as 0.8 ft/sec were required to transport the debris material from the debris injection tubes to the test screen.

Table 5.3. PNNL Series 2 Test Matrix

Test Case No.	Test ID	Target Debris Bed NUKON Loading (g/m^2)	Target Debris Bed CalSil Loading (g/m^2)	CalSil to NUKON Mass Ratio	Total Target Debris Bed Loading (g/m^2)	Target Fluid Temperature (°C)	Screen Material Used(a)	NRC Priority No. for Test(b)
PO1	060804_PO_0000_LP1	0	0	N/A	0	21	plate	13
PO2	060804_PO_0000_LP2	0	0	N/A	0	54	plate	13
PO3	060805_PO_0000_LP1	0	0	N/A	0	82	plate	13
NO3a	060425_NO_2703_LP1	1450	0	0.00	1450	21	plate	1
NO3b	060425_NO_2703_LP2	1450	0	0.00	1450	54	plate	1
NO3c	060425_NO_2703_LP3	1450	0	0.00	1450	82	plate	1
NO6a(c)	060731_NO_2703_LP1	1450	0	0.00	1450	54	plate	1
NO6b(c)	060731_NO_2703_LP2	1450	0	0.00	1450	21	plate	1
NO7a(c)	060802_NO_2703_LP1	1450	0	0.00	1450	82	plate	1
NO7b(c)	060802_NO_2703_LP2	1450	0	0.00	1450	54	plate	1
CO1a	060512_CO_8108_LP1	0	4350	N/A	4350	21	plate	2 +200%(d)
CO1b	060512_CO_8108_LP2	0	4350	N/A	4350	54	plate	2 +200%(d)
CO1c	060512_CO_8108_LP3	0	4350	N/A	4350	82	plate	2 +200%(d)
NC1	060427_NC_0252_LP1	108	27	0.25	135	21	plate	7
NC2	060428_NC_0453_LP1	108	135	1.25	243	21	plate	8
NC4	060509_NC_0505_LP1	217	54	0.25	271	21	plate	9
NC5a	060426_NC_0708_LP1	217	163	0.75	380	21	plate	6
NC5b	060426_NC_0708_LP2	217	163	0.75	380	82	plate	6
NC6a	060517_NC_0808_LP1	217	217	1.00	434	21	plate	N/A
NC6b	060517_NC_0808_LP2	217	217	1.00	434	82	plate	N/A
NC9	060331_NC_2024_LP1	724	362	0.50	1086	21	plate	4
NC10	060404_NC_2698_LP1	724	724	1.00	1448	21	plate	5
NC15a(c)	060807_NC_0708_LP1	217	163	0.75	380	54	plate	6
NC15b(c)	060807_NC_0708_LP2	217	163	0.75	380	21	plate	6
NC16a(c)	060809_NC_0708_LP1	217	163	0.75	380	82	plate	6
NC16b(c)	060809_NC_0708_LP2	217	163	0.75	380	54	plate	6
NC17a(c)	060817_NC_2024_LP1	724	362	0.50	1086	54	plate	4
NC17b(c)	060817_NC_2024_LP2	724	362	0.50	1086	21	plate	4

(a) Screen = 5-mesh woven wire cloth, plate = perforated plate with 1/8-inch holes.
(b) Test Priority number from the "Modification to the Statement of Work" for the performance period of 4/1/05 to 12/30/06.
(c) Debris bed formed at an elevated fluid temperature.
(d) The initial priority 2 test called for a CalSil mass loading of 1450 g/m^2. Benchtop testing demonstrated this to be insufficient mass loading to form a complete debris bed. Therefore, the mass loading for the large-scale test was increased an additional 200% (refer to Section 7.3).

Table 5.4. PNNL Coatings Materials Test Matrix

Test Case No.	Test ID	Target Debris Bed Processed Coating Loading (g/m^2)	Target Debris Bed 1/4 in. Square Coating Loading (g/m^2)	Total Target Debris Bed Loading (g/m^2)	Target Fluid Temperature (°C)	Screen Material Used(a)
ALK1a	060501_PQC_2609_LP1	700	700	1,400	21	plate
ALK1b	060501_PQC_2609_LP2	700	700	1,400	82	plate
ALK2	060502_POC_2609_LP1	1400	0	1,400	21	plate
ZE1	060504_PQZ_2609_LP1	700	700	1,400	21	plate
ALKBT	060428_PQC_1136_BP1	700	700	1,400	21	plate

(a) Screen = 5-mesh woven wire cloth, plate = perforated plate with 1/8-inch holes.

5.1.5 Benchtop Tests

The PNNL test program used the benchtop loop to conduct 79 NUKON-only, 8 CalSil-only, 25 NUKON/CalSil tests, and 1 Coatings test. These tests were conducted to assess debris preparation procedures and associated metrics; develop the debris loading system design, technique, and procedures; investigate the effects of the debris loading sequence; evaluate repeatability and data trends such as with flow history; and provide initial scoping results to help refine the test matrix and velocity sequence. The bulk of the benchtop results are discussed in Sections 3 and 6.

Table 5.5 includes a list of benchtop tests that were conducted in the same manner as the large-scale tests and whose results are included in the presentation of large-scale results in Section 7. The head loss measurements from these tests are included in the Quick Look reports for the related large-scale test cases listed in the far right column of Table 5.5. The test matrixes for the additional NUKON-only and NUKON/CalSil tests conducted in the benchtop loop are included in Appendixes M and N.

Table 5.5. PNNL Benchtop Tests Directly Associated with Large-Scale Test Conditions

Test Case No.	Test ID	Target Debris Bed NUKON Loading (g/m^2)	Target Debris Bed CalSil Loading (g/m^2)	CalSil to NUKON Mass Ratio	Total Target Debris Bed Loading (g/m^2)	Target Fluid Temperature (°C)	Screen Material Used[(a)]	Related Large-Scale Test Case No.
NOBT1	060223_NO_1363_B1	1681	0	0	1681	21	screen	NO6, NO7
NOBT1	060228_NO_1363_B1	1681	0	0	1681	21	screen	NO6, NO7
COBT1	060406_CO_1176_BP1	0	1450	N/A	1450	21	plate	CO1a, CO1b, CO1c
COBT2	060510_CO_1469_BP1	0	1812	N/A	1812	21	plate	CO1a, CO1b, CO1c
COBT3	051227_CO_0411x_B1	0	2174	N/A	2174	21	screen	CO1a, CO1b, CO1c
COBT4	051227_CO_1763_B2	0	2174	N/A	2174	21	screen	CO1a, CO1b, CO1c
COBT5	060510_CO_1763_BP2	0	2175	N/A	2175	21	plate	CO1a, CO1b, CO1c
COBT6	060510_CO_2351_BP3	0	2900	N/A	2900	21	plate	CO1a, CO1b, CO1c
COBT7	060511_CO_3527_B2	0	4350	N/A	4350	21	plate	CO1a, CO1b, CO1c

(a) Screen = 5-mesh woven wire cloth, plate = perforated plate with 1/8-inch holes.

5.2 Approach for Developing Test Procedures

The test preparation procedure is specified in an attempt to control the initial conditions at which the debris bed is formed on the screen. Test preparation consists of establishing the test loop conditions, preparing of the debris material, introducing the debris to the test loop, and forming the debris bed.

This section summarizes the approach taken to meet the objectives presented in Section 1.2. The primary driver in developing the test setup and test procedures was to maximize the repeatability of the head loss measurements obtained from separate debris beds having the same debris mass loading, ratio of debris constituents, and flow conditions (screen approach velocity and fluid temperature). To accomplish this, an attempt was made to identify the parameters to which the resulting pressure drop across the debris bed may be sensitive and then to ensure those parameters were monitored and controlled. The goal was to ensure that scatter obtained in the measured data would be due to random uncertainty and variability in the debris bed formation as opposed to changes in a critical parameter not being monitored or held constant.

The main parameter postulated to have a significant impact on the head loss was the structure of the debris bed. In other words, given the same quantity of debris materials, it was assumed that a wide range of pressure drops could be obtained for a given screen approach velocity depending how the material was loaded onto the screen. Therefore, controlling the initial conditions of the test that may influence the debris bed formation or structure of the final debris bed was given significant attention. These parameters included:

- The size or consistency of the debris material introduced into the loop. Repeatable debris preparation procedures and methods for characterizing the resulting debris were determined to be critical for obtaining repeatable results. Therefore, a significant effort was put forth to develop debris preparation procedures, evaluate the impact of changes to the debris preparation procedures, and monitor or characterize the prepared debris materials. The goal was to introduce the same material into the loop each time.
- The rate, concentration, and order in which debris reaches the test screen. It was postulated that the structure of the debris bed (and thus the resulting pressure drop) might vary if the order in which the various components of the debris were applied to the screen was altered. Therefore, significant emphasis was placed on developing a debris injection system and associated procedures that provided repeatable injection of the debris material into the flow stream upstream of the test screen. Emphasis was also placed on ensuring that the process could be monitored.
- The test screen configuration. To eliminate pressure drops associated with discontinuities in the flow path or complications associated with an unsecured screen, the test screen was designed so the screen material terminated at the pipe wall with no support structure affecting the flow path and no crevice in the pipe wall to retain debris material. To ensure the test screen could not flutter, vibrate, or change configuration, the screen was secured in a support collar that was sandwiched between the two halves of the custom-fabricated TTS.

The intent was to use the same material for each test and apply it to the test screen in the same manner each time. Therefore, the structure of the debris beds for repeat tests would only differ due to the variability associated with the deposition of the debris on the screen.

The second priority was to ensure that the measured pressure drop across the debris bed corresponded to known conditions on the screen. After debris bed formation, numerous data points were recorded as the screen approach velocity was varied. The desire was to ensure the measured pressure drop could be associated with a well-characterized debris bed. To assist with improving the characterization of the debris, the following issues were addressed:

- Continual formation of the debris bed. Initial benchtop tests indicated that a significant fraction (on the order of 0.15 to 0.4) of the target mass loading was not being retained on the screen during the duration of loop operation. It was postulated that debris material may continue to be deposited on the debris bed as the capture efficiency of the debris bed improved with increased debris accumulation. If this were the case, the concern existed that for most of the pressure drop measurements made across the debris bed, the mass loading would be unknown. To address this issue, minimum debris bed formation criteria (e.g., number of loop circulations) were specified in the procedures, and a bag filter system was added to the test loop. The filter system allowed suspended debris material to be filtered from the flow at any prescribed point during a test, thus reducing the potential for mass addition to occur during a test.

- In situ characterization of the debris bed. To obtain characterization of the debris bed at each velocity point, several systems for in situ characterization of the debris bed and flow stream were investigated. The development of an optical triangulation system for obtaining in situ debris bed height measurements was pursued, and a system was installed at the end of the Series 1 tests. The in situ bed height measurements allowed changes in the debris bed thickness to be monitored at each velocity point.
- Determining mass loading of individual constituents on the test screen. With the benchtop result indicating that 15 to 40% of the target mass would not be retained on the test screen, mass measurements indicated that the uncertainty in the CalSil mass loading for NUKON/CalSil debris beds would exceed 100%. These high uncertainties would make it difficult to evaluate trends in the debris bed pressure drop associated with the CalSil mass loading. To resolve the issue, Ca^{++} ISE probes were employed to determine the concentration of CalSil from HCl solutions used to dissolve the retrieved debris beds.

The following additional issues were addressed to reduce the variability in the test results:

- The presence of gas in the fluid and potentially the debris bed as the pressure drop within the test loop is increased. To eliminate pressure drop associated with a gas phase and the variability that could exist if the presence of gas was periodic, an argon cover gas system was applied to the expansion tank so that the static pressure of the entire test loop could be raised to maintain gas in solution.
- Flow profile upstream of the test screen. To minimize changes or disruptions to the flow field as the screen approach velocity is varied (e.g., swirl component) 20-plus diameters of straight seamless pipe were installed upstream of the test screen. To ensure steady, true pressure-drop measurements, 10-plus diameters of straight seamless pipe were installed downstream of the test section allowing for the downstream pressure tap to be located 10 diameters downstream of the test section.
- Contamination from settled debris and cleaning of the test loop. The benchtop testing demonstrated that insulation debris materials that settled in sections of pipe or flex hose were readily mobilized and flushed at higher fluid velocities. However, the testing also indicated that the debris materials, especially CalSil, had an affinity for crevices such as those created by flanged joints. This created the potential for contamination from settled materials and having to perform extensive, time-consuming cleaning operations. To reduce the impact of this issue, the pipe was butt-welded as much as possible, and flex hoses that were readily removed for inspection and cleaning were used in the large-scale loop.

5.3 Overview of Test Procedure

This section provides an overview of the procedures used to conduct the head loss tests. Each series of tests was conducted with a fixed set of procedures with several exceptions:

- The screen approach velocity during the Series 1 tests was changed from 0.2 ft/sec to 0.1 ft/sec (refer to Section 5.3.2).

- During the test program, several changes were made to the debris bed retrieval procedure in an attempt to increase the reliability of the process to recover the debris bed intact.

Slight changes were made to some procedures between test series. These changes will be summarized in the following sections. Unless otherwise noted, the description of the procedures applies to all of the test series described in Section 5.1.

There are several instances where the test operators deviated from the test procedures due to extenuating circumstances related to the individual tests. Examples include:

- Omitting the velocity sequence from Test Case NC10 due to the high head loss encountered at the completion of the debris bed formation.
- Repeating the velocity sequence for ALK2 after the peak screen approach velocity was increased to mobilize material and allow the bed formation process to continue.

Instances where a deviation from the test procedure occurred are explained in the individual Quick Look Reports, which are in Appendixes G through K. Section 5.3.1 discusses the pretest preparations, Section 5.3.2 discusses the test procedure used to obtain the head loss measurements, and Section 5.3.3 discusses the post-test operations and debris bed assessment.

5.3.1 Pretest Preparation

The Series 1 tests used laboratory process water and the Benchmark and Series 2 tests used DI water with a conductivity < 2 µS/cm. After each Series 1 test, the entire inventory of water was drained from the loop for disposal. For the Series 2 and Benchmark tests, the DI water was drained to a holding tank and reused. The conditioning of the water after each test consisted of circulating the water for multiple passes through a 10-µm bag filter. To control biological growths in the test fluid, the loop inventory was treated periodically with Mt. Hood 480 biocide, as prescribed in vendor instructions. Because of the rubber flex hoses used in the test loop, the conductivity of the DI water was increased using potassium chloride (KCl) to ensure protection of the instrumentation from the buildup of static charge. The salt was added to reach a target conductivity on the order of 80 µS/cm. Approximately 32 g of KCl were added to an inventory of approximately 200 gal of DI water. Periodic adjustments were made as water inventory was lost, and additional DI water was added. The conductivity of the process water was measured to be approximately 160 µS/cm.

Prior to testing, the screen material was placed in the TTS and the loop filled with water. When the perforated plate was installed, the rounded edges of the perforations were placed facing upstream. The loop was degassed by circulating the loop inventory through the main line with the isolations valves partially closed to increase the local pressure drop and drive gas out of solution. The flow rate through the loop was periodically reduced and passed through the bag filter housing where the configuration of the filter housing and the filter itself helped to scrub gas bubbles from the flow. The accumulated gas was then bled/purged from the top of the filter housing.

DAS instrument checks included:

- Purging the delta-pressure transmitter manifold, isolating each transmitter and using the transmitter bypass valves to check the true instrument zero readings.

- Isolating the high-pressure side of the delta-pressure transmitter array manifold and comparing the water column readings for all of the transmitters installed.
- Isolating the Micro Motion flow meters and performing zero checks.
- Closing the main line throttle valve so that all main line flow passed through the injection lines, this flow configuration put the main line Micro Motion in Series with the injection line Micro Motions. The mass flow readings for the main line Micro Motion were compared for consistency to those from the injection line units through the upper range limit of the injection line Micro Motions.

DAS zero readings were recorded and the screen approach and injection line velocities adjusted to 0.1 ft/sec and 0.8 ft/sec, respectively except as noted above. After the adjustment of the flow rates, the test loop was considered ready for debris injection.

5.3.1.1 Debris Preparation

The NUKON debris preparation for all test series except the Benchmark series targeted an R4 value of 11±1. The debris preparation was conducted as specified in Section 3.3. The variations to the debris preparation for the Benchmark tests are discussed in Section 5.1.2.

The debris preparation was always performed after the test loop had been prepared for testing and the initial screen approach and injection line velocities had been set. Following preparation, the debris slurry was continually agitated as it was taken from the wet lab to the test loop.

5.3.1.2 Debris Injection and Debris Bed Formation

For the Series 1 tests, the CalSil and NUKON materials were prepared separately and introduced into the loop using independent injection loops for each constituent. The constituents were introduced into the test loop simultaneously but had no interaction before entry into the test loop. Based on the variation in the head loss measurements obtained between tests from the Series 1 tests, it was postulated that the Series 1 debris introduction procedure created variability in the sequence at which debris material arrived at the test screen. To investigate the variation observed in the Series 1 head loss measurements, the debris loading sequence investigation presented in Section 6.3 was conducted. Following the investigation of the loading sequence, the NRC staff decided that future tests would be conducted by premixing the debris constituents prior to introduction into the test loop.

For the Benchmark and Series 2 NUKON/CalSil tests, the debris material was prepared separately but then mixed together prior to introduction into the debris injection line. For NUKON-only and CalSil-only tests, no difference existed in the debris injection procedures.

To introduce the debris slurry to the debris injection lines, the flow through the injection line(s) was terminated and the injection-line flex hose isolated. The debris slurry was then poured into the debris injection-line flex hose and water added to fill the hose. The connection of the injection line hose allowed an air bubble to be trapped in the injection line flex hose. With the injection line hose isolated from the rest of the injection line, the air bubble was used to continually agitate (performed manually) and disperse the debris material within the flex hose.

The debris injection system contained two parallel injection lines so that debris constituents could be loaded separately or with a lag time between debris introductions. If the second line was used, the first hose was manually manipulated while the second hose was filled and similarly manipulated. To initiate the introduction of debris to the test loop the debris injection line isolation valves were opened.

The first Series 1 tests were conducted with the screen approach velocity initially set to 0.2 ft/sec, and the pump speed was held constant as debris accumulated on the test screen. The pressure drop across the screen increased with the accumulation of debris on the screen, and the resulting screen approach velocity was allowed to decline. Tests NO4, NC3, and NC14 were conducted in this manner. Following test NC14, NRC staff determined that the debris beds should be formed at a constant screen approach velocity of 0.1 ft/sec. Therefore, for the remainder of the test program, the screen approach velocity was set to 0.1 ft/sec and the pump speed adjusted as needed to maintain the constant screen approach velocity.

Because of the slow buildup in head loss observed during debris bed formation in the benchtop loop, a minimum requirement of 20 loop circulations was specified before the steady-state criterion could be evaluated for the completion of the debris bed formation process. For the first three tests of Series 1, the minimum circulation requirement took approximately 95 minutes, which was extended to 185 minutes (20 circulations at 0.1 ft/sec) for the remainder of the Series 1 tests and the Benchmark tests.

In reviewing the test data for debris bed formation from the Benchmark tests, it was observed that the head loss across the debris bed was fairly constant after approximately 6 to 7 calculated circulations through the loop—approximately one hour. A more substantial impact to the head loss appeared to be created by cycling the screen approach velocity. Therefore, for the Series 2 tests, the minimum bed formation time was reduced to one hour at 0.1-ft/sec screen approach velocity from the time the debris material initially reached the screen/plate.

The DAS recorded instrument readings throughout the debris bed formation process. However, transient head loss associated with debris bed formation is beyond the scope of this report and is not presented. Following the minimum number of circulations (debris bed formation time) required for bed formation, the steady-state criterion was evaluated for acceptance.

The Series 1 tests were conducted at higher screen approach velocities and therefore at higher-pressure drops than the rest of the tests. The Series 1 steady-state criterion used for debris bed formation was less than a 2-in. change in the head loss over a span of 10 minutes.

For the Benchmark and Series 2 tests, the steady-state head loss criterion for debris bed formation following the completion of the minimum number of circulations was an absolute change in head loss of less than 2% over 10 minutes based on a 1-minute running average. The criterion is expressed as

$$0.02 \geq \left| \frac{\Delta P_{t_1} - \Delta P_{t_2}}{\Delta P_{t_1}} \right|$$

where

ΔP_{t1} = the measured head loss across the bed at time t_1.

ΔP_{t2} = the measured head loss across the bed at time t_2.

$t_1 - t_2 \geq 10$ minutes

Following the completion of the minimum bed formation time and achieving the steady-state criterion, the debris bed was visually observed to determine whether a complete debris bed was formed. A complete debris bed was defined as a debris bed that covered the entire screen leaving no open channels for preferential flow. If a complete debris bed had been formed, the pretest procedure was considered complete, and the test procedure was initiated.

If a complete debris bed had not formed, the following steps were executed:

1. Head loss measurements were taken at 0.1 ft/sec after the bed formation criteria with respect to steady state head loss had been met.
2. The screen approach velocity was increased to 0.2 ft/sec for 20 minutes and observations made as to whether the debris bed formation process was continuing such that channeling would be mitigated. After 20 minutes at 0.2 ft/sec:
    a. If the visual observation of the debris bed surface indicated the channeling was being mitigated, the head loss was monitored for acceptance of the bed formation criterion assuming time zero started at the completion of the initial 20-minute duration at 0.2 ft/sec.
        i. If a complete debris bed had formed and no channeling existed, then steady-state data were recorded for test point No. 2 (refer to Table 5.8 in Section 5.3.2), filtering was initiated, and execution of the normal test procedure continued from the point of filtration.
        ii. If the bed formation criteria were met but channeling existed, proceed to item b.
    b. If visual observation of the debris bed surface indicated that the channeling was not being reduced and minimal change in the head loss was observed (steady state criterion < 0.05), then filtering was initiated. The velocity sequence matrix in Table 5.8 was replaced with the velocity sequence presented in Table 5.6.

Table 5.6. Truncated Velocity Sequence for an Incomplete Debris Bed

Test Point	Velocity (ft/sec)	Test Phase
Initial condition	0.10	Bed formation
1	0.10	Increase in static pressure of test loop ramp up 1
2 (prefiltering)	0.20	Ramp up 1 (prefiltering)
2 (post-filtering)	0.20	Ramp up 1 (post-filtering)
3	0.10	Ramp down 1
5	0.02	Ramp down 1
6	0.10	Ramp up 2

5.3.2 Test Procedure

While data was recorded throughout the entire debris injection and debris bed formation process, the actual testing was considered to begin after the debris bed had been formed. At the completion of bed formation the following were recorded:

- Optical triangulation photographs of the debris bed (optical triangulation system not available for the Series 1 tests)
- Manual in situ measurements of the debris bed thickness
- Time duration between debris introduction and steady-state head loss readings.

After the minimum bed formation time and the steady-state criterion for debris bed formation had been met, the static pressure of the test loop was increased using the cover gas pressure in the expansion tank. To maintain gas in solution and avoid gas bubbles during testing, the pressure was raised approximately 2.5 atm (37 psi [253 kPa]). After the loop pressure had been set, execution of the velocity sequence was initiated.

For the Series 1 tests, the velocity sequence for each test was determined from the velocities used in the past study (Shaffer et al. 2005). Therefore, the velocity sequence used for each Series 1 test was unique. Tables 5.7 and 5.8 contain the velocity sequences used for the Benchmark and Series 2 tests.

At each test point in the velocity sequence, the head loss was monitored for steady-state conditions. The steady-state criteria were the same as those specified for bed formation with the time duration cut in half. For the peak velocity at the end of each velocity ramp up, the steady-state criterion was the same as that for debris bed formation. After steady-state conditions were reached at each test point, the debris bed was photographed with the optical triangulation system, and in situ manual measurements of the debris bed height were recorded.

For the Series 1 and Benchmark tests, no filtering of the test fluid was performed during the test. For the Series 2 tests, after steady-state conditions were reached at the completion of ramp up 1 (0.2 ft/sec), the entire main line flow was diverted through the 10-µm bag filter. Filtering was conducted for a minimum of 20 minutes and was maintained until the steady-state criterion for a peak flow was reached. After reaching steady-state conditions, the main-line valve configuration was returned to bypassing the bag filter housing. Testing continued through the remainder of the velocity sequence with no additional filtering.

Table 5.7. Velocity Sequence for the Benchmark Tests

Test Point	Velocity (ft/sec)	Test Sequence
Initial condition	0.10	Bed Formation
1	0.10	Increase in static pressure of test loop Ramp down 1
2	0.05	Ramp down 1
3	0.02	Ramp down 1
4	0.05	Ramp up 1
5	0.10	Ramp up 1
6	0.05	Ramp down 2
7	0.02	Ramp down 2
8	0.10	Ramp up 2
9	0.15	Ramp up 2
10	0.20	Ramp up 2
11	0.15	Ramp down 3
12	0.10	Ramp down 3
13	0.15	Ramp up 3
14	0.20	Ramp up 3
15	0.10	Ramp down 4
16	0.05	Ramp down 4
17	0.02	Ramp down 4
18	0.10	Ramp up 4

Table 5.8. Velocity Sequence for the PNNL Series 2 Tests

Test Point	Velocity (ft/sec)	Test Phase
Initial condition	0.10	Bed Formation
1	0.10	Ramp up 1
2 (prefiltering)	0.20	Ramp up 1 (prefiltering)
2 (post-filtering)	0.20	Ramp up 1 (post-filtering)
3	0.10	Ramp down 1
4	0.05	Ramp down 1
5	0.02	Ramp down 1
6	0.10	Ramp up 2
7	0.20	Ramp up 2
8	0.10	Ramp down 2
9	0.02	Ramp down 2
10	0.10	Ramp up 3
11	0.20	Ramp up 3
12	0.10	Ramp down 3
13	0.02	Ramp down 3
14	0.10	Ramp up 4

At the completion of the velocity sequence, if the test fluid was not to be heated, the test was considered complete, and the post-test procedure was initiated to retrieve the debris bed.

If the test fluid was to be heated, the heaters were turned on to the desired temperature set point. The screen approach velocity was maintained at 0.1 ft/sec, and the fluid temperature was monitored. At the completion of the heat up, the velocity sequence was repeated.

5.3.3 Post-Test Procedures

At the completion of testing, the main objective was to recover the debris bed intact. Debris bed retrieval is discussed in Section 5.3.3.1. The post-test evaluation of the debris bed consisted of obtaining post-test debris bed height measurements with the debris bed still in the TTS and obtaining the dry retrieved mass of the debris bed. The post-test measurements are described in Section 5.3.3.2

The intact NUKON/CalSil debris beds were dissolved to determine the retrieved CalSil mass loading. The CalSil assessment is discussed in Section 5.3.3.3. The other possible post-test evaluation consisted of sectioning the debris bed (see Sections 2.5.4.3 and 6.4). Only debris beds from the benchtop loop were sectioned. No sectioning of the large-scale debris beds was performed, and the sectioning process is not described in this section. The current methodology does not allow a debris bed to be both sectioned and assessed for CalSil content. Both processes use and consume the entire debris bed.

5.3.3.1 Debris Bed Retrieval

The debris bed retrieval procedure will not be described in detail because it was continually being refined to enhance the chances of recovering the intact debris bed. The critical requirements for successfully retrieving the debris beds were:

- Maintaining a positive flow through the debris bed until the water was drained below the debris bed
- Avoiding the release of gas bubbles or exposure of the bed to pressure pulses, either of which could rupture the debris bed or cause the bed to lift off the screen.

Initially, the argon cover gas was used to generate flow through the debris bed and ensure a positive differential pressure existed across the debris bed until the loop was successfully drained and vented. Later in the test program an additional drain valve was added to the discharge of the test loop pump. The drain line allowed the loop's main pump to be used to continually draw flow though the debris bed while discharging fluid from the loop. After the test loop was drained and vented, the TTS was removed from the test loop with the debris bed still intact within the TTS.

5.3.3.2 Post-Test Evaluation

While the debris bed was still intact in the TTS, the top of the TTS was used as a reference plane to obtain a coarse topography of the retrieved debris bed. A metal scale was used to obtain measurements from the debris bed surface to the reference plane at the top of the TTS. The measurements were taken along two perpendicular diameters of the TTS. The reference position of the screen was used to transform the measurements into debris bed heights.

The debris bed and test screen were then removed from the TTS, and the debris bed was photographed. The wet debris bed mass was obtained. The debris bed was placed in a fume hood and allowed an initial drying period at ambient conditions for several hours to several days. Final drying consisted of placing the debris in a 194°F (90°C) oven and periodically measuring the debris bed mass until constant readings were obtained.

5.3.3.3 CalSil Assessment

For the NUKON/CalSil debris beds, the effects of the CalSil mass loading and the CalSil-to-NUKON mass ratio on the resulting pressure drop across the debris bed were to be evaluated. Benchtop testing demonstrated that for some of the proposed NUKON/CalSil mass loadings, the test screen only retained approximately 60 to 85% of the target mass loading based on mass measurements of the initial constituents introduced into the loop and the dry mass of the retrieved debris bed. The benchtop results indicated that for some of the proposed NUKON/CalSil test cases, the uncertainty in the CalSil mass loading based on the mass measurements would be well over 100%.

Therefore, a method was desired to either separate the CalSil from the NUKON or detect the concentration of one of the constituents. After a preliminary investigation, the process of dissolving the debris beds in an HCl solution consisting of 37.6% HCl diluted in DI water at a ratio of 2:3 and detecting the concentration of calcium using a calcium ion selective electrode (ISE) was chosen (see Section 2.5.4.2).

The ISE probe voltage is a function of the calcium concentration in solution. However, there may be other factors (i.e., constituents) that influence the resulting ISE probe reading when submerged in an unknown solution. The approach used for assessing the CalSil mass content was to correlate the CalSil concentration in performance standards with the ISE probe voltage. To develop the performance curve, performance standards of varying CalSil concentrations in HCl solutions were generated over the range of interest defined by the spectrum of target CalSil mass loadings in the varying test series. Based on the effective concentration range of the ISE probe, which is ion specific, aliquots were prepared from the performance standards. The process of preparing the aliquots included adding sodium hydroxide (NaOH) to neutralize them to a pH of 7 and adding potassium chloride (KCl) as an ionic strength adjuster.

Because the ISE probe readings can change with time due to aging or contamination of the membrane, a fixed performance curve was not used. The aliquots from the performance standards were measured at the time that aliquots from the debris beds were evaluated. Therefore, the performance curves were generated for a specific set of measurements taken at a specific time. The objective was to obtain relative probe readings from known samples and correlate the readings to the CalSil concentration. The probe reading from the debris bed sample was then used to predict a CalSil concentration in the debris bed aliquot through inverse linear regression. Knowing the dilution used to generate the debris bed aliquot, the concentration of CalSil in the dissolved debris sample can then be calculated.

In developing the performance curve for the ISE probe, the following parameters should be considered:

- the number of CalSil concentrations at which performance standards are made
- the number of performance standards made for each concentration
- the number of aliquots drawn from each performance standard
- the number of readings taken in each aliquot
- the number of ISE probes used to obtain the readings.

Based on the time and resources required to perform the assessment, it is much more efficient to evaluate a suite of debris beds at one time rather than one debris bed at a time. The assessment of the Series 1 debris beds was performed based on the experience of the initial evaluation used to assess the methodology and develop the initial procedures. The assessment of the Series 2 debris beds was able to take advantage of the lessons learned from the Series 1 debris bed assessment. Based on the results of the Series 1 CalSil assessment, statistical modeling was used to optimize the test plan for generating the performance curves to reduce the uncertainty of the results. The modeling took into account the resources available to conduct the test, so that the uncertainty was optimized with respect to the resources allocated for the task. For the parameters listed above, Table 5.9 lists the values used for the Series 1 and Series 2 CalSil assessments of the NUKON/CalSil debris beds.

This optimization is the reason for the significant difference between the 95% upper and lower inverse confidence limits reported for the Series 1 and 2 CalSil mass loadings reported in Section 7.4.. Not all of the measurements obtained for the Series 1 data were fully analyzed; therefore, additional analyses of the Series 1 data could reduce the difference between the upper and lower confidence limits reported for the Series 1 results.

Table 5.9. Parameter List for Developing the ISE Probe Performance Curves

Parameter Description	Values for Series 1 CalSil Assessment Performance Curve	Values for Series 2 CalSil Assessment Performance Curve
Number of CalSil concentrations used to generate performance curve	5	5
Number of performance standards generated for each CalSil concentration	1	4
Number of aliquots prepared from each performance standard	1	3
Number of probe readings made in each aliquot	1	1
Number of ISE probes used to take readings	2	1

6.0 Phenomenological Results and Discussion

To ensure the adequacy of the data obtained from tests performed on the large-scale loop, testing was conducted in the benchtop loop to evaluate the effect of parameters associated with the initial conditions on the measured pressure drop across debris beds. These parameters are potential sources of variability and may explain differences observed between the results of the PNNL tests and other testing efforts. An example of such a parameter is the degree of debris disassociation or fragmentation discussed in Section 3.2.1.2. This section discusses the results obtained for the following four parameters:

- Debris preparation associated with presoaking fiber material at elevated temperature to simulate a 30-minute lag time between the occurrence of a LOCA and the start of the sump recirculation (Section 6.1).
- Sump screen material (Section 6.2).
- The debris loading sequence used to generate the debris bed. Section 6.3 contains the pressure drop measurements for various debris loading sequences, and Section 6.4 presents observations made using SEM.
- The flow history to which the debris bed has been subjected (Section 6.5). The effects of time at flow and the cycling of the approach velocity are discussed.

6.1 Debris Preparation

Section 3.2.3.3 shows that NUKON debris preparation accomplished by mixing in a blender can significantly affect debris bed formation and subsequent head loss results. The degree of disassociation or fragmentation of the insulation material to create debris is quantified using the R4 metric discussed in Section 3. Previous investigations of the head loss associated with NUKON debris beds prepared the debris by boiling it for 10 to 15 minutes to break down organic binders before introducing it to the loop (Shaffer et al. 2005). Based on conversations with Dr. W.J. Shack at ANL, other researchers presoaked the debris material in 140°F water for 30 minutes before introducing it into the loop to simulate the approximately 30-minute delay that would exist between the occurrence of a LOCA and the start of the sump recirculation. Boiling the NUKON debris, both before and after blender preparation, apparently reduces the R4 metric for the debris, as discussed in Section 3.1.2.

Debris bed loading conditions similar to Test Case 1a from NUREG/CR-6874 (Shaffer et al. 2005), which was a NUKON-only test with a debris loading of 1681.4 g/m^2, have been used to study some effects of varying debris preparation procedures. This test condition will be referred to as NOBT1a. Repeat tests in the benchtop loop for test condition NOBT1a using both boiled and non-boiled debris material are considered to evaluate the effects on resulting debris bed formation and head loss.

6.1.1 Test Conditions

Tests were conducted in the PNNL benchtop loop (Section 2.3) using the test procedures similar to those summarized in Section 5.3. All NUKON debris (the bulk of the benchtop loop tests were conducted using the initial shredded NUKON that had no specific lot number; see Section 3) was prepared to an R4 value of 10–12 for each test. Some of the debris was tested without prior boiling; other samples of debris were boiled at 212°F (100°C) for 10 minutes, allowed to cool to approximately 86°F (30°C) with frequent mixing using a kitchen spatula, then introduced into the loop. The target debris loading of 1681.4 g/m^2 corresponds to 13.63 g of NUKON debris for the 4 in.-diameter test section of the benchtop loop. All of these tests employed a perforated plate as the sump screen material, which is described in Section 2.2.

An initial screen approach velocity of 0.20 ft/sec (0.06 m/s) was used to form the debris bed. The velocity was allowed to decay over the 20-minute bed formation time (constant pump speed), resulting in approximately 27 circulations through the loop. Debris bed formation was considered complete when steady conditions were achieved for the preset pump speed. The steady-state criterion for bed formation and at each recorded velocity was assumed to be achieved when the pressure drop exhibited a change of less than 2-in. of H_2O over a 5-minute period. All reported pressure drop measurements are for steady-state conditions. Pressure drops are reported in inches of H_2O at a reference temperature of 68°F (20°C).

The velocity sequence used for Test Case 1a (Shaffer et al. 2005) was used as the basis for selecting the velocity sequence to be used for test condition NOBT1a. This is the same velocity sequence used for large-scale test cases NO6 and NO7. To reduce the test time, the velocity sequence was truncated. Also the limitations of the benchtop loop precluded testing at the peak velocities obtained for Test Case 1a during previous work (Shaffer et al. 2005). The tables presented in Sections 6.1.2 and 6.2.2 contain blank lines to represent Test Case 1a test points that were skipped during the individual benchtop loop tests.

Two non-boiled tests, 060228_NO_1363_BP2 and 060421_NO_1363_BP1, and three BAP tests, 060327_NO_1363_BP1, 060328_NO_1363_BP1, and 060523_NO_1363_BAP1 were conducted. An additional BAP test, 060324_NO_1363_BP1, was conducted, but contamination of the debris bed with rust particulate rendered the data suspect, and those results are not included in this evaluation. The rust contamination consisted of flakes of material that were readily visible. Visual observation of the retrieved bed determined whether contamination was present. The replacement of some loop components and a change in the loop preparation procedures greatly reduced the occurrence and severity of contamination.

6.1.2 Test Results

Head-loss results as a function of screen approach velocity for the non-boiled and boiled prepared NUKON debris for test condition NOBT1a are presented in Table 6.1. The percent difference and average of the measured head loss for corresponding velocities for the non-boiled and boiled tests are provided in Table 6.2. Comparison is made based on the averages.

The differences in the non-boiled and boiled results are similar to the respective non-boiled and boiled differences. However, the results of the boiled tests are typically lower. Thus, the results indicate that boiling the debris results in lower head loss for the same preparation conditions.

Different results may be obtained due to boiling if the debris preparation procedures are different than those described for the non-boiled and boiled tests (consider debris preparation results in Section 3). It was shown, as depicted in Figure 6.1, as a function of the R4 metric, that the head loss increased with increasing blender preparation time (lower R4) to a point approximately coincident with the chosen PNNL NUKON debris preparation target R4 value and then began to decrease. It was also shown that boiling the debris reduced the R4 metric result. Thus, boiling, which has been shown to decrease the R4 metric, might be expected to increase head loss if a larger initial value of R4 was used (right side of Figure 6.1). In contrast, for PNNL testing with debris prepared near peak head loss with respect to R4, boiling (i.e., decreasing R4) would be expected to reduce the head loss (left side of Figure 6.1).

Table 6.1. Benchtop Non-Boiled and Boiled Debris Results for Test Condition NOBT1a[(a)]

Test Preparation	060228_NO_1363_BP2 Non-Boiled		060421_NO_1363_BP1 Non-Boiled		060327_NO_1363_BP1 Boiled		060328_NO_1363_BP1 Boiled		060523_NO_1363_BAP1 Boiled	
Test Phase	**Screen Approach Velocity (ft/sec)**	**Head Loss (in. H2O)(b)**	**Screen Approach Velocity (ft/sec)**	**Head Loss (in. H2O)(b)**	**Screen Approach Velocity (ft/sec)**	**Head Loss (in. H2O)(b)**	**Screen Approach Velocity (ft/sec)**	**Head Loss (in. H2O)(b)**	**Screen Approach Velocity (ft/sec)**	**Head Loss (in. H2O)(b)**
Ramp up 1	0.13	23	0.14	30	0.14	27	0.14	31	0.15	34
	0.20	39	0.20	46	0.20	40	0.20	41	0.20	46
	0.40	86	0.40	103	0.40	103	0.40	104	0.40	118
	0.57	164	0.57	167	0.57	160	0.57	157	0.57	183
	0.70	227	0.70	226	0.70	215	0.70	195	0.70	237
	0.88	322	0.88	343	0.88	293	0.88	266	0.88	326
Ramp down 1	Point skipped	NA	Point skipped	NA	Point skipped	NA	Point skipped	NA	Point skipped	NA
	0.70	245	0.70	257	0.70	219	0.70	199	0.70	244
	0.56	187	0.56	196	0.56	165	0.56	149	0.56	185
	0.41	129	0.41	134	0.41	113	0.41	102	0.41	126
	0.20	55	0.20	57	0.20	47	0.20	42	0.20	54
Ramp up 2	0.30	90	0.30	93	0.30	77	0.30	69	0.30	88
	0.41	129	0.41	134	0.41	113	0.41	103	0.41	130
	0.56	193	0.56	198	0.56	166	0.56	152	0.56	187
	0.71	263	0.71	269	0.71	225	0.71	208	0.71	250
	0.88	355	0.88	362	0.88	302	0.88	278	0.88	336
Ramp down 2	Point skipped	NA	Point skipped	NA	Point skipped	NA	Point skipped	NA	Point skipped	NA
	Point skipped	NA	Point skipped	NA	Point skipped	NA	Point skipped	NA	Point skipped	NA
	Point skipped	NA	Point skipped	NA	Point skipped	NA	Point skipped	NA	Point skipped	NA
	Point skipped	NA	Point skipped	NA	Point skipped	NA	Point skipped	NA	Point skipped	NA
	Point skipped	NA	Point skipped	NA	Point skipped	NA	Point skipped	NA	Point skipped	NA
	Point skipped	NA	Point skipped	NA	Point skipped	NA	Point skipped	NA	Point skipped	NA
Ramp up 3	0.30	93	0.30	96	0.30	79	0.30	71	0.30	88
	0.88	360	0.88	372	0.88	304	0.88	284	0.88	341
	Point skipped	NA	Point skipped	NA	Point skipped	NA	Point skipped	NA	Point skipped	NA
Ramp down 3	Point skipped	NA	Point skipped	NA	Point skipped	NA	Point skipped	NA	Point skipped	NA
	Point skipped	NA	Point skipped	NA	Point skipped	NA	Point skipped	NA	Point skipped	NA
	Point skipped	NA	Point skipped	NA	Point skipped	NA	Point skipped	NA	Point skipped	NA
	Point skipped	NA	Point skipped	NA	Point skipped	NA	Point skipped	NA	Point skipped	NA
	0.2	57	0.2	60	0.2	48	0.2	44	0.2	54
Ramp up 4	Point skipped	NA	Point skipped	NA	Point skipped	NA	Point skipped	NA	Point skipped	NA
	Point skipped	NA	Point skipped	NA	Point skipped	NA	Point skipped	NA	Point skipped	NA
	Point skipped	NA	Point skipped	NA	Point skipped	NA	Point skipped	NA	Point skipped	NA
Ramp down 4	Point skipped	NA	Point skipped	NA	Point skipped	NA	Point skipped	NA	Point skipped	NA
	Point skipped	NA	Point skipped	NA	Point skipped	NA	Point skipped	NA	Point skipped	NA
	Point skipped	NA	Point skipped	NA	Point skipped	NA	Point skipped	NA	Point skipped	NA
	Point skipped	NA	Point skipped	NA	Point skipped	NA	Point skipped	NA	Point skipped	NA
	Point skipped	NA	Point skipped	NA	Point skipped	NA	Point skipped	NA	Point skipped	NA
Ramp up 5	Point skipped	NA	Point skipped	NA	Point skipped	NA	Point skipped	NA	Point skipped	NA
	Point skipped	NA	Point skipped	NA	Point skipped	NA	Point skipped	NA	Point skipped	NA

(a) The blank lines represent velocity points in the original test case 1a velocity sequence that were skipped during the individual benchtop loop tests.

(b) In. of H_2O are for a reference temperature of 68°F (20°C).

Table 6.2. Comparison of Results for Benchtop Non-Boiled and Boiled Debris Results for Test Condition NOBT1a[a]

Test Phase	Screen Approach Velocity (ft/sec)	% Difference Between PNNL Non-Boiled Tests (%)	Non-Boiled Average (in. H_2O)[a]	% Difference Boiled Test 1 to 2	% Difference Boiled Test 1 to 3	% Difference Boiled Test 2 to 3	Boiled Average (in. H_2O)[a]	% Difference Non-Boiled to Boiled
Ramp up 1	0.14	30	27	15	26	10	31	16
	0.20	18	43	3	15	12	42	0
	0.40	20	95	1	15	13	108	15
	0.57	2	166	-2	14	17	167	1
	0.70	0	227	-9	10	22	216	-5
	0.88	7	333	-9	11	23	295	-11
Ramp down 1	0.70	5	251	-9	11	23	221	-12
	0.56	5	192	-10	12	24	166	-13
	0.41	4	132	-10	12	24	114	-14
	0.20	4	56	-11	15	29	48	-15
Ramp up 2	0.30	3	92	-10	14	28	78	-15
	0.41	4	132	-9	15	26	115	-12
	0.56	3	196	-8	13	23	168	-14
	0.71	2	266	-8	11	20	228	-14
	0.88	2	359	-8	11	21	305	-15
Ramp down 2	Point skipped	NA	NA	NA	NA	NA	NA	NA
Ramp up 3	0.30	3	95	-10	11	24	79	-16
	0.88	3	366	-7	12	20	310	-15
Ramp down 3	0.2	5	59	-8	13	23	49	-17
Ramp up 4	Point skipped	NA	NA	NA	NA	NA	NA	NA
Ramp down 4	Point skipped	NA	NA	NA	NA	NA	NA	NA
Ramp up 5	Point skipped	NA	NA	NA	NA	NA	NA	NA

(a) Inches. of H_2O are for a reference temperature of 68°F (20°C).

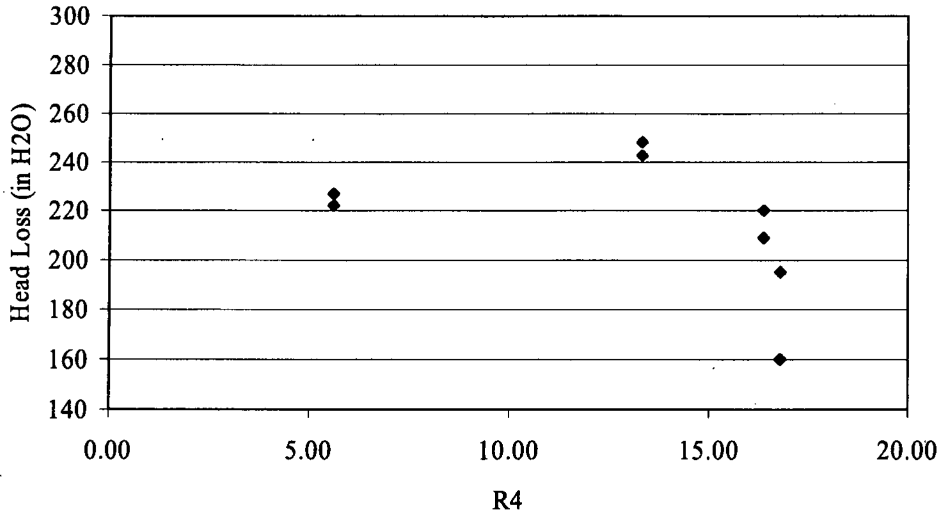

Figure 6.1. Debris Bed Head Loss as a Function of R4 for a Target Debris Loading of 1449.5 g/m²

The non-boiling to boiling test results were considered in regards to the readily quantifiable aspects of debris bed formation: height, mass, and appearance. The representative approximate debris bed body heights for the tests are given in Table 6.3 along with the dry retrieval debris bed mass and computed density. The measured debris bed heights are referred to as approximate because of the limitations of the measurement technique; the debris bed "body" measurements (plane area of the bed, not the outer rim) are inferred from a 1-mm-increment ruler placed beside the debris bed in a vertical orientation. This gross technique is only employed for the benchtop evaluations and provides a relative means of comparison. The dry retrieved debris bed mass is approximately equivalent across the tests, while the representative height apparently increases, thereby reducing the computed density. The highest head loss results are achieved for the highest density debris bed, 060421_NO_1363_BP1. Thus, considering the minimal differences and approximate nature of the results, boiling the debris is apparently discernable in the resulting height and mass of the debris bed.

The visual appearance of the debris beds in Figures 6.2, 6.3, 6.4, 6.5 and 6.6 does not provide any evidence that head loss differences may be expected (see Section 3.2.3.3 related debris bed appearance as a function of debris preparation to head loss).

Table 6.3. Benchtop Non-Boiling and Boiling Preparation Debris Bed Data for Test Condition NOBT1a

Test	Preparation	Approximate Measured Debris Bed Body Height (in.)	Dry Debris Bed Mass (g)	Computed Density (g/mL)
060228_NO_1363_BP2	Non-boiled	0.35	12.53	0.17
060421_NO_1363_BP1	Non-boiled	0.31	12.96	0.20
060327_NO_1363_BP1	boiled	0.39	12.93[a]	0.16
060328_NO_1363_BP1	boiled	0.39	12.81[a]	0.16
060523_NO_1363_BAP1	boiled	0.43	13.05	0.15

(a) Rust flakes from benchtop loop components were visually observable on the debris bed. The mass of this contaminant is not readily quantifiable.

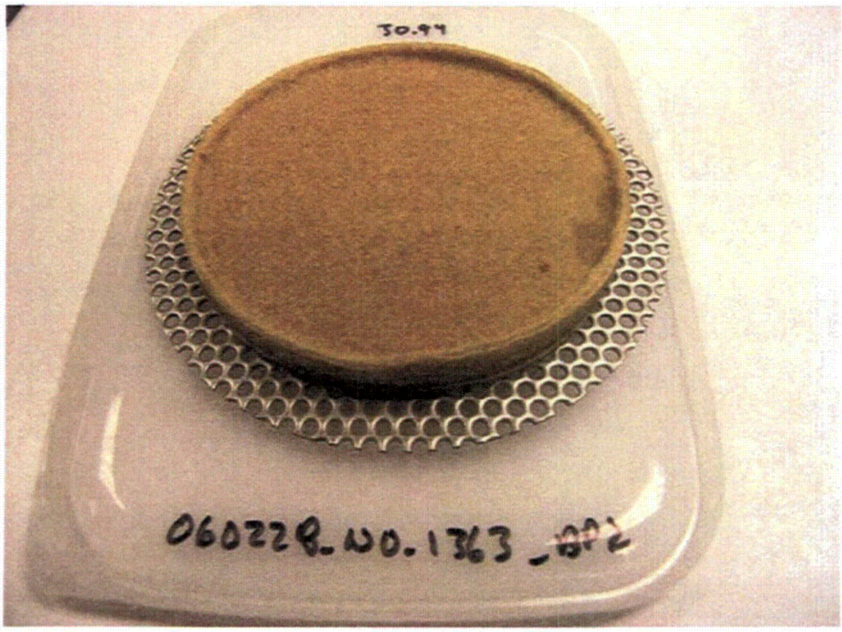

Figure 6.2. 060228_NO_1363_BP2, Non-Boiled

Figure 6.3. 060421_NO_1363_BP1, Non-Boiled

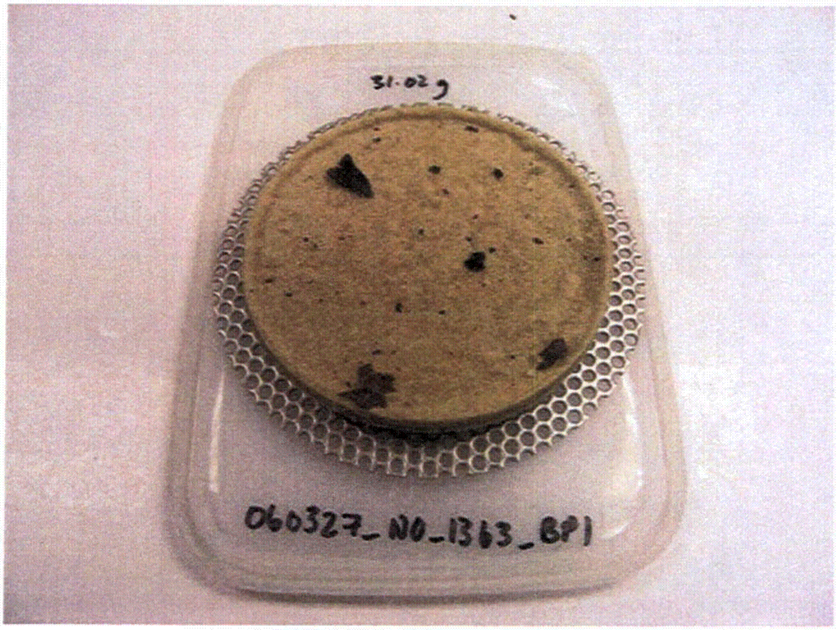

Figure 6.4. 060327_NO_1363_BP1, Boiled

Figure 6.5. 060328_NO_1363_BP1, Boiled

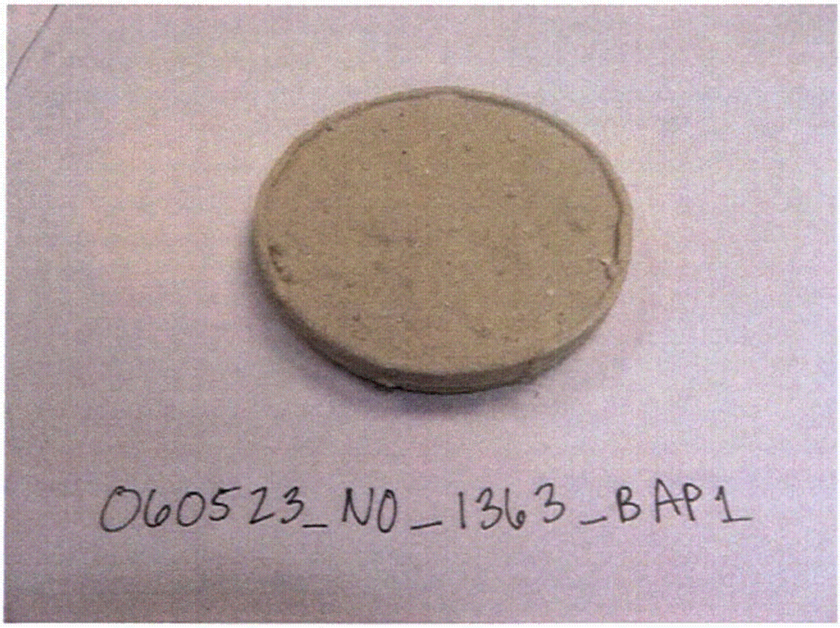

Figure 6.6. 060523_NO_1363_BAP1, Boiled

6.2 Sump Screen Material Comparison

PNNL employed both 5-mesh screen and a perforated plate with 1/8-inch-diameter holes as sump screen material. (Refer to Section 2.2 for descriptions of the sump screen materials.) Repeat tests in the bench-top loop with test condition NOBT1a (NUKON-only, target debris loading 1681.4 g/m^2) using both the

5-mesh screen and the perforated plate as sump screen material are considered to evaluate the effect on the resulting debris bed formation and head loss.

6.2.1 Test Conditions

Tests were conducted in the PNNL benchtop loop using test procedures similar to those discussed in Section 5.3. All NUKON debris material (i.e., the initial shredded NUKON with no specified lot number, as discussed in Section 3), was prepared to an R4 value of 11 ± 1 for each test. The target debris loading of 1681.4 g/m^2 corresponds to 13.63 g of NUKON debris for the 4-in.-diameter test section of the benchtop loop.

An initial screen approach velocity of 0.20 ft/sec (0.06 m/s) was used to form the debris bed. The velocity was allowed to decay over the 20-minute bed formation time (constant pump speed), resulting in approximately 27 circulations through the loop. Debris bed formation was determined to be complete when steady-state conditions were achieved for the preset pump speed. The steady-state criterion for bed formation and at each recorded velocity was assumed to be achieved when the pressure drop exhibited a change of less than 2-in. H_2O over a 5-minute period. Pressure drop readings were taken after steady-state conditions were achieved after bed formation and after steady-state conditions were reached at a matrix of predefined velocities. All reported pressure drop measurements are for steady-state conditions. Pressures are reported in inches of H_2O at a reference temperature of 68°F (20°C).

The velocity sequence used for Test Case 1a (Shaffer et al. 2005) was used as the basis for selecting the velocity sequence to be used for test condition NOBT1a. This is the same velocity sequence used for the large-scale test cases NO6 and NO7. To reduce the test time, the velocity sequence was truncated. Also, the limitations of the benchtop loop precluded testing at the peak velocities obtained for Test Case 1a during previous work (Shaffer et al. 2005). The tables presented in Sections 6.1.2 and 6.2.2 contain blank lines to represent Test Case 1a test points that were skipped during the individual benchtop loop tests.

Two tests were conducted with the 5-mesh screen, 060223_NO_1363_B1 and 060228_NO_1363_B1, and two tests were conducted with the perforated plate, 060228_NO_1363_BP2 and 060421_NO_1363_BP1.

6.2.2 Test Results

Head loss results from the benchtop loop as a function of screen approach velocity for the 5-mesh screen and perforated plate conducted at test condition NOBT1a are presented in Table 6.4. The percent difference and average of the measured head loss for corresponding velocities for the two materials are also provided in Table 6.4. Average values are compared in the table.

The differences between the measured head loss for 5-mesh screen and perforated plate were not sufficiently distinct from the respective 5-mesh and plate differences to make a conclusion about whether the sump screen material significantly affected the debris bed head loss. These results are considered with regard to the readily quantifiable aspects of debris bed formation, height, mass, and appearance.

The representative approximate debris bed body heights for the tests are given in Table 6.5 along with the dry retrieval debris bed mass. (The measured debris bed heights are referred to as approximate because of the limitations of the measurement technique; the debris bed body measurements (plane area of the bed, not the outer rim) are inferred from a 1-mm-increment ruler placed vertically beside the debris bed. This

Table 6.4. Benchtop 5-Mesh and Plate Test Results for Test Condition NOBT1a

Test	060223_NO_1363_B1		060228_NO_1363_B1		060228_NO_1363_BP2		060421_NO_1363_BP1		Comparison				
Sump Screen	5-mesh		5-mesh		Plate		Plate						
Test Phase	Screen Approach Velocity (ft/sec)	Head Loss (in. H_2O)(a)	Screen Approach Velocity (ft/sec)	Head Loss (in. H_2O)(a)	Screen Approach Velocity (ft/sec)	Head Loss (in. H_2O)(a)	Screen Approach Velocity (ft/sec)	Head Loss (in. H_2O)(a)	% Difference 5-Mesh	5-Mesh Average (in. H_2O)(a)	% Difference Plate	Plate Average (in. H_2O)(a)	% Difference Plate to 5-mesh
Ramp up 1	0.16	35	0.16	28	0.13	23	0.14	30	-20.0	32	30.4	27	-15.9
	0.20	45	0.2	43	0.20	39	0.20	46	-4.4	44	17.9	43	-3.4
	0.40	112	0.4	89	0.40	86	0.40	103	-20.5	101	19.8	95	-6.0
	0.57	203	0.57	161	0.57	164	0.57	167	-20.7	182	1.8	166	-9.1
	0.70	246	0.7	206	0.70	227	0.70	226	-16.3	226	-0.4	227	0.2
	0.88	344	0.88	304	0.88	322	0.88	343	-11.6	324	6.5	333	2.6
	Point skipped	NA	Point skipped	NA	Point skipped	NA	Point skipped	NA	NA	NA	NA	NA	NA
Ramp down 1	Point skipped	NA	Point skipped	NA	Point skipped	NA	Point skipped	NA	NA	NA	NA	NA	NA
	0.70	265	0.7	226	0.70	245	0.70	257	-14.7	246	4.9	251	2.2
	0.56	202	0.56	168	0.56	187	0.56	196	-16.8	185	4.8	192	3.5
	0.41	147	0.41	122	0.41	129	0.41	134	-17.0	135	3.9	132	-2.2
	0.20	70	0.2	45	0.20	55	0.20	57	-35.7	58	3.6	56	-2.6
Ramp up 2	0.30	104	0.3	89	0.30	90	0.30	93	-14.4	97	3.3	92	-5.2
	0.41	148	0.41	126	0.41	129	0.41	134	-14.9	137	3.9	132	-4.0
	0.56	227	0.56	187	0.56	193	0.56	198	-17.6	207	2.6	196	-5.6
	0.71	297	0.71	246	0.71	263	0.71	269	-17.2	272	2.3	266	-2.0
	0.88	398	0.88	324	0.88	355	0.88	362	-18.6	361	2.0	359	-0.7
	Point skipped	NA	0.96	NA	Point skipped	NA	Point skipped	NA	NA	NA	NA	NA	NA
Ramp down 2	Point skipped	NA	0.88	NA	Point skipped	NA	Point skipped	NA	NA	NA	NA	NA	NA
	Point skipped	NA	0.69	236	Point skipped	NA	Point skipped	NA	NA	NA	NA	NA	NA
	Point skipped	NA	0.56	188	Point skipped	NA	Point skipped	NA	NA	NA	NA	NA	NA
	Point skipped	NA	0.4	127	Point skipped	NA	Point skipped	NA	NA	NA	NA	NA	NA
	Point skipped	NA	0.29	86	Point skipped	NA	Point skipped	NA	NA	NA	NA	NA	NA
	Point skipped	NA	0.2	47	Point skipped	NA	Point skipped	NA	NA	NA	NA	NA	NA
Ramp up 3	0.30	104	0.3	88	0.30	93	0.30	96	-15.4	96	3.2	95	-1.6
	0.88	416	0.88	322	0.88	360	0.88	372	-22.6	369	3.3	366	-0.8
	Point skipped	NA	0.96	NA	Point skipped	NA	Point skipped	NA	NA	NA	NA	NA	NA
Ramp down 3	Point skipped	NA	0.87	NA	Point skipped	NA	Point skipped	NA	NA	NA	NA	NA	NA
	Point skipped	NA	0.7	245	Point skipped	NA	Point skipped	NA	NA	NA	NA	NA	NA
	Point skipped	NA	0.41	126	Point skipped	NA	Point skipped	NA	NA	NA	NA	NA	NA
	Point skipped	NA	0.29	84	Point skipped	NA	Point skipped	NA	NA	NA	NA	NA	NA
	Point skipped	NA	0.2	55	0.2	57	0.2	60	NA	NA	5.3	58.5	NA
Ramp up 4	Point skipped	NA	0.41	130	Point skipped	NA	Point skipped	NA	NA	NA	NA	NA	NA
	Point skipped	NA	0.7	263	Point skipped	NA	Point skipped	NA	NA	NA	NA	NA	NA
	Point skipped	NA	0.96	NA	Point skipped	NA	Point skipped	NA	NA	NA	NA	NA	NA
Ramp down 4	Point skipped	NA	0.69	NA	Point skipped	NA	Point skipped	NA	NA	NA	NA	NA	NA
	Point skipped	NA	0.41	130	Point skipped	NA	Point skipped	NA	NA	NA	NA	NA	NA
	Point skipped	NA	0.2	63	Point skipped	NA	Point skipped	NA	NA	NA	NA	NA	NA
	Point skipped	NA	0.1	31	Point skipped	NA	Point skipped	NA	NA	NA	NA	NA	NA
	Point skipped	NA	0.05	6	Point skipped	NA	Point skipped	NA	NA	NA	NA	NA	NA
	Point skipped	NA	0.02	6	Point skipped	NA	Point skipped	NA	NA	NA	NA	NA	NA
Ramp up 5	Point skipped	NA	0.1	31	Point skipped	NA	Point skipped	NA	NA	NA	NA	NA	NA
	Point skipped	NA	0.2	68	Point skipped	NA	Point skipped	NA	NA	NA	NA	NA	NA

(a) In. of H_2O are for a reference temperature of 68°F (20°C).

Note: The blank lines (point skipped) represent velocity points in the original Test "Case 1a velocity sequence that were skipped during the individual benchtop loop tests.

gross technique is employed only for the benchtop evaluations and provides a qualitative means of comparison.) For both the 5-mesh screen and the perforated plate, the head loss is elevated for those tests with more mass retained in the debris bed. The trend is not apparent between the sump screen materials; however, as the 5-mesh test 060228_NO_1363_B1yeilded lower head loss results than the plate test, 060421_NO_1363_BP1, which has a lower retained dry debris bed mass. (The unquantified contaminant mass [see Table 6.5] is ignored.) However, the indicated decrease in debris bed body height for test 060421_NO_1363_BP1 results in the greater computed density (see Table 6.5), suggesting that the discussed "mass-trend" discrepancy is therefore plausible. The "density effect" is not consistent (head loss trend with density) either, however. Thus, it is not possible to correct for debris bed formation conditions to further evaluate sump screen material effects.

Likewise, the visual appearance of the debris beds in Figures 6.7, 6.8, 6.9, and 6.10 does not provide any evidence that head loss differences may be expected (see Section 3.2.3.3 for related debris bed appearance as a function of debris preparation to head loss).

6.3 Debris Loading Sequence

As reported in *Quick-Look Report for PNNL Test 051128_NC_2776_L2, Test Case 6e2 Conditions,* in Appendix J, the values of the head loss measured during that test were significantly higher than those obtained from previous tests of debris beds with the same and similar target mass constituent ratios (0.5 and 0.55) and the same (1522 g/m^2) and greater (up to 2246.7 g/m^2) total target mass loadings (see Figure 6.11). The evaluation of the impact the debris loading sequence has on the head loss was initiated in an attempt to explain the elevated head loss measurements obtained for test 051128_NC_2776_L2. Test Cases 6e and 6e2 are identifications used by the previous head loss investigation reported in NUREG/CR-6874 (Shaffer et al. 2005) and are similar to tests replicated for the Series 1 test matrix (see Section 5.1). Test Cases 6e and 6e2 correspond to PNNL Test Cases NC12 and NC13; the target mass loadings for this test condition are 993 g/m^2 of NUKON and 496 g/m^2 of CalSil for a total mass loading of 1489 g/m^2

The head loss measured for 051128_NC_2776_L2 (test case NC13) was approximately twice that of test 051117_NC_2776_L1 (test case NC12), even with approximately 6% less measured mass (based on post-test measurements) retained on the screen. Head loss results from test 051117_NC_2776_L1 (test case NC14) appear to trend, in terms of higher head loss with higher target debris loading, with tests 051110_NC_0595_L1 (test case NC3), 051121_NC_1587_L1 (test case NC7), and 051115_NC_4098_L1 (test case NC14). Based on the results presented in Figure 6.11, test 051123_NC_2181_L1 is observed to also have elevated (out of the trend) head loss results.

Initial benchtop tests (prior to the initiation of large-scale loop testing) with debris beds generated from the same target mass constituent ratio and a target debris loading of 2174.2 g/m^2 produced similar dramatic variations in the measured debris bed head loss. For two of these tests, the pump in the benchtop loop was effectively insufficient to provide flow through the bed, while for two other tests, flow was easily maintained. These four referenced tests, 050831_NC_1763_1, 050831_NC_1763_2, 050901_NC_1763_1, and 050901_NC_1763_2, were performed as part of an initial scoping evaluation to evaluate the suitability of the debris loading techniques; head loss as a function of screen approach velocity was not investigated.

Table 6.5. Benchtop 5-mesh Screen and Perforated Plate Debris Bed Data for Test Condition NOBT1a

Test	Screen Material	Approximate Measured Debris Bed Body Height (in)	Dry Debris Bed Mass (g)	Computed Density (g/mL)
060223_NO_1363_B1	5-mesh	0.35	13.45	0.18
060228_NO_1363_B1	5-mesh	0.35	13.30[(a)]	0.18
060228_NO_1363_BP2	plate	0.35	12.53	0.17
060421_NO_1363_BP1	plate	0.31	12.96	0.20

(a) Rust flakes from benchtop loop components were visually observable on the debris bed. The mass of this contaminant is not readily quantifiable.

Figure 6.7. 060223_NO_1363_B1, 5-Mesh

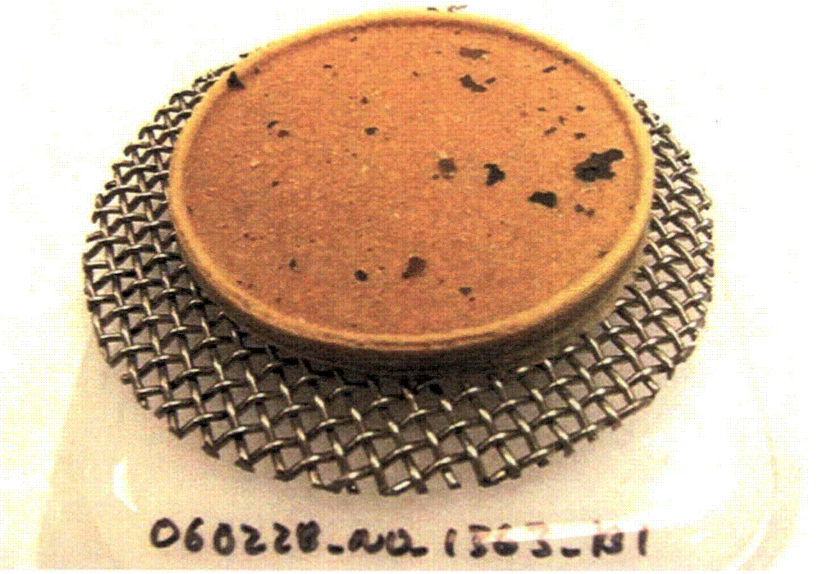

Figure 6.8. 060228_NO_1363_B1, 5-Mesh. Flakes are rust from benchtop loop components.

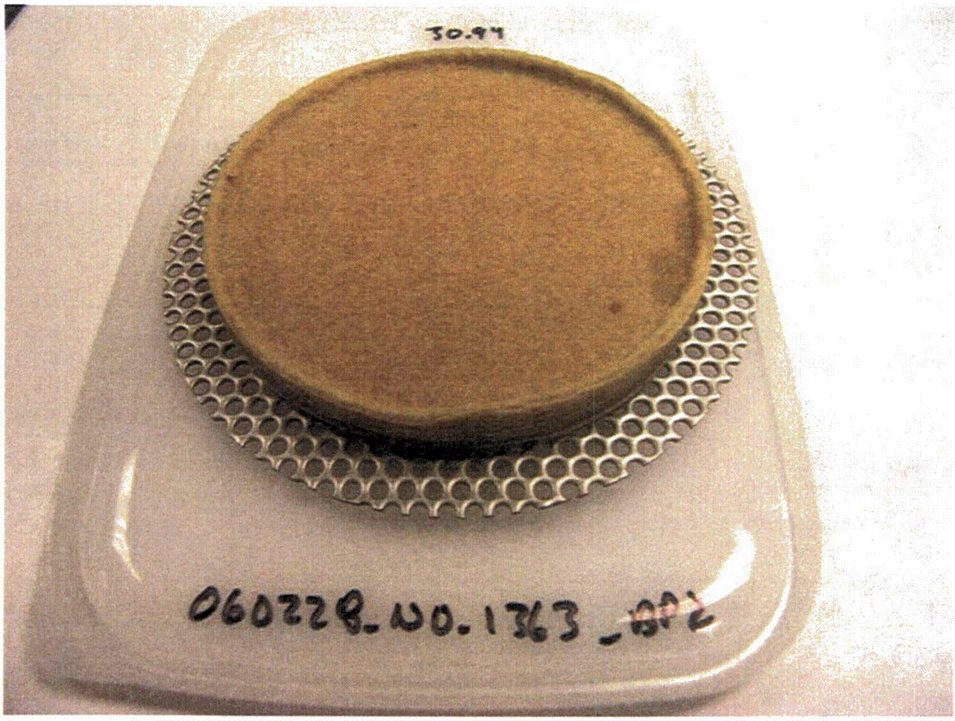

Figure 6.9. 060228_NO_1363_BP2, Plate

Figure 6.10. 060421_NO_1363_BP1, Plate

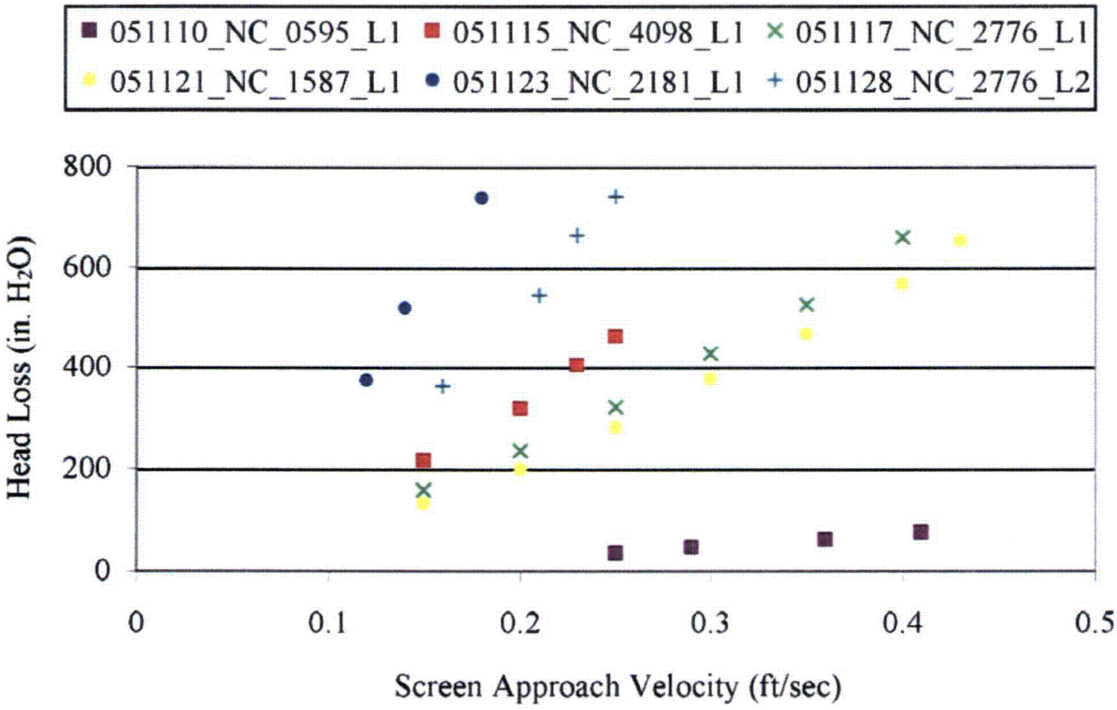

Figure 6.11. Debris Bed Head Loss as a Function of Screen Approach Velocity for NUKON/CalSil Debris Beds Formed in the PNNL Large-Scale Loop During Series 1 Tests. The data points plotted are all from ramp up 3 of each velocity sequence. All of the data are from PNNL Quick-Look Reports, related to each specific test, that are contained in Appendixes H and J.

As was subsequently done in the large-scale loop, the same procedures were followed for each of these benchtop tests, and extreme care was taken to ensure that initial conditions (sample preparation, handling, introduction into loop, etc.) were similar for each test. Simple and rapid out-of-loop tests were conducted to try to identify the cause of the altered debris bed head loss performance (mass to volume considerations depending on NUKON and CalSil slurry handling evaluated via R4 test). No readily apparent mechanisms were identified.

It was suggested by PNNL staff that the relatively high target CalSil to NUKON mass constituent ratio (0.5) may be the cause of the varied results; the extremely high head loss results were not repeated at a mass constituent ratio of 0.25 in the benchtop loop (Tests 050908_NC_1469_1, 050908_NC_1469_2, 050919_NC_1469_1, 051004_NC_1469_1, and 051006_NC_1469_1). These results possibly indicated that there is a critical amount of CalSil particulate that can fill the pore space of the NUKON fibers to drastically reduce the flow paths through a debris bed.

Visual observations made during and after large-scale tests 051123_NC_2181_L1 (Test Case NC13) and 051128_NC_2776_L2 (Test Case NC15) indicated that the initial material reaching the screen was CalSil and that the flow rate in the horizontal sections of the test loop at a screen approach velocity of 0.1 ft/sec (0.03 m/s) was not sufficient to keep the CalSil particulate well mobilized (fully suspended). It was therefore hypothesized that the relatively elevated head loss results discussed above for the large-scale loop were caused by the bulk of the CalSil reaching an already-formed NUKON debris bed. This scenario could occur in the Series 1 debris introduction scheme if a significant portion of the CalSil were to reach the screen prior to a NUKON debris bed forming or if CalSil particulate settled and resuspended prior to initially reaching the screen. In each case, CalSil particulate that had not been captured by the debris bed would potentially be available to fill in the flow paths through and/or deposit onto a pre-existing NUKON debris bed. This hypothetical post-fibrous layer formation deposition of the particulate CalSil could form a relatively close-packed layer of particulate. The close-packed layer has the potential to have a high resistance to flow resulting in a higher head loss at low flow rates. Benchtop tests were conducted to evaluate the effect of these possible scenarios of debris loading sequence on the resulting debris bed head loss.

6.3.1 Benchtop Loop Investigation

The significantly varied head loss results for debris beds in both the benchtop and large-scale tests with the same target debris loading raised questions regarding both the ability to provide statistically meaningful results with regard to repeatability as well as conservatism of the results in terms of a safety-basis use. The postulated mechanisms whereby head loss results could be significantly altered were therefore investigated. These mechanisms include the following:

- A critical particulate-to-fiber mass ratio exists at which the packing minimizes the bulk debris bed porosity. Depending on debris bed formation conditions, CalSil particulate may deposit more densely into the debris bed flow paths.
- The formation of a closely packed layer of particulate (layer of relatively small diameter particulate having a lower porosity than a layer of relatively large fibers) on the surface of the debris bed. The layer of small particulate forming on the top of the bed is readily conceived. However, it is possible that the close-packed layer could form at the discharge side or exit surface depending on how the bed was formed and how long the bed has been in existence. Loop operation for a longer time period could tend to push the particulates to the outlet end of the debris bed.

6.3.1.1 Benchtop Test Cases

Investigations to assess the potential effects of these postulated mechanisms were conducted in the benchtop loop. The introduced debris mass was scaled to match the target debris loading of tests 051117_NC_2776_L1 (Test Case NC14, Condition 6e) and 051128_NC_2776_L2 (Test Case NC15, Condition 6e2). CalSil-only debris beds with higher target loadings were also investigated. The NUKON and CalSil debris materials were prepared the same as for the Series 1 tests.

A 5-mesh screen was used in the benchtop loop. Debris beds were formed, when possible, at an initial screen approach velocity of 0.2 ft/sec. Two velocity cycles of ramp up and -down cycles were typically conducted. Note that the benchtop loop does not have the degassing capability of the large-scale loop; the quantity of gas in the test section was visually observed to vary to some degree between the test cases. Also, the data presented herein from the instrumentation of the benchtop loop should not be considered to have the same resolution as the Series 1 data from the large-scale loop. All of the test data were recorded electronically; however, the data presented here were recorded manually from the DAS meters displayed on the computer screen. The test cases considered and the associated tests are tabulated in Table 6.6. Individual tests for the same test case indicate repeated tests with the exception of the Case 3 tests and one Case 4 test, as described below.

Table 6.6. Summary of Test Cases Conducted in the Benchtop Loop to Evaluate the Effects of the Debris Loading Sequence

Test Number	Test Case	Test Case Description
051214_NC_1234_B1	1A	Introduction of the CalSil material after a NUKON debris bed has completely formed (steady-state criteria met).
051214_NC_1234_B2	1B	
051215_NC_1234_B1	2A	Introduction of the NUKON and CalSil material as pre-mixed slurry.
051215_NC_1234_B2	2B	
051216_NC_1234_B1	2C	
051227_CO_0411x_B1	3A	Introduction of the CalSil material only. If a CalSil-only debris bed could be formed, NUKON material would be added.
051227_CO_1763_B2	3B	
051228_NC_1234_B1	4A	Introduction of the NUKON material following the CalSil material being introduced into the flow loop. The duration between the CalSil being introduced and the initiation of the NUKON addition is referred to as the "lag time"
051228_NC_1234_B2	4B	
051228_NC_1234_B3	4C	

The possible effect of the delay or lag time for the introduction of the NUKON material for Case 4 has also been considered. In the Case 4 tests of Table 6.6, the NUKON material was introduced when, by visual observation, all of the CalSil material had been introduced into the flow loop. The results from the lag time analysis are presented in subsection 6.3.1.2.1.

6.3.1.2 Benchtop Test Head Loss Results and Discussion

Initial results confirm that CalSil particulate introduced onto a pre-formed NUKON debris bed, either by post NUKON-debris bed formation or by initial pass-through, has significant effects on the resulting head loss (Figure 6.12). The data presented in Figure 6.12 are tabulated with the complete test results in Appendix F. (Due to the range [0 to 1,000 inches H_2O] of the pressure transducer used in the benchtop loop and the incomplete debris bed formation for the CalSil-only test cases, essentially no head loss was observed, and the data are therefore not reported in the Appendix.). Referring to Table 6.6, two repeat tests were performed for Case 1; 051214_NC_1234_B1 and 051214_NC_1234_B2. Three tests were performed for Case 2, 051215_NC_1234_B1, 051215_NC_1234_B2, and 051216_NC_1234_B1. As shown in Figure 6.12, the Case 1 head loss results were significantly higher than Case 2 results. This result is not surprising given that the Case 1 tests resulted in an observable layer of relatively fine particulate that could reasonably be expected to be packed such that flow paths were limited compared with the expectedly dispersed particulate tests of Case 2. As discussed, the variation in size and shape between the NUKON fibers and CalSil particulate may be expected to provide a tightly packed condition with subsequently limited flow paths, but there may be insufficient particulate to reach this condition when it is dispersed throughout the fibrous debris layer.

Two tests were performed for Case 3. For test 051227_CO-0411x_B1 (Case 3A), the initial CalSil mass introduced to the benchtop loop was 4.11 g (target CalSil debris loading for Test Case-6e [NC12] and Test Case-6e2 [NC13]). A complete CalSil debris bed was not formed at this concentration due to the existence of exposed screen and open channels (debris bed formation criteria included no visually observable open screen mesh openings in the debris bed. Refer to Section 3). CalSil material was therefore subsequently added in an attempt to form a debris bed. Four incremental loadings of 3.38 g of CalSil was added to yield a peak target mass loading of 2175 g/m^3. This mass loading was the maximum

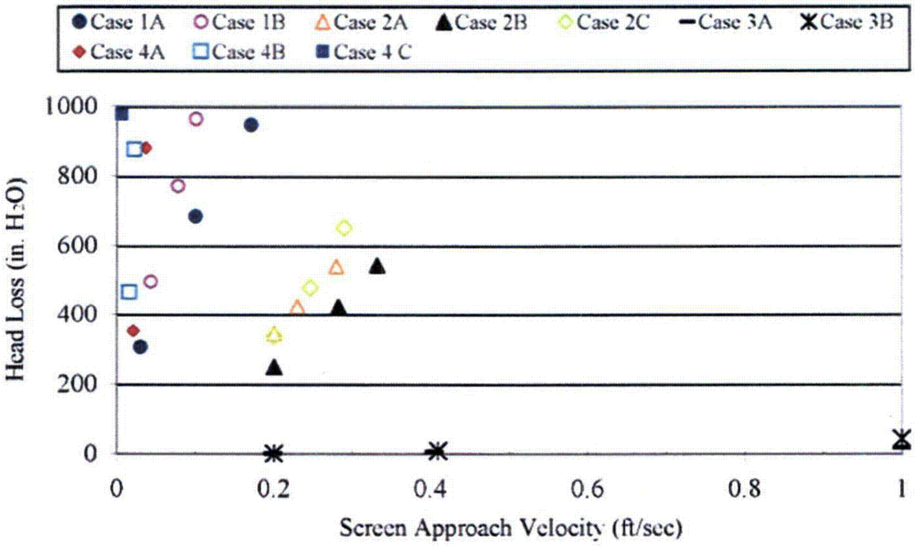

(a)

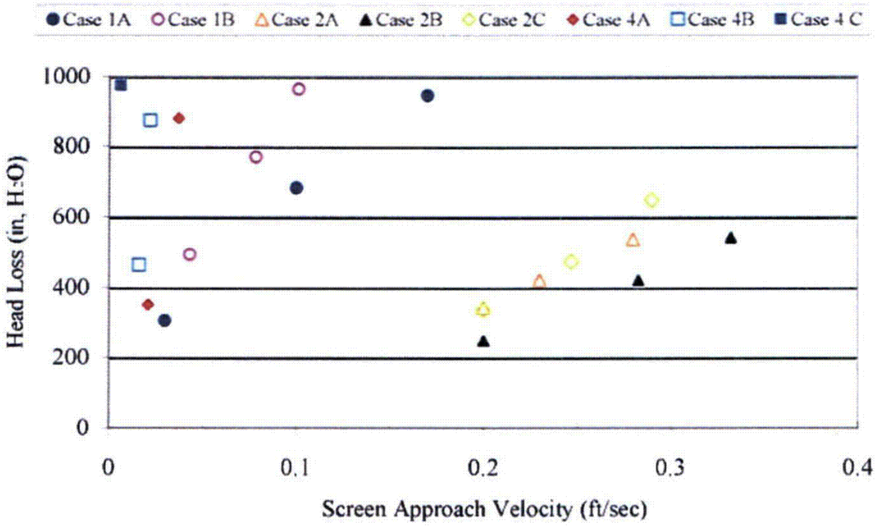

(b)

Figure 6.12. Debris Bed Head Loss as a Function of Screen Approach Velocity for Debris Beds Formed in the PNNL Benchtop Loop. The data presented are for the final ramp up of each velocity sequence. The tests were conducted for various sequences of debris loading; (a) contains all four cases of the load sequence investigation; Case 3 has been excluded from (b) allowing greater resolution of the screen approach velocity to be shown.

CalSil debris loading from the NRC proposed test matrix. After each addition of CalSil, head loss measurements were monitored for steady-state conditions, and time was allowed for the debris bed to form. Although measurable head loss was achieved (Figure 6.12), a complete CalSil debris bed was not considered to have formed (Figure 6.13).

For the second Case 3 test 051227_CO_1763_B2 (Case 3B), the maximum CalSil debris loading from the proposed test matrix (2175 g/m^3) was added in a single introduction. Again, a complete CalSil debris bed was not considered to have formed (Figure 6.14). The head loss measurements for the single addition of CalSil were higher than those obtained after the incremental introductions (see Figure 6.12). The head losses from these CalSil-only tests were negligible compared with the other debris loading scenarios evaluated.

Three tests were performed for Case 4: 051228_NC_1234_B1, 051228_NC_1234_B2, and 051228_NC_1234_B3. As shown in Figure 6.12, these tests resulted in the highest measured head loss of all the cases evaluated. This result may suggest that the postulated critical particulate-to-fiber mass ratio mechanism or conditions used for debris bed formation have more effect on the head loss than a distinct particulate layer (the apparent lack of a distinct particulate layer for these tests is discussed below). Conditions for debris bed formation include factors such as the initial screen approach velocity, control of the approach velocity during bed formation, sequence of debris introduction, rate of debris injection, fluid temperature, and concentration of debris as it reaches the test screen. This concept is corroborated by investigations of particulate filtration and related literature (Konstandopoulos 2000, Merkel et al. 2003, Mizuno and Suzuki 2004).

While both the benchtop and large-scale tests had elevated head loss with debris introduction possibly similar to the benchtop Case 4 tests, the large-scale head loss results (Test 051128_NC_2776_L2) at the same screen approach velocity are approximately 40 times less than those from the benchtop Case 4 tests. There are a number of possible explanations for this behavior discussed below, none of which were investigated.

- The introduction of CalSil first results in a larger percentage of the debris mass circulating through the entire loop. The differences in loop configurations and the significantly longer flow path with increased vertical rise of the large-scale loop allows for the possibility of greater segregation of the various size particles of debris. If a significant amount of segregation occurred, the difference in debris bed structure between the large-scale and benchtop loop beds may explain the variation in results. The debris beds from the benchtop loop would be expected to display a greater degree of uniformity from top to bottom compared with the large-scale beds, which would possess a greater degree of stratification.

- Variations in the concentration of the debris reaching the screen may also contribute to variations in the debris bed structure.

- The configuration of the large-scale loop may have allowed a significant portion of the CalSil to initially settle in the loop. Therefore, the ratio of CalSil to NUKON during the bed formation process was different from that of the benchtop loop tests. The settled CalSil may have then been deposited on the surface of the bed when the screen approach velocity was increased.

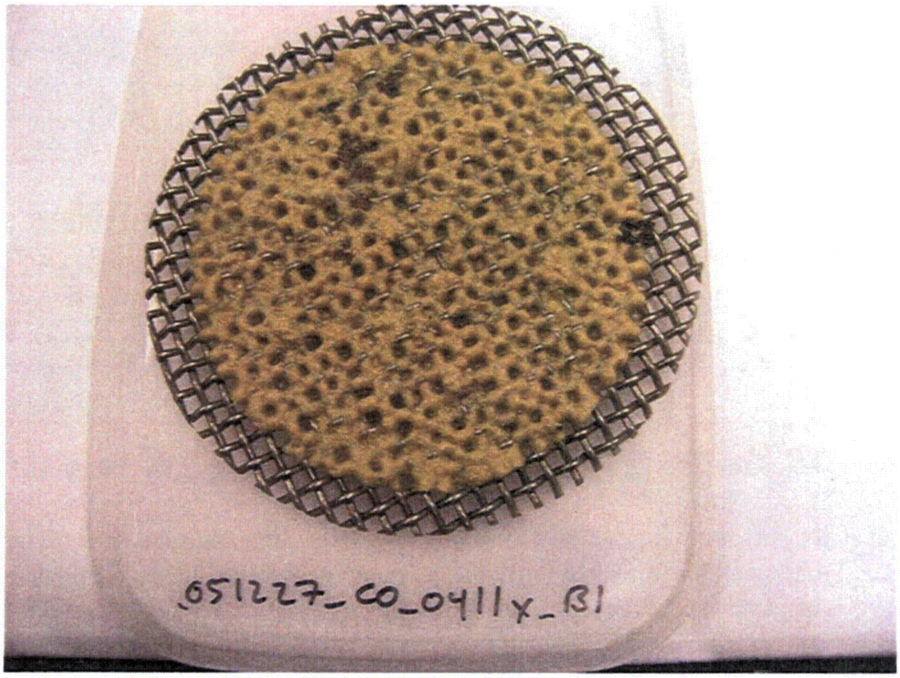

Figure 6.13. Test 051227_CO_0411x_B1 CalSil Debris Bed for Case 3A; target CalSil mass, 17.63 g; rust particulate and chunks from loop visible on surface.

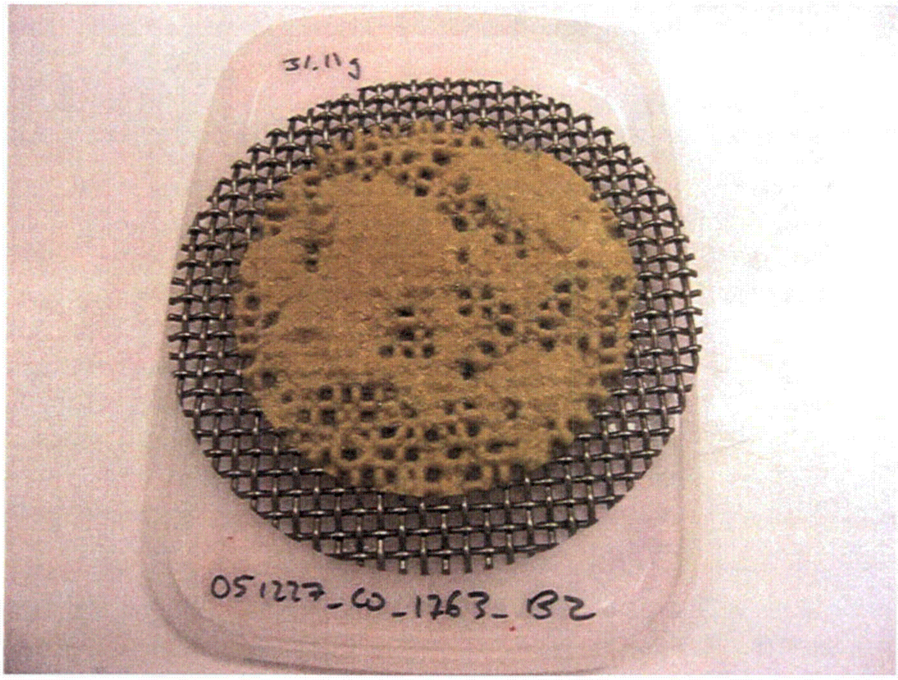

Figure 6.14. Test 051227_CO_1763_B2 CalSil Debris Bed for Case 3B

The high head loss of benchtop tests 051228_NC_1234_B1 and 051228_NC_1234_B2 (Cases 4A and 4B) occurred even with possible channeling in one location on the edge of the beds, as shown in Figures 6.15 and 6.16, respectively. The time or conditions at which these possible channels were formed are unknown, although the initial head loss at high velocity was approximately 10% higher for each debris bed than the subsequent head loss when the velocity was again ramped up.

It was suggested by PNNL investigators that the head loss for the Case 4 tests (CalSil immediately followed by NUKON) are higher than the Case 1 tests (CalSil introduced onto a preformed NUKON debris bed) as a result of the fibrous material in the CalSil. This fibrous material could be deposited on the debris bed surface during the Case 1 tests while the majority may be expected to be in the interior of the debris bed for the Case 4 tests (the fiber will hold up on the screen with or without NUKON fiber present). This fibrous material from the CalSil insulation may provide a structure or flow paths in the CalSil surface layer of the Case 1 tests. This potential effect was indirectly considered for test 051228_NC_1234_B3 (Case 4C). In this test, as-received CalSil was ground with a mortar and pestle to disassociate the fibrous material from the particulate. The bulk material was then separated by sieving through a 212-μm-opening screen mesh. The CalSil material for test 051228_NC_1234_B3 was then taken from this "fiber-less" CalSil and prepared as for the other tests. The maximum head loss of any of the benchtop tests was achieved for test 051228_NC_1234_B3; approximately 975 in. H_2O at a screen approach velocity of 0.006 ft/sec (0.002 m/s). It is not believed that the possible channels in the other two debris beds of the Case 4 tests were the sole reason for the observed difference. When debris bed formation was occurring, the attainable screen approach velocity at the maximum pump speed for debris bed B3 was 50 to 60% of that for debris beds B1 and B2.

As discussed, it may be expected that introducing CalSil particulate on top of a preformed NUKON debris bed will result in a higher head loss than a debris bed formed from premixed debris. Further, the suggestion above that the fibrous material in the CalSil may provide flow paths or reduce the packed density of CalSil appears plausible and may be supported, at first glance, by the results of test 051228_NC_1234_B3. However, the difference between the surface appearance of the debris beds for Case 1, those of Case 4A and 4B, and the one for Case 4C is striking and may indicate that the critical particulate to fiber mass ratio and formation conditions are more significant.

As postulated, the variation in particle size and shape between the NUKON and CalSil may be expected to provide a tightly packed uniformly distributed debris bed with limited flow paths, even more so than a particulate surface layer, when sufficient particulate is available. Visual observation of the debris beds in Figures 6.17 through 6.20 from Case 1 shows distinct CalSil layers. Visual observation of Case 4 debris beds 051228_NC_1234_B1 and 051228_NC_1234_B2 does not show such distinct CalSil layers (see Figures 6.15 and 6.16). In fact, these debris beds do not appear dissimilar to the Case 2 debris beds (see Figure 6.21). This is also true for Case 4C, 051228_NC_1234_B3 (see Figure 6.22), which produced the highest head loss during the evaluation of the debris load sequence.

Reasonably good agreement (relative to the magnitude of the head loss between different test cases) was achieved between the large-scale and benchtop results for relatively similar debris injection scenarios (simultaneous separate injection lines compared to premixed) as shown in Figure 6.23. Consider head loss results from tests 051127_NC_2776_L1 (NC12) and 051128_NC_2776_L2 (NC13) performed in the large-scale loop and contained in Figure 6.23. For these tests, the debris constituents were introduced separately but simultaneously according to the Series 1 procedures. The head loss results from

Figure 6.15. Test 051228_NC_1234_B1 NUKON/CalSil Debris Bed for Case 4A. Possible flow channel at 5:00 orientation.

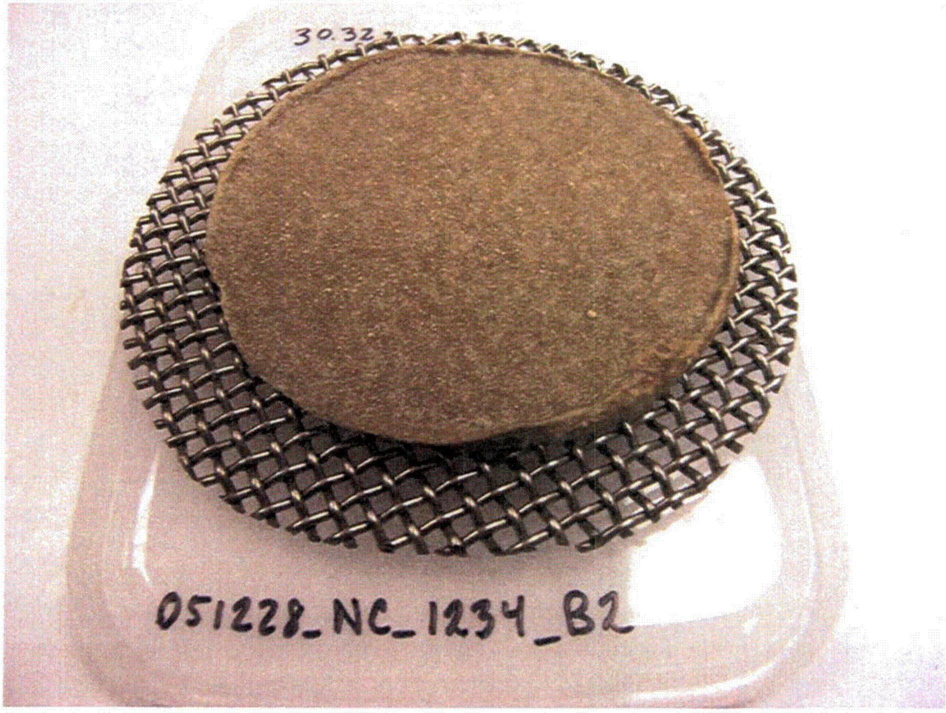

Figure 6.16. Test 051228_NC_1234_B2 NUKON/CalSil Debris Bed for Case 4B. Possible flow channel at 4:30 orientation.

Figure 6.17. Test 051214_NC_1234_B1 NUKON/CalSil Debris Bed for Case 1A. Debris Bed Surface is Mostly CalSil.

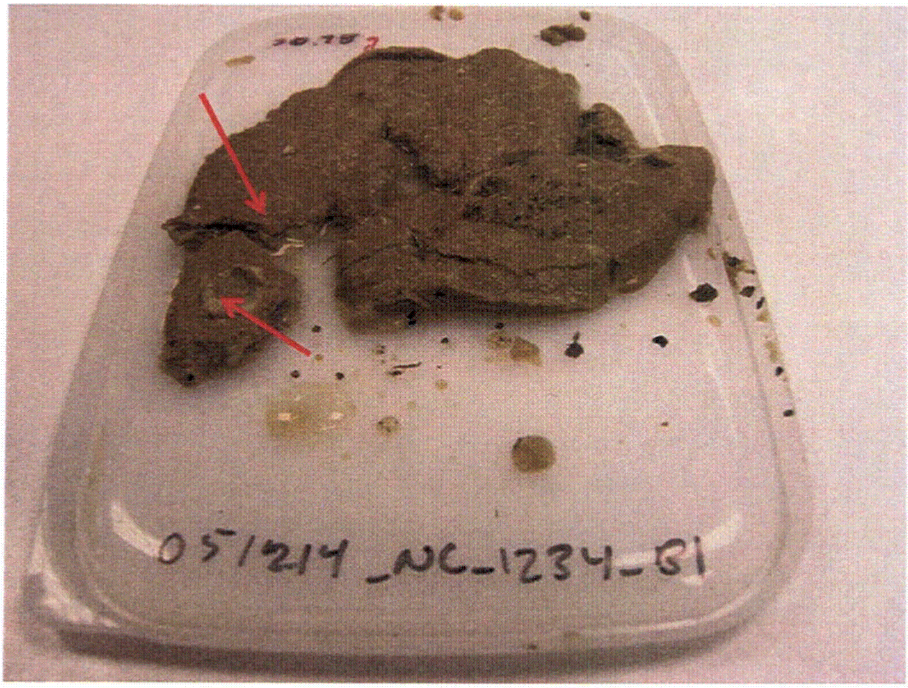

Figure 6.18. Test 051214_NC_1234_B1 NUKON/CalSil Debris Bed for Case 1A. Observation of CalSil Layer after attempt made to remove retrieved debris bed from the test screen. Brown "chunks" are rust from loop captured at screen surface.

Figure 6.19. Test 051214_NC_1234_B2 NUKON/CalSil Debris Bed for Case 1B. Debris Bed Surface is CalSil. Apparent Post-Test Rupture Caused After Drainage of the Test Loop During Separation of Test Section.

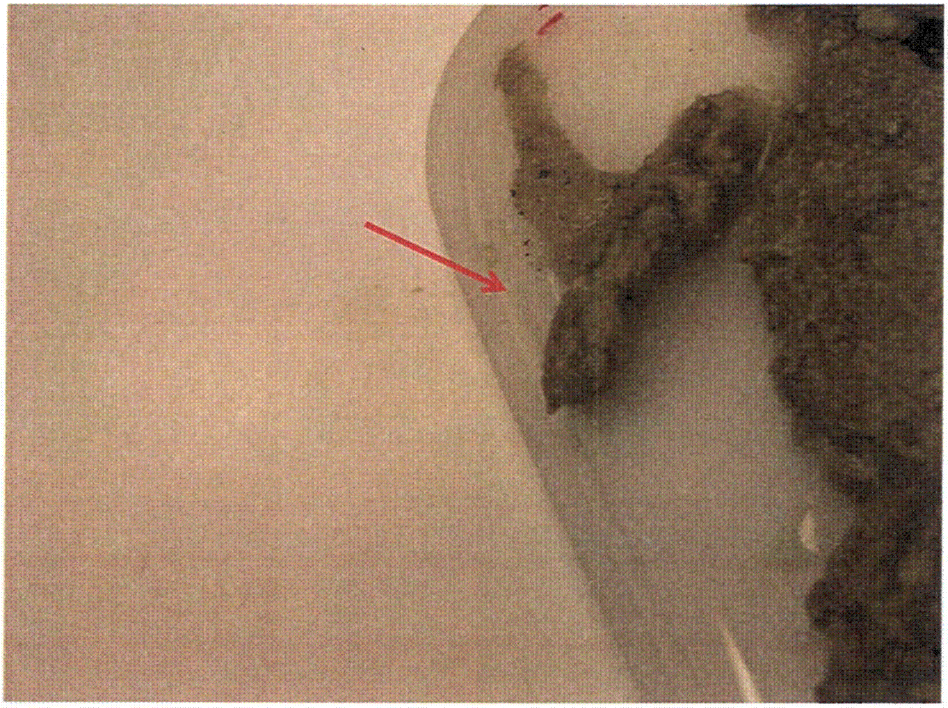

Figure 6.20. Test 051214_NC_1234_B2 NUKON/CalSil Debris Bed for Case 1B. Observation of CalSil Layer. Debris Bed Piece Tipped on Side. Brown "Specks" Are Rust From Loop Captured at Screen Surface.

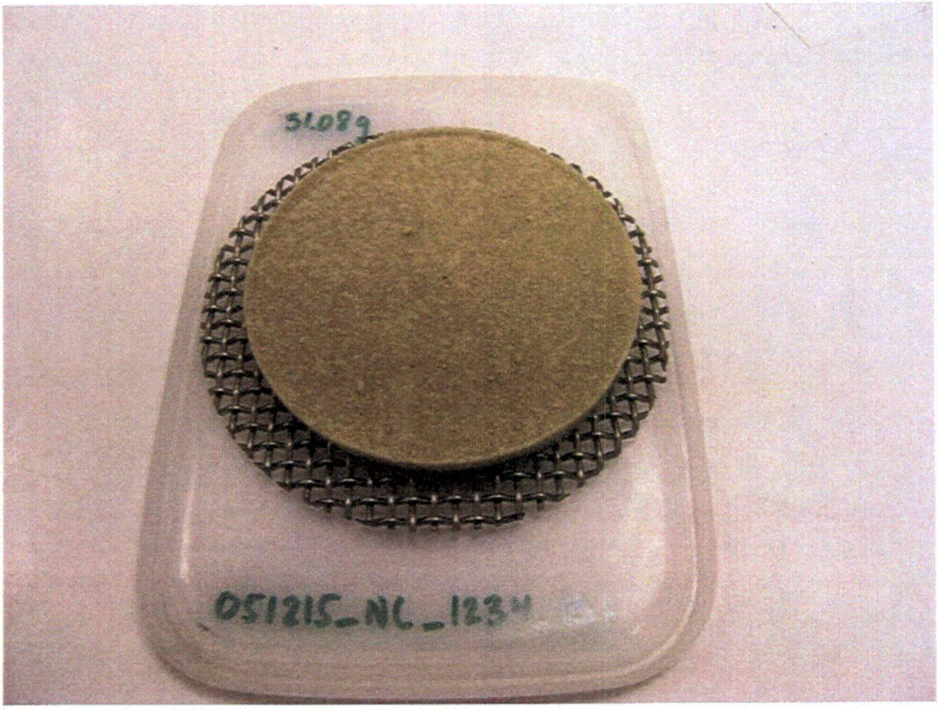

Figure 6.21. Test 051215_NC_1234_B1 NUKON/CalSil Debris Bed for Case 2A.

Figure 6.22. Test 051228_NC_1234_B3 NUKON/CalSil Debris Bed for Case 4C

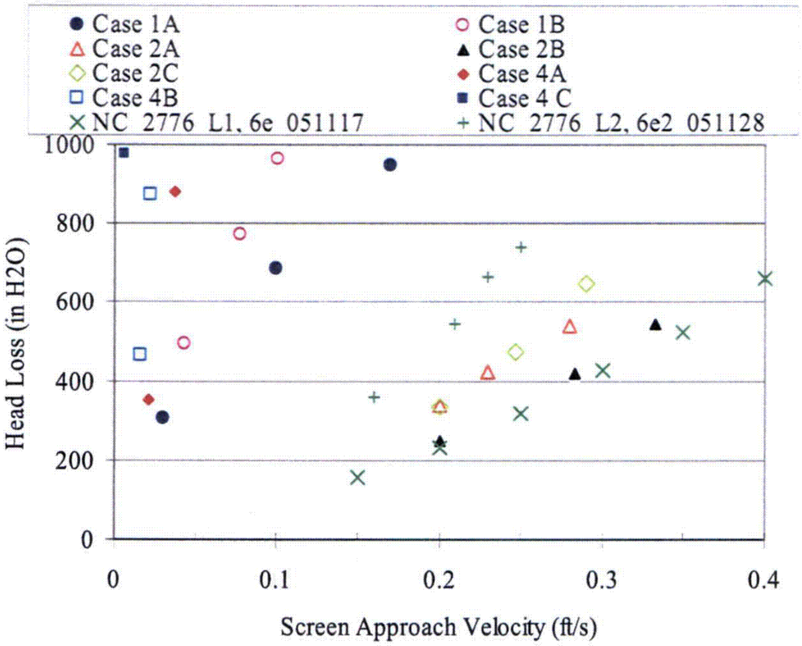

Figure 6.23. **Comparison of Debris Bed Head Loss as a Function of Screen Approach Velocity for NUKON/CalSil Debris Beds Formed with Different Debris Loading Sequences in the PNNL Large-Scale and Benchtop Loops (data from Figures 6.11 and 6.12).**

051127_NC_2776_L1 fall with the range of those obtained for the Case 2 tests, indicating the debris may have been well mixed before reaching the screen. The head loss results from 051128_NC_2776_L2 fall between those obtained for Case 2 (premixed debris) and Case 1 (CalSil introduced after NUKON-only bed formed). These results suggest the simultaneous injection of the NUKON and CalSil debris can result in premixed debris or allow for a fraction of the CalSil to be deposited on the surface of debris bed resulting in an elevated head loss for the same target mass loading.

The variation in the head loss results for the two Series 1 tests appears to be greater than for any of the other loading scenarios evaluated. Thus, the quantity of CalSil particulate potentially available for deposition on a preformed bed is at a maximum in the sequential introduction (Case 1), at a minimum in the premixed condition (Case 2), and somewhere in between for the simultaneous injection employed as the standard procedure for the Series 1 large-scale tests. However, as evidenced from the Case 4 tests, in particular test 051228_NC_1234_B3, significantly elevated head loss results are achievable without an apparent CalSil (particulate) top layer.

It may be that a critical particulate-to-fiber mass ratio is approached when the amount of particulate in the CalSil debris mass is increased by pre-sieving out the fiber (see above discussion of CalSil material preparation for test 051228_NC_1234_B3). This potential effect is addressed in subsection 6.3.1.2.1.

Furthermore, formation conditions such as CalSil particulate preferentially depositing into the flow path of a forming debris bed are believed to also play a significant role. For a given particle-to-fiber ratio, premixing results in a lower head loss as the particulate distributes throughout the debris bed. Therefore, some of the particulate occupies pore space that is not in a flow path and therefore does not contribute to flow resistance or blockage. When the CalSil particulate is introduced to the loop before the introduction of NUKON and allowed to become distributed throughout the flow (as in the Case 4 tests), CalSil particulate is available to be continually added to the forming debris bed, allowing it to be used more effectively and transported to block flow paths as the NUKON debris accumulates in the debris bed. This scenario may result in the particulate being more efficiently (optimally with respect to increasing flow resistance) distributed by the flow within the debris bed as the bed is formed, rather than:

- Being uniformly distributed within the debris bed and possibly having some particulate adhere to the NUKON prior to debris injection as a result of the premixed debris condition.
- The CalSil reaching the surface of the preformed NUKON debris bed thus limiting the dispersing of CalSil within debris bed to transport via flow from the debris surface through the packed NUKON fiber bed.

6.3.1.2.1 Case 4 Lag Time Investigation

As postulated, when the particulate is added during the bed formation, particulate may be used more effectively and transported to block flow paths. The possible effect of the delay or lag time for the introduction of the NUKON material for Case 4 has therefore been considered. Altering the lag time would potentially alter the distribution of the particulate through the debris bed and thus potentially alter the resulting head loss.

In the Case 4 tests of Table 6.6, the NUKON debris was introduced when, by visual observation, all of the CalSil material had been introduced into the flow loop. The actual lag time from the introduction of the CalSil to that of the NUKON for these tests is provided in Table 6.7 along with lag times for subsequently performed specific lag time tests.

The lag times of the 051228 Case 4 tests, 11, 17, and 19 seconds (Table 6.7), correspond to approximately 0.25, 0.39, and 0.43 of the calculated circulation time, respectively (subsequently referred to as the circulation fraction). To provide substantial differentiation to the 051228 tests as well as the calculated circulation time, a 30 second lag time, corresponding to an approximately 0.68 circulation fraction, was chosen for investigation.

The head loss results for tests 060207_NC_1234_B1 and 060303_NC_1234_B2 are provided in Figure 6.24. The 051228 Case 4 test results are included for comparison. All test data are tabulated in Appendix F. The results in Figure 6.24 indicate that increasing the lag time (i.e., increasing the circulation fraction) elevates the head loss for the tests considered. These results underscore the importance the debris bed formation conditions and process can have.

Table 6.7. Lag Time Benchtop Test Summary for Case 4 Conditions

Test Number	Lag Time (sec)	Circulation Fraction
051228_NC_1234_B1 (Case 4A)	11	0.25
051228_NC_1234_B2 (Case 4B)	17	0.39
051228_NC_1234_B3 (Case 4C)	19	0.43
060207_NC_1234_B1	30	0.68
060303_NC_1234_B2	30	0.68

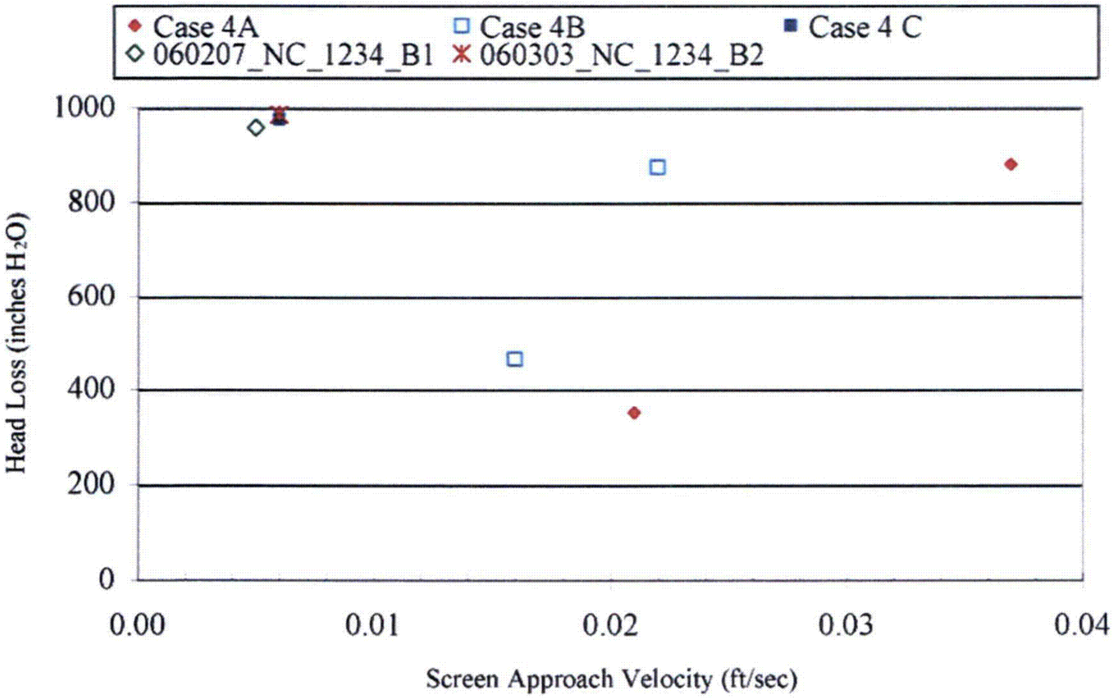

Figure 6.24. Debris Bed Head Loss as a Function of Screen Approach Velocity for Case 4 Lag Time Investigation. Data is for the final ramp up in velocity. Debris beds formed in the PNNL benchtop loop.

The essential replication of the 051228_NC_1234_B3 (Case 4C) head loss by the 060207_NC_1234_B1 and 060303_NC_1234_B2 tests indicate that closely approaching or perhaps reaching the critical particulate to fiber mass ratio by increasing the amount of particulate in the CalSil debris mass by pre-sieving out the fiber (see Section 6.3.1.2 discussion of CalSil material preparation for test 051228_NC_1234_B3) is not a strong contributor to the elevated head loss results. It does seem plausible however that the introduction of true particulate mass without fibers (due to sieving) may serve to increase the effect of the elevated circulation fraction (19 sec compared to 30 sec; refer to Table 6.7).

There is no visually observable difference in the 060207_NC_1234_B1 and 060303_NC_1234_B2 debris beds (Figures 6.25 and 6.26, respectively) compared with the 051228_NC_1234_B1, 051228_NC_1234_B2, and 051228_NC_1234_B3 debris beds (Figures 6.15, 6.16, and 6.22, respectively).

As discussed in subsection 6.3.1.2 regarding Figures 6.15 and 6.16, the 051228_NC_1234_B1 and 051228_NC_1234_B2 debris beds showed signs of channeling in one location at the test section wall. This raises the question as to whether the presence of these channels negates the apparent effect of the lag time depicted in Figure 6.24. As discussed, the time or conditions at which these possible channels were formed is unknown, although the initial head loss at high velocity was elevated by approximately 10% for each debris bed over the subsequent head loss when the velocity was again ramped up. Further, and more conclusively, an edge channel was visually observed to form during debris bed formation for the debris bed of benchtop test 060303_NC_1234_B1. (The 0.68 circulation fraction was being evaluated with test 060303_NC_1234_B1. The formation of the channel and the subsequent flow history resulted in the test

Figure 6.25. 060207_NC_1234_B1 NUKON/CalSil Debris Bed for Case 4 30 sec Lag Time

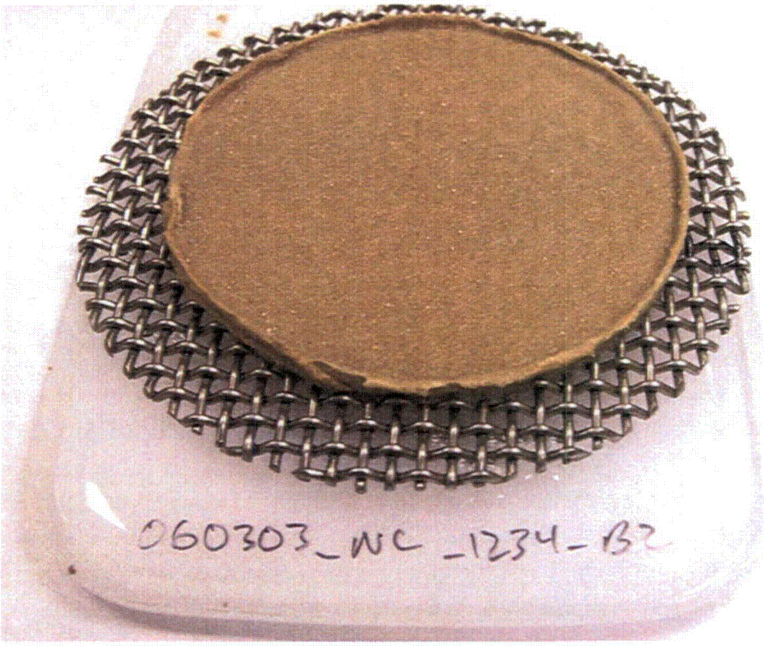

Figure 6.26. 060303_NC_1234_B2 NUKON/CalSil Debris Bed for Case 4 30 sec Lag Time

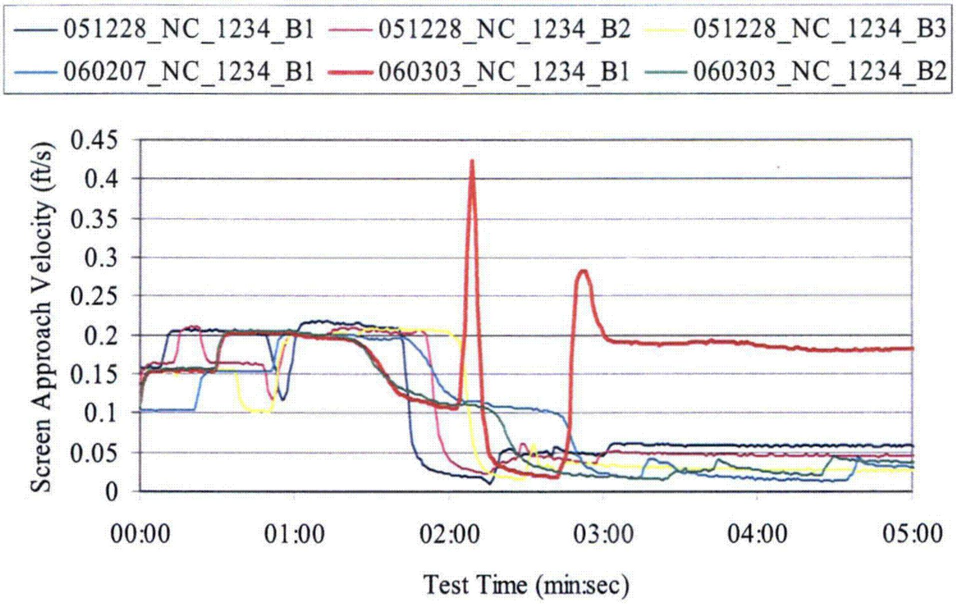

Figure 6.27. Screen Approach Velocity as a Function of Test Time, Case 4 Tests

being prematurely terminated and no head loss results are therefore presented.) The flow history during debris bed formation as illustrated by the attainable velocity of test 060303_NC_1234_B1 compared to all of the other Case 4 tests shows the effect of the observed channel, see Figure 6.27. (For each Case 4 test, the pump speed was maximized to maintain flow through the debris bed. The pump speed was reduced after the first velocity spike for test 060303_NC_1234_B1.) The similarity of the flow histories for the remaining tests suggests that the lag time effects evidenced in Figure 6.24 are real and not a result of channeling in the lower circulation fraction tests. Further lag time tests would support or negate this statement.

6.3.1.3 Post-Test Debris Bed Evaluation

Additional visual comparison may be made of the characteristics of the debris beds. The debris bed rim is not as pronounced in Case 1 (Figures 6.17 and 6.19) as in Cases 2 (Figure 6.21) and 4 (Figures 6.15, 6.16, 6.22, 6.25, and 6.26). (The lag time test debris beds of Section 6.3.1.2 are included with the Case 4 debris beds.) The approximate debris bed body heights for the test cases are given in Table 6.8. The appearance and visually observed thickness of the CalSil layers are also reported. The measured debris bed heights are referred to as "representative" because of the limitations of the measurement technique; the debris bed "body" measurements (plane area of the bed, not the outer rim, see Figure 6.16 for example) are inferred from a 1-mm-increment ruler placed vertically beside the debris bed. This gross technique is used only for the benchtop evaluations and provides a relative means of comparison.

The debris beds with elevated head loss results, Cases 1 and 4, had approximate measured debris bed body heights nominally 67% as thick as those from Case 2. As presented below, the Cases 1 and 4 dried debris beds had 86% of the mass of the Case 2 beds on average. Thus, the elevated head loss for the thinner debris beds may be expected due to the higher bulk densities for the debris beds. The manually measured approximate debris bed body heights for retrieved, dried beds from the Series 1 large-scale loop

Table 6.8. Relative Comparison of Approximate Debris Bed Body Height Measurements from Benchtop Investigation of NUKON/CalSil Debris Beds

Test	Approximate Measured Debris Bed Body Height (in.) (mm)	Approximate Measured CalSil Top Layer Height at Edge (in.) (mm)
051214_NC_1234_B1	0.20 (5.1)	0.04 (1.0)
051214_NC_1234_B2	0.22 (5.6)	0.06 (1.5)
051215_NC_1234_B1	0.31 (7.9)	No CalSil Layer Apparent
051215_NC_1234_B2	Rupture on Retrieval, N/A	No CalSil Layer Apparent
051216_NC_1234_B1	0.31 (7.9)	No CalSil Layer Apparent
051227_CO_0411x_B1	N/A	N/A
051227_CO_1763_B2	N/A	N/A
051228_NC_1234_B1	0.20 (5.1)	No CalSil Layer Apparent
051228_NC_1234_B2	0.22 (5.6)	No CalSil Layer Apparent
051228_NC_1234_B3	0.22 (5.6)	No CalSil Layer Apparent
060207_NC_1234_B1	0.24 (6.1)	No CalSil Layer Apparent
060303_NC_1234_B2	0.20 (5.1)	No CalSil Layer Apparent

tests exhibiting elevated head loss were 0.21 in (5.3 mm) for 051128_NC_2776_L2, and 0.24 in (6.1 mm) for test 051117_NC_2776_L1 (refer to Appendix J). This relatively minor thickness difference, 0.03 in. (0.8 mm), is the inverse of the expected result given the resultant head losses (similar mass quantities were retrieved). However, as shown in Figure 6.23, the head loss difference for these two large-scale tests is much less significant than for the benchtop results.

The relatively greater reduction in thickness of the benchtop Case 1 and 4 debris beds compared with the reduction in mass of the Case 2 debris beds may further support the significance of the formation conditions and the critical mass ratio of particulate on influencing the resultant head loss. Particulate packing into a flow path, while increasing the head loss, may not increase the bulk volume of the debris bed. As suggested, the diverse particle and fiber sizes in a premixed debris bed may pack relatively tightly. It may be, however, as suggested by the debris bed results, that the particulate intermingled with the fiber in the premixed condition causes a decrease in the bulk density despite a potential reduction in the local porosity.

It was observed that the Case 1 and Case 4 debris beds were significantly weaker structurally than those of Case 2, as judged by their behavior during removal from the screen. A flat metal ruler was used to remove and lift the debris beds off the screens. For debris from the Case 1 debris beds sagged and fell where it was not directly supported by the ruler. The Case 4 debris beds, while not actually removed from the screen, were evaluated on the debris bed edge, and similar behavior was observed. The Case 2 debris beds could be lifted in their entirety off the screen with the ruler, as could the NUKON-only debris. NUKON-only debris beds were easily removed from their screens and appeared to be stronger structurally than the Case 1 and 4 debris beds. This result is somewhat surprising, given the higher head loss of the Case 1 and 4 debris beds.

The relative structural strength of debris beds may be related to the water content of the debris bed, which may be compared using their computed immediate post-retrieval water mass fraction. The water mass fraction, w_H, is computed from

$$w_H = \frac{m_W - m_D}{m_W} \tag{6.1}$$

where m_D and m_W are the dry and wet retrieved debris bed masses, respectively. Essentially equivalent water mass fractions are computed for Cases 1 and 4 as well as for the Case 2 debris beds (see Table 6.9). Thus, the water content apparently does not contribute to the observed strength differences.

The total dry debris mass that accumulated on the test screen is also reported in Table 6.9. The dry debris bed mass is lower for the Case 1 and 4 debris beds compared with those from the Case 2 tests (approximately 0.82 dry solid retrieval fraction of the initial added mass compared to approximately 0.94). This result may be expected given the premixing of the debris for the Case 2 tests allows material interaction to occur prior to introduction. However, perhaps much more crucial is the fact that the extremely high head loss results achieved for the Case 1 and 4 tests limited the available flow rate, thus significantly decreasing the number of loop circulations completed during these tests. It is somewhat remarkable to compare the CalSil-only debris bed pictures (Figures 6.13 and 6.14) with their dry mass and retrieval fraction. Nominally only 10% of the material was retained on the screen (observed rust material from the loop is included in the measured dry mass).

The water mass consideration can also theoretically be used to determine a representative porosity assuming the debris bed is completely saturated with no interstitial air. The higher head loss debris beds may be expected to have a lower porosity. The density of water, ρ_H, is taken as 1 g/mL. The representative porosity of the debris bed, ϕ_W, can then be determined from

$$\phi_W = \left(1 - \frac{m_D}{m_W}\right)\frac{\rho_W}{\rho_H} \tag{6.2}$$

where ρ_W is the wet debris bed density computed from

Table 6.9. Debris Bed Measured Mass from Benchtop Investigation of NUKON/CalSil Debris Beds

Test Number	Test Case	Wet Mass (g)	Dry Mass (g)	Dry Solid Retrieval Fraction of Target	Water Fraction Eq. (6.1)	Dry Debris Bed Porosity Eq. (6.5)
051214_NC_1234_B1	1A	65.27$^{(a)}$	10.76$^{(a)}$	0.87	0.84	0.91
051214_NC_1234_B2	1B	64.01$^{(a)}$	10.17$^{(a)}$	0.82	0.84	0.92
051215_NC_1234_B1	2A	72.98	11.58	0.94	0.84	0.94
051215_NC_1234_B2	2B	97.39	11.42	0.93	0.88	No h$^{(b)}$
051216_NC_1234_B1	2C	65.3	11.66	0.94	0.82	0.94
051227_CO_0411x_B1	3A	N/A$^{(a)}$	1.49$^{(a)}$	0.08	N/A	No h$^{(b)}$
051227_CO_1763_B2	3B	19.36	2.26	0.13	0.88	No h$^{(b)}$
051228_NC_1234_B1	4A	63.16	10.15	0.82	0.84	0.92
051228_NC_1234_B2	4B	62.92	10.33	0.84	0.84	0.92
051228_NC_1234_B3	4C	64.26	9.6	0.78	0.85	0.93
060207_NC_1234_B1	NA	64.2	9.3	0.75	0.86	0.94
060303_NC_1234_B2	NA	66.22	9.44	0.76	0.86	0.92

(a) Rust debris from loop observed in/on debris bed.
(b) No height measurement, see Table 6.8.

$$\rho_W = \frac{m_W}{\frac{\pi}{4}d^2h} \tag{6.3}$$

where d is the test section diameter (4 in.) and h is the debris bed body height. Imperfections in the debris bed and the rim are neglected. Calculation of the representative porosity using Eq. (6.2) and (6.3) from the data of Tables 6.8 and 6.9 is rendered suspect, however, when porosities greater than 1 are achieved.

Consider, therefore, that the bulk wet density may be expressed by

$$\rho_W = \frac{1}{\frac{1-w_H}{\rho_S} + \frac{w_H}{\rho_H}} \tag{6.4}$$

where ρ_S is the dry solid density. Also, the density of the dry debris material, assuming relatively constant particulate to fiber mass ratios between the respective debris beds, should be relatively constant. In application of Eq. (6.3) and (6.4), the dry debris material density is computed to range from -1.5 to 3.3 g/mL. Because this is a nonsensical result, and the solid density should in fact be relatively constant, the nonphysical results from Eq. (6.2) are understandable and not considered further.

Consider instead the average porosity of the dry debris bed, which may be evaluated from

$$\phi_D = 1 - \frac{m_D}{\frac{\pi}{4}d^2h\rho_S} \tag{6.5}$$

With a representative dry solid density of 3 g/mL, relatively consistent results are achieved (see Table 6.9). A representative constant dry solid density of 3 g/mL is chosen loosely based on data from Zigler et al. (1995), Shaffer et al. (2005), Weast (1975) and preliminary PNNL work. An attempt was made to minimize the error of the difference between ρ_W from Eq. (6.3) and (6.4) by solving for ρ_S; convergence was not achievable. Acknowledging the uncertainties of the analysis, the average porosity of the Case 2 debris beds appears to be only slightly elevated over the Case 1 and Case 4 debris beds in keeping with, but having a surprisingly small difference with regard to, the head loss results. The apparent relatively constant average porosity does make sense in relation to the argument that the formation conditions in terms of particulate distribution play a significant role. To reiterate, it is suggested that, when added during the debris bed formation, particulate may be collected in the flow paths by selective mass transport as opposed to being more homogeneously distributed from a premixed condition.

The apparent structural strength issue is not explained by examination of the average porosity. Insight into the internal structure of the debris bed may possibly be gained by a literature review of the relative strength of fiber particulate matrixes as related to their inner structure. It is striking to note that the Case 1 debris beds are apparently weaker than NUKON-only debris beds. Consider that the Case 1 debris beds consist of CalSil deposited onto a preformed NUKON-only debris bed. Apparently, therefore, the addition of CalSil to a preformed NUKON debris bed weakens or changes the structure of a NUKON debris bed with respect to post test handling. Contrary to this observation, testing in the benchtop loop has repeatedly shown that a formed NUKON-only debris bed will rupture if subjected to no-flow conditions while still submerged. However, the apparent weaker (based on post test handling) 051228_NC_1234_B3 NUKON/CalSil debris bed sat submerged at no-flow conditions during retrieval for approximately 10 minutes (water in the test section above the debris bed had to be siphoned out; there was no flow through the debris bed with approximately 2.5 ft of water on it). The observations with respect to structural strength may be related to the compressibility of the debris beds and changes that may occur when the differential pressure is removed and the debris bed is no longer submerged (removed from the water).

6.3.2 Investigation Conclusions

The results of the benchtop tests discussed herein support the conclusion that the elevated head loss results observed in the initial benchtop tests as well as large-scale Series 1 tests 051123_NC_2181_L1 and 051128_NC_2776_L2 were due to slight differences in CalSil and NUKON debris introduction process/sequences. All investigated changes in loading sequences resulted in divergent head loss results. The investigated debris loading sequences were ranked from the highest measured head loss to the lowest as follows:

1. CalSil introduction followed by the introduction of NUKON after a slight time lag (Case 4). Increasing the lag time between the introduction of the CalSil and NUKON increased the resultant head loss.
2. CalSil introduction onto a preformed NUKON-only debris bed (Case 1).
3. Premixed NUKON and CalSil (Case 2) had the lowest measured head loss of the NUKON and CalSil sequences investigated.

These debris loading sequence issues should be considered in terms of both the statistically meaningful results with regard to repeatability, conservatism of the results for real applications in terms of a safety-basis use, and identification of required correlation parameters. The data suggest, in accordance with other particulate filtration studies, that the particulate-to-fiber mass ratio (i.e., internal decrease in debris bed porosity due to the addition/buildup of particulate) has a more significant effect on the resulting head loss than just the formation of a closely packed layer of particulate on the surface of the debris bed.

Other test sequences such as additional variations in the time lag for Case 4, CalSil debris bed formation followed by the addition of NUKON, CalSil addition followed by NUKON followed by CalSil, and sequential tests may provide additional information. Insight into the underlying physical phenomena may be achieved through bed sectioning and associated analyses as well as debris deposition modeling and packing/porosity calculations based on particulate and fiber size distributions.

6.4 Debris Bed Sectioning

Debris beds 060303_NC_1234_B2 and 060516_NC_1234_B1 generated in the benchtop loop as part of the load sequence evaluation (Section 6.3) were selected for cross-sectional analysis. Both debris beds had a target CalSil mass loading of 507 g/m^2 and a target NUKON mass loading of 1015 g/m^2, for a total target mass loading of 1522 g/m^2. This is essentially the same target mass loading as test cases NC12 and NC13. Debris bed 060303_NC_1234_B2 had 76% of the target mass retained on the screen for a retrieved mass loading of 1164 g/m^2. The final dry mass for bed 060516_NC_1234_B1 is not available;

however, other benchtop debris beds with the same mass target mass loading subjected to repeat tests of the test procedure used for 060516_NC_1234_B1 had an average of 86% of the target mass retained on the screen for an average retrieved mass loading of 1306 g/m^2.

Debris bed 060516_NC_1234_B1 was generated to Case 1 test conditions (refer to Section 6.3.1) with a complete NUKON debris bed formed before introducing the CalSil debris. Bed 060303_NC_1234_B2 was generated to Case 4 test conditions with a 30 second lag time between the introduction of the CalSil and NUKON debris materials.

After being dried at 90°C, the debris beds were impregnated with an epoxy resin and sectioned; cross-sectional samples were imaged using SEM, as described in Section 2.5.3.3. The samples were taken along the center wire of the square grid and along a diagonal, as shown in Figure 6.28. A photograph of the mounted samples for bed 060516_NC_1234_B1 is shown in Figure 6.29. A series of images was taken through the depth and along the top surface for each sample.

Under visual examination, both debris beds appeared to consist of three distinct regions: the wire support, a thick region with high porosity, and a very thin high-density region on the upstream (inlet) surface of the debris bed. A series of SEM images for each of the last two regions is shown in Figures 6.30 through 6.33 for bed 060303_NC_1234_B2 and Figures 6.34 through 6.36 for bed 060516_NC_1234_B1. The orientation of the images is such that the vertical axis of the debris bed appears horizontal in the image with the direction of flow through the debris bed having been from right to left in the image.

The porous center region shown in Figures 6.30 and 6.31 consists almost entirely of cylindrical NUKON fibers ranging from 5 to 15 microns in diameter, based on analyses of SEM photos. The elliptical cross-sectional shapes indicate where a fiber is at an angle with respect to the cut surface. Based on the images, it appears the predominant orientation of the fibers is approximately parallel to the debris bed surface (assumed to be at right angles to the direction of flow). The light-shaded areas indicate CalSil material. The center region also includes gaps (voids) between the NUKON fiber regions, as shown in Figure 6.31. One possible explanation for these gaps is that the procedure for flooding the sample with epoxy induced separation. Another possible explanation, since the benchtop did not have the ability to increase the static pressure of the loop to maintain gas in solution, is that the void may have been created by a gas bubble forming within or at the base of the debris bed as the pressure drop increased. If the bubble was formed at the bottom of the bed, it may have migrated upward in the bed as the flow was reduced or during the debris bed retrieval process.

Digital analysis of the SEM images indicate that the porous center regions, excluding gaps, consist of a NUKON fiber concentration of 6.1 ±1.7 vol% (060303_NC_1234_B2) and 8.3 ±1.9 vol% (060516_NC_1234_B1) and a CalSil concentration of 1.4 ±0.6 vol% (060303_NC_1234_B2) and 3.7 ±1.2 vol% (060516_NC_1234_B1). These concentrations are consistent throughout the center porous region of the bed, with no discernable trend as a function of location. The thickness of the center porous region is approximately 8.2 and 4.5 mm, respectively. The total thickness of the debris beds is 8.7 and 5.5 mm, respectively.

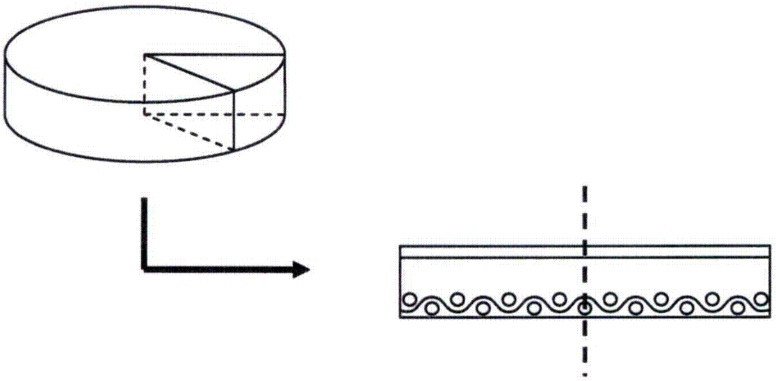

Figure 6.28. Schematic of Debris Bed Cross-Section Used for SEM Imaging

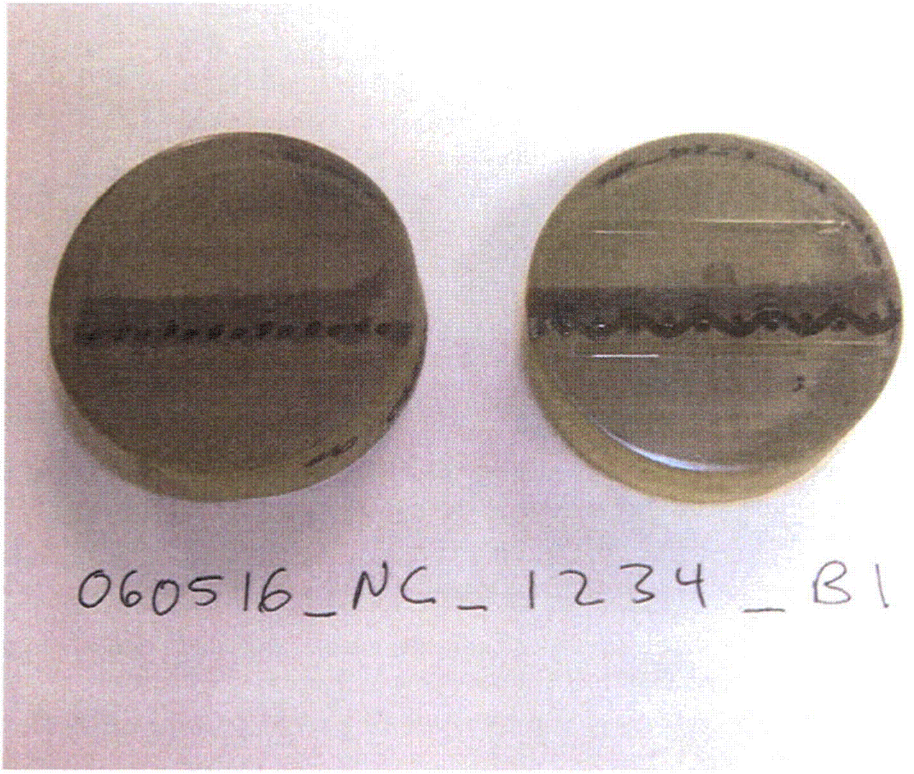

Figure 6.29. Mounted Debris Bed Samples Used for SEM Imaging

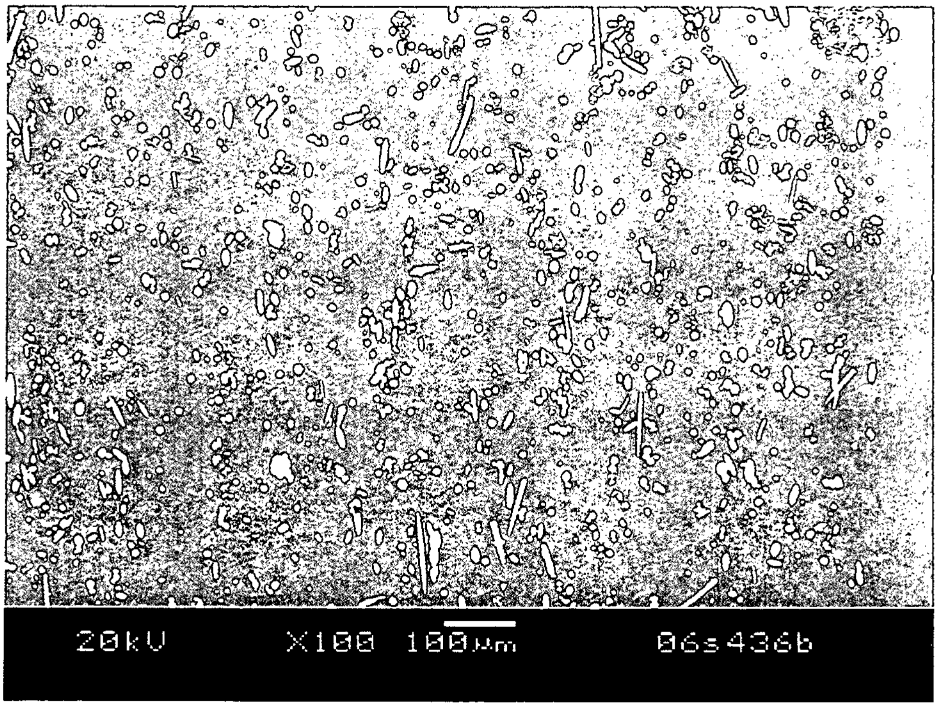

Figure 6.30. SEM Image of the NUKON Fiber Region in Debris Bed 060303_NC_1234_B2 (Case 4)

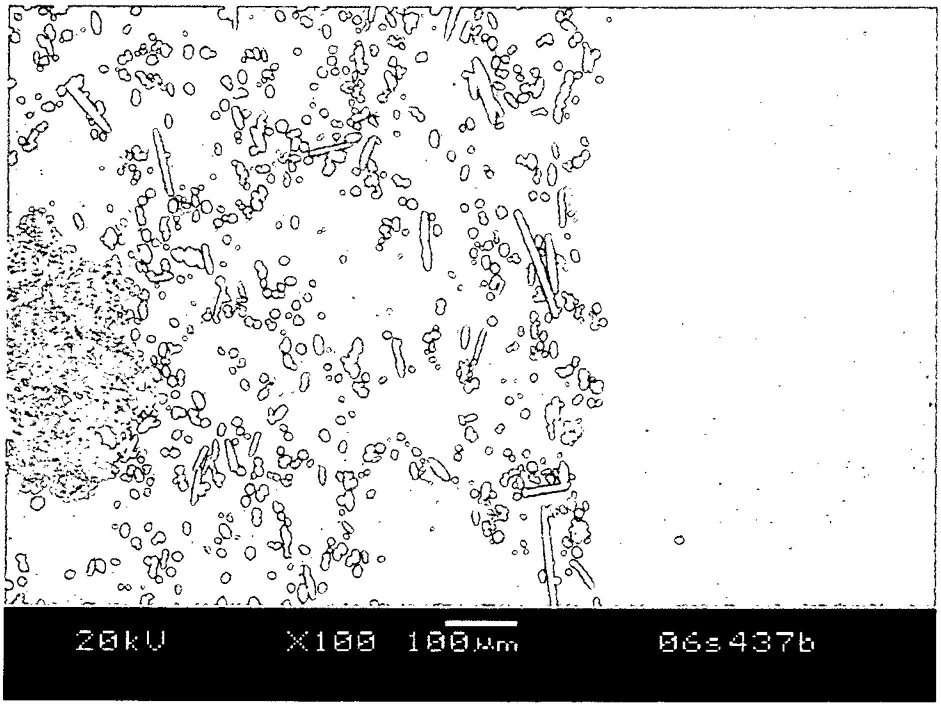

Figure 6.31. SEM Image of NUKON Fiber Region in Debris Bed 060303_NC_1234_B2 (Case 4) Showing Gap or Void Region

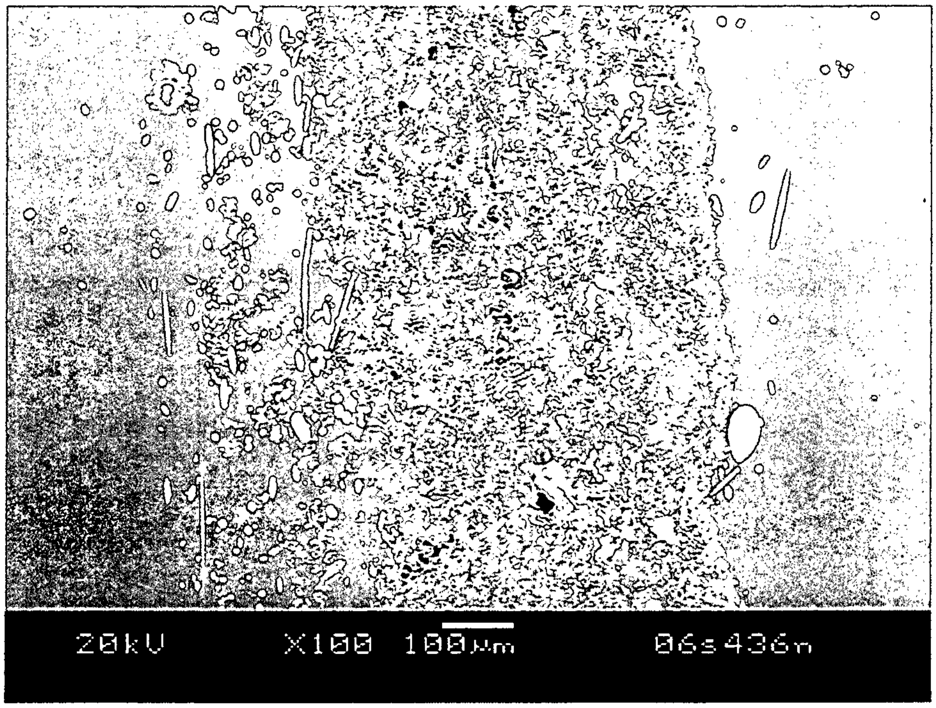

Figure 6.32. SEM Image of the CalSil Surface Layer for Debris Bed 060303_NC_1234_B2 (Case 4)

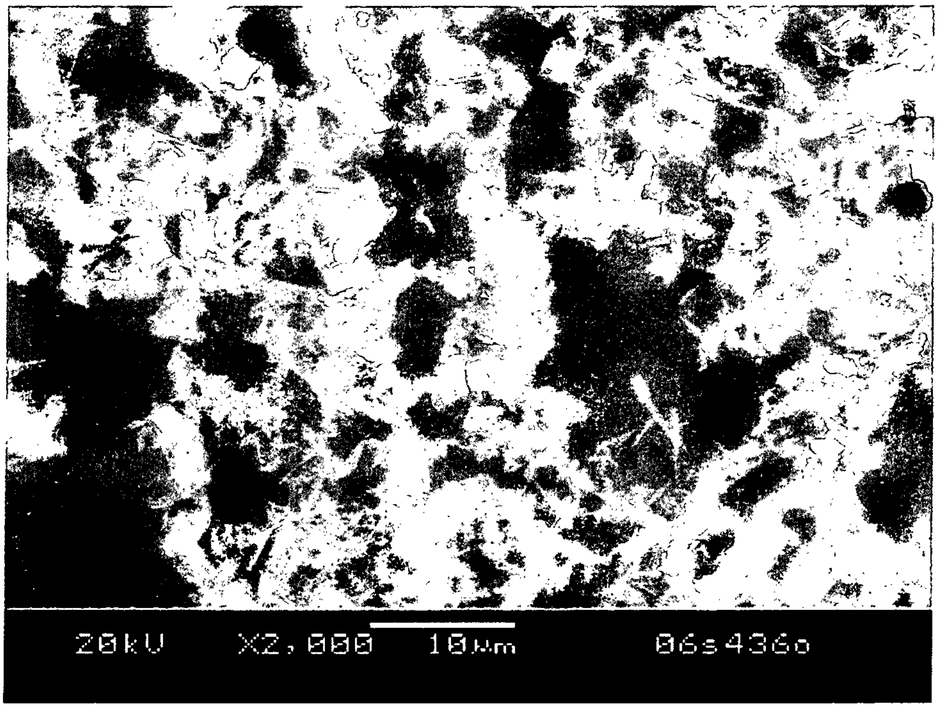

Figure 6.33. High-Magnification SEM Image of the CalSil Surface Layer for Debris Bed 060303_NC_1234_B2 (Case 4)

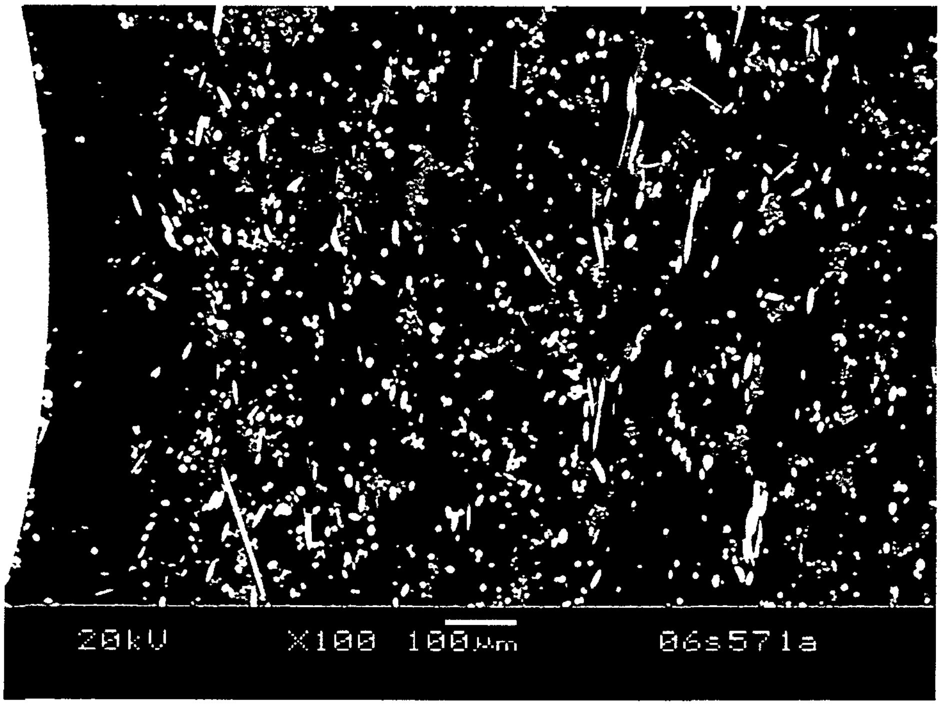

Figure 6.34. NUKON Fibers near Metal Grid for Debris Bed 060516_NC_1234_B1 (Case 1)

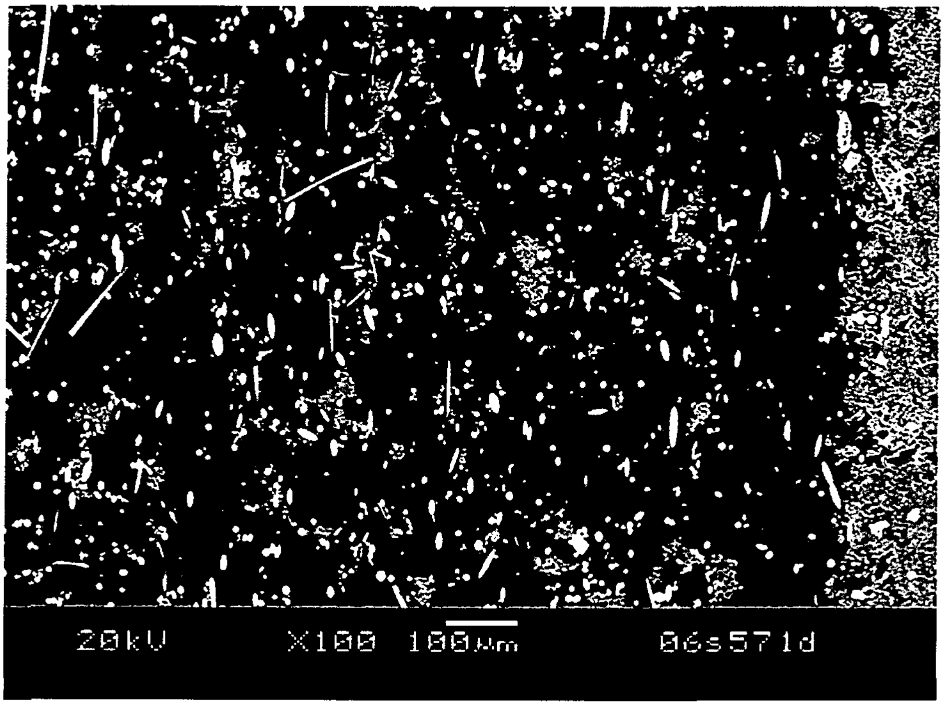

Figure 6.35. NUKON Fibers near Surface Region for Debris Bed 060516_NC_1234_B1 (Case 1)

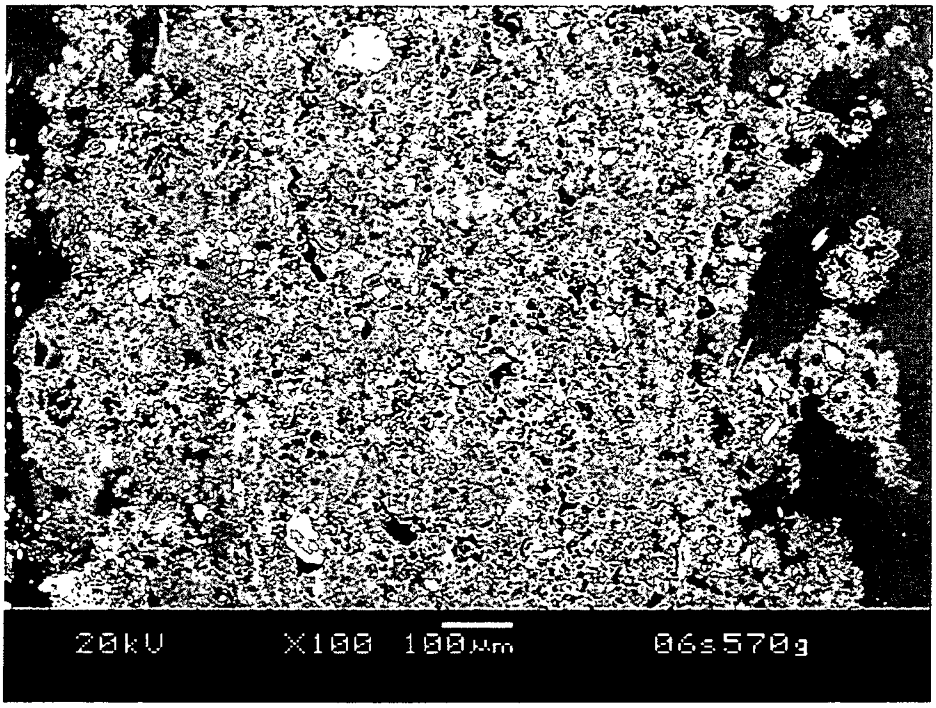

Figure 6.36. Cross-Section of Surface Region (CalSil layer) for Debris Bed 060516_NC_1234_B1 (Case 1)

The high-density surface layer shown in Figures 6.32 and 6.33 consists primarily of CalSil particulate supported by NUKON fibers. The layer is relatively uniform across the debris bed with measured thicknesses of 0.52 ±0.06 mm and 1.05 ±0.09 mm, respectively. Digital image analysis results indicate that the surface layer consists of CalSil concentrations of 59 ±7 vol% (060303_NC_1234_B2) and 64 ±4 vol% (060516_NC_1234_B1) and a NUKON fiber concentration of 6.5 ±0.5 vol% and 5.5 ±0.6 vol%, respectively. Figure 6.33 is a high-magnification SEM image of the CalSil surface layer. Much of the calcium silicate has the form of micron sized needle-like crystals that have agglomerated together.

The structure of the two debris beds suggests a sequence of filtration mechanisms. The original wire grid is not effective in capturing the CalSil particles, but the long aspect ratio NUKON fibers begin to form a mat on the grid surface. The particles continue to pass through the grid until the density of the fiber mat increases to the point where the gaps are roughly the size of the particle diameters. The fiber mat then acts as the particle filter and the surface layer begins to form.

The composition results presented for the porous center region are for a bed that is not loaded and compressed. The NUKON fibers may have elastic properties that allow the bed to change its structure in response to forces resulting from the flow resistance of the surface layer. The dynamic behavior of the fiber mat due to pressure fluctuations may also allow the release of CalSil particles trapped in the center region.

The total flow resistance of the debris bed is determined by the permeability and thickness of both the center and surface regions under flow conditions. The center region resistance will be relatively insensitive to the applied flow rate. However, the thickness and permeability of the center region will decrease significantly as the flow rate increases. The flow resistance of the surface layer will result in a lithostatic load compressing the fiber bed. The increase in fiber density will result in a lower permeability and higher flow resistance in the center region. This resistance adds to the lithostatic load on the downstream fiber bed, compressing it even further.

A major difference between the two debris beds is the thickness of the fiber bed center region, which is approximately 8.2 mm (060303_NC_1234_B2) and 4.5 mm (060516_NC_1234_B1), not quite a factor of 2. The second bed also has a significantly higher concentration of CalSil particles, which could interfere with the compression and sealing of the bed. The use of microscale simulations may be used to determine the permeability of both the surface region and the fiber bed region as a function of compression. This information, along with the elastic strength of the NUKON fibers, could be used to predict the overall flow resistance of the debris bed under different flow conditions.

6.5 Flow History

Head loss for a given screen approach velocity has been observed to increase as the velocity is cycled through the test range and returns to the given velocity either as part of a ramp up or ramp down of the velocity sequence (see Sections 6.1–6.3). Section 5.3 describes the velocity matrixes applied for the various test series. Flow history, the time and flow a debris bed has been subjected to prior to attaining a specific velocity, has also been observed to have an impact on the measured head loss (see head loss data in Section 6.2 of complete and truncated velocity matrixes). Specific repeated-cycle benchtop tests have been conducted to investigate the magnitude of the effect of flow history on the debris bed head. The tests were conducted using test condition 1a (NUKON-only, target debris loading 1681.4 g/m^2).

6.5.1 Test Conditions

Tests were conducted in the PNNL benchtop loop (Section 2.3) using test procedures similar to those described in Section 5.3. The non-boiled NUKON debris was prepared to an R4 value of 11 ± 1 for each test. The target debris loading of 1681.4 g/m^2 corresponds to 13.63 g of NUKON debris in the 4 in.-diameter test section of the benchtop loop. All tests employed 5-mesh screen as the test screen material, which is described in Section 2.2.

The initial screen approach velocity was 0.20 ft/sec, and the velocity was allowed to decay over the 20-minute bed formation time (constant pump speed), resulting in approximately 27 circulations through the loop. The steady-state criterion for bed formation and at each subsequent velocity was taken as less than a 2-in.-H_2O change in head loss over a 2-minute period. Repeated cycling through the screen approach velocity matrix (0.20, 0.45, and 0.75 ft/sec screen approach velocities) was conducted. Extended half-hour hold periods at constant screen approach velocities (same as cycling points) were also performed. Two flow history tests were performed, 060418_NO_1363_B1 and 060419_NO_1363_B1.

6.5.2 Test Results

Head loss results as a function of screen approach velocity for flow history tests 060418_NO_1363_B1 and 060419_NO_1363_B1 are presented in Table 6.10. The approximate 20% difference in test results compares with similar test comparisons observed in Sections 6.1 and 6.2. For each flow history test, the head loss at a given screen approach velocity increased with the number of cycles (refer to Table 6.10 and Figures 6.37 and 6.38. The average increase in head loss with cycling is typically at a maximum for cycles 1–3, as observed in Table 6.11. It may also be observed from Table 6.11 that the average change in head loss per velocity cycle was typically greater at the higher screen approach velocities.

Table 6.10. 060418_NO_1363_B1 and 060419_NO_1363_B1 Flow History Tests Data

Test		060418_NO_1363_B1	060419_NO_1363_B1
Test Phase[a]	**Screen Approach Velocity (ft/sec)**	**Head Loss (in. H_2O)**	**Head Loss (in. H_2O)**
Ramp up 1	0.2	41	37
	0.45	120	102
	0.75	236	197
Ramp Down 1	0.45	128	105
	0.2	49	40
Ramp up 2	0.45	128	105
	0.75	244	203
Ramp Down 2	0.45	132	108
	0.2	51	41
Ramp up 3	0.45	131	108
	0.75	249	206
Ramp Down 3	0.45	134	110
	0.2	51	41
T1	0.2 (T)	51, 52	41, 43
	0.45 (T)	135, 135	111, 112
	0.75 (T)	256, 256	213, 211
Ramp up 4	0.2	53	43
	0.45	137	111
	0.75	260	213
Ramp Down 4	0.45	140	113
	0.2	54	43
Ramp up 5	0.45	139	112
	0.75	262	214
Ramp Down 5	0.45	141	115
	0.2	54	43
Ramp up 6	0.45	140	114
	0.75	266	216
Ramp Down 6	0.45	142	115
	0.2	55	44
T2	0.2 (T)	55, 57	44, 46
	0.45 (T)	145, 146	118, 118
	0.75 (T)	276, 276	225, 222
Ramp up 7	0.2	57	45
	0.45	147	117
	0.75	278	223
Ramp Down 7	0.45	149	119
	0.2	58	45
Ramp up 8	0.45	149	117
	0.75	280	223
Ramp Down 8	0.45	150	119
	0.2	58	45
Ramp up 9	0.45	150	119
	0.75	281	224
Ramp Down 9	0.45	152	120
	0.2	59	46
T3	0.2 (T)	59, 61	46, 48
	0.45 (T)	155, 156	122, 123
	0.75 (T)	293, 291	232, 228

(a) T1 = T2 = T3 = 0.5 hour hold period. Double entries indicate the head loss at the beginning and end of the hold periods, respectively.

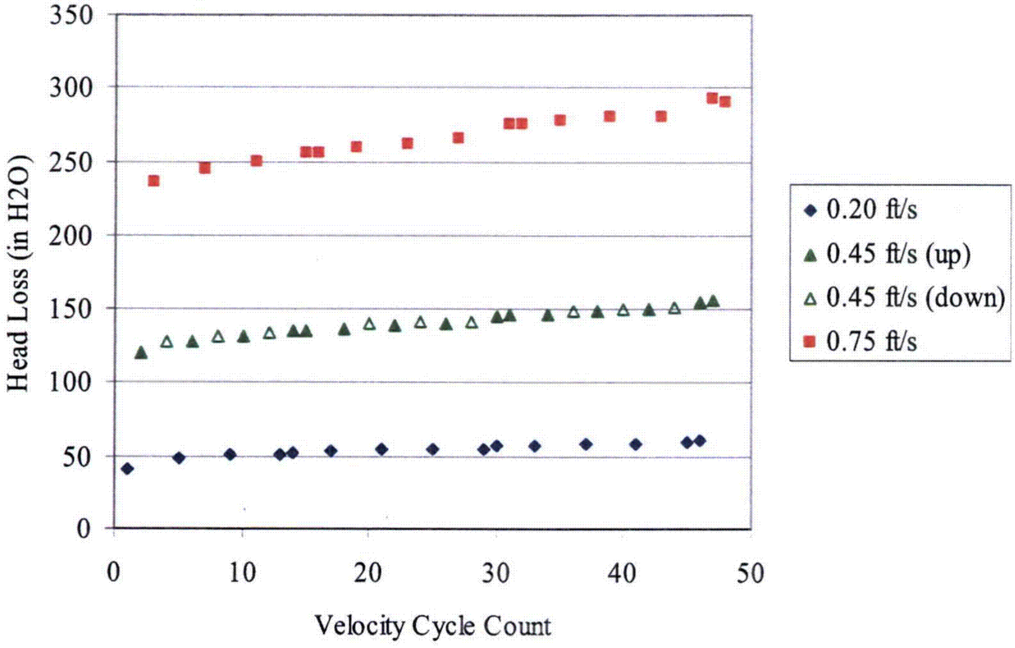

Figure 6.37. 060418_NO_1363_B1 Head Loss as a Function of the Velocity Cycle Count (number of cycles of velocity ramp up and ramp down completed)

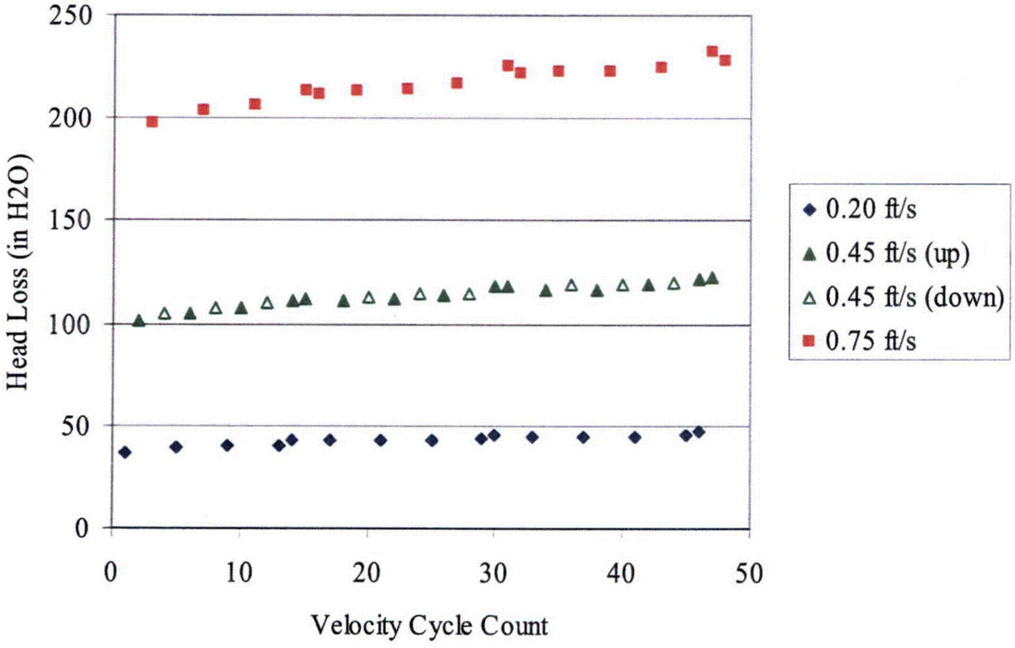

Figure 6.38. 060419_NO_1363_B1 Head Loss as a Function of Velocity Cycle Count (number of cycles of velocity ramp up and ramp down completed)

Table 6.11. Average Change in Head Loss per Velocity Cycle

Parameter	Average Change in Head Loss per Velocity Cycle Count (in H_2O/Cycle)		
Screen Approach Velocity (ft/sec)	0.20	0.45	0.75
Test	060418_NO_1363_B1		
Cycles 1–3	3.3	5.0	6.7
Cycles 4–6	0.7	2.7	2.0
Cycles 7–9	0.7	1.3	5.0
Test	060419_NO_1363_B1		
Cycles 1–3	1.3	3.0	5.3
Cycles 4–6	0.3	2.3	4.0
Cycles 7–9	0.3	1.7	3.0

The results from the half-hour hold periods at constant screen approach velocities indicate a different trend (see Table 6.10); it appears that at the higher velocities the head loss remains constant or decreases over the hold period.

The representative approximate debris bed body heights and dry debris bed masses for debris beds of the flow history tests are provided in Table 6.12. Similar height and mass results lead to essentially equivalent computed bulk densities. The debris bed appearances in Figures 6.39 and 6.40 are similar as well.

Table 6.12. 060418_NO_1363_B1 and 060419_NO_1363_B1 Flow History Tests Debris Bed Data

Test	Approximate Measured Debris Bed Body Height (in)	Dry Debris Bed Mass (g)	Computed Density (g/mL)
060418_NO_1363_B1	0.39	13.23	0.16
060419_NO_1363_B1	0.39	13.03	0.16

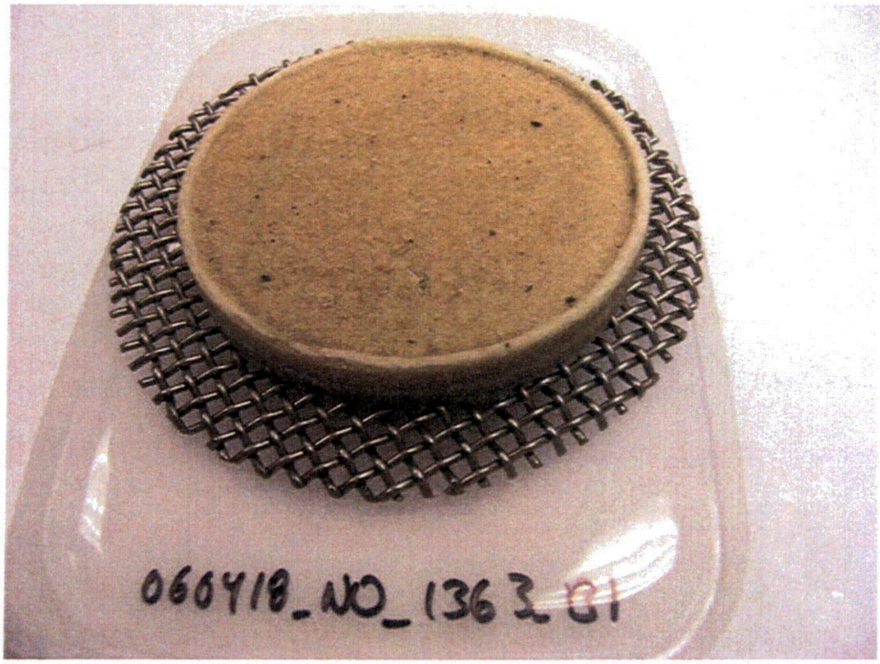

Figure 6.39. 060418_NO_1363_B1 Flow History Test

Figure 6.40. 060419_NO_1363_B1 Flow History Test